

Anomalous elasticity, fluctuations and disorder in elastic membranes

Pierre Le Doussal

CNRS-Laboratoire de Physique Théorique de l'Ecole Normale Supérieure, 24 rue Lhomond, 75231 Paris Cedex, France*

Leo Radzihovsky

Department of Physics, University of Colorado, Boulder, CO 80309 and
Kavli Institute for Theoretical Physics, University of California, Santa Barbara, CA 93106†

Motivated by freely suspended graphene and polymerized membranes in soft and biological matter we present a detailed study of a tensionless elastic sheet in the presence of thermal fluctuations and quenched disorder. The manuscript is based on an extensive draft dating back to 1993, that was circulated privately. It presents the general theoretical framework and calculational details of numerous results, partial forms of which have been published in brief Letters [1, 2]. The experimental realization atom-thin graphene sheets [3] has driven a resurgence in this fascinating subject, making our dated predictions and their detailed derivations timely. To this end we analyze the statistical mechanics of a generalized D -dimensional elastic “membrane” embedded in d dimensions using a self-consistent screening approximation (SCSA), that has proved to be unprecedentedly accurate in this system, *exact* in three complementary limits: (i) $d \rightarrow \infty$, (ii) $D \rightarrow 4$, and (iii) $D = d$. Focusing on the critical “flat” phase, for a homogeneous two-dimensional ($D = 2$) membrane embedded in three dimensions ($d = 3$), we predict its universal roughness exponent $\zeta = 0.590$, length-scale dependent elastic moduli exponents $\eta = 0.821$ and $\eta_u = 0.358$, and an anomalous Poisson ratio, $\sigma = -1/3$. In the presence of random uncorrelated heterogeneity the membrane exhibits a glassy wrinkled ground state, characterized by $\zeta' = 0.775$, $\eta' = 0.449$, $\eta'_u = 1.101$ and a Poisson ratio $\sigma' = -1/3$. Motivated by a number of physical realizations (charged impurities, disclinations and dislocations) we also study power-law correlated quenched disorder that leads to a variety of distinct glassy wrinkled phases. Finally, neglecting self-avoiding interaction we demonstrate that at high temperature a “phantom” sheet undergoes a continuous crumpling transition, characterized by a radius of gyration exponent, $\nu = 0.732$ and $\eta = 0.535$. Many of these universal predictions have received considerable support from simulations. We hope that this detailed presentation of the SCSA theory will be useful to further theoretical developments and corresponding experimental investigations on freely suspended graphene.

Contents

I. Introduction	2
A. Preamble and modern graphene motivation	2
B. Motivation and background	4
1. Membranes	4
2. Elastic membrane and its critical “flat” phase	4
3. Crumpling transition and the crumpled phase	5
4. Quenched disorder heterogeneity in an elastic membrane	5
C. Self-consistent screening approximation (SCSA)	6
D. Outline of the manuscript	7
II. Generalized model of a polymerized membrane	8
A. Homogeneous membrane: mean-field theory	8
B. Homogeneous membrane: thermal fluctuations	10
C. Model of a heterogeneous membrane: quenched disorder	11
III. SCSA of homogeneous membrane in the flat phase	13
A. Background	13
B. Effective model for the out-of-plane height fluctuations	14

*Electronic address: ledou@lpt.ens.fr

†Electronic address: radzihov@colorado.edu

C. Derivation of the SCSA equations for a homogeneous membrane	16
D. Analysis of the SCSA equations for a homogeneous membrane	18
E. Discussion of the SCSA predictions for a homogeneous membrane	20
IV. The crumpling transition	23
A. Derivation of the SCSA equations	23
B. Analysis and results	24
V. Flat phase of an elastic membrane with quenched disorder	27
A. Effective flat-phase model of a heterogeneous elastic membrane	27
B. The SCSA equations for the heterogeneous membrane	28
VI. Analysis of the SCSA equations for the heterogeneous membrane with short-range disorder	32
A. Perturbative regime of short length, large $q \gg q_{nl}$ scales	32
B. Non-perturbative regime of long-length, small $q \ll q_{nl}$ scales	33
1. Disorder-dominant, $T = 0$, short-range correlated disordered fixed point	34
2. Search for a $T > 0$ marginal fixed point	37
3. Thermal fixed point with short-range disorder	38
4. Stress-only disorder ($\Delta_\kappa = 0$) analysis	39
VII. Analysis of the SCSA equations for the heterogeneous membrane in long-range disorder	40
A. Realization of long-range disorder	40
B. Long-range quenched disorder	41
C. Stress-only disorder	41
D. Non-zero curvature disorder	43
1. Disorder-dominated phases: $\zeta' > \zeta$	43
2. Temperature-dominated phases, $\zeta' < \zeta$	47
3. Marginal phases, $\zeta' = \zeta$	50
VIII. Conclusions	52
Acknowledgments	53
A. Useful integrals and identities	53
1. Area of a D -dimensional Sphere	53
2. A Class of Spherically Symmetric Integrals	54
3. Spherical Average of $\hat{p}_{\alpha_1} \hat{p}_{\alpha_2} \dots \hat{p}_{\alpha_m}$	54
4. Feynman Parameters Integrals	56
5. Two Propagator Integrals of Products $q_{\alpha_1} q_{\alpha_2} \dots q_{\alpha_m}$	56
6. Summary	59
B. Results for the SCSA integrals	59
C. Crumpling transition integrals	60
References	62

I. INTRODUCTION

A. Preamble and modern graphene motivation

In this manuscript we present a detailed statistical mechanics study of a tensionless elastic sheet, as realized by graphene and polymerized membranes in soft and biological matter, in the presence of thermal fluctuations and quenched disorder. The manuscript is based on a draft dating back to 1993, that was circulated privately. Recent experimental realization of a freely suspended graphene [4] following the 2004 pioneering works of Geim and Novoselov [3], has led to a renaissance of this subject [5, 6] making our dated predictions and their detailed derivations timely. Some of the predictions have appeared in our earlier Letters [1, 2] in a rather terse form, challenging researchers

to reproduce and utilize our results in the modern graphene context. This motivated us to complete this detailed manuscript.

As we will discuss in detail, the key qualitative ingredient of a low-tension elastic sheet is that (in contrast to its tension-controlled counterpart), at an arbitrary low temperature and weak disorder its out-of-plane fluctuations $h_{rms} \sim L^\zeta$ grow unboundedly with its in-plane linear size L , where ζ is the universal roughness exponent of the “flat” phase of the fluctuating membrane. As a result of such strong thermally and disorder-driven fluctuations in the flat phase (first emphasized for the former by Nelson and Peliti[7]), nonlinear elasticity is always qualitatively important, *nonperturbatively* so, beyond a nonlinear length scale $\xi_{nl}(T)$. On longer scales the fluctuating flat sheet is *critical* at zero tension without any fine-tuning – a “critical phase” – and is characterized by universal power-law correlations, manifested by its anomalous elasticity driven by thermal fluctuations and/or quenched disorder. Namely, as predicted by theory [1, 8, 9], it is characterized by universal length-scale-dependent (enhanced) bending rigidity $\kappa(\mathbf{q}) \sim q^{-\eta}$, and in-plane (softened) elastic moduli $\mu(\mathbf{q}) \sim \lambda(\mathbf{q}) \sim q^{\eta_u}$, with a universal negative Poisson ratio of $-1/3$ [1]. All these and other properties of such a tensionless membrane, e.g., a spectacular absence of a linear elastic response with power-law universal nonlinear elasticity, then follow and are controlled by an infrared stable fixed point. Although in the presence of tension these universal singularities will be cut off by the corresponding tension-dependent length scale, they can, nevertheless, be experimentally observable in graphene for a sufficiently low tension.

In our work [1, 2], detailed here, we derived and explored these properties extensively in the presence of thermal fluctuations and random quenched disorder using a field-theoretic method that we developed in the context of membranes, the Self-Consistent Screening Approximation (SCSA), leading to accurate predictions for the exponents. As can be seen in Fig. (1) these predictions were confirmed in numerical simulations already in the 90’s.

Graphene, as the most prominent modern realization of an atom thin elastic sheet, is subject to strong thermal fluctuations, and the nonlinear length $\xi_{nl}(T)$ is reduced to the scale of its nanometer lattice constant. The renormalization of the Young modulus, $K_0(\mathbf{q}) \sim q^{\eta_u}$, predicted by the theory, has been recently observed experimentally on graphene sheets using the defect density as a control parameter for the relevant wavevector q [10, 11] (see also [12]). The best fitting value $\eta_u \approx 0.36$ found in this experiment is in close agreement with the SCSA prediction [1], $\eta_u = 0.358$. Note that, contrarily to the claim there [11], the ϵ -expansion [8], which predicts a nearly vanishing value $\eta_u = 2 - \frac{24}{25}\epsilon \approx 0.08$, strongly underestimates the renormalization of K_0 by thermal out-of-plane fluctuations, which is much more accurately captured by the SCSA method employed here. A similar renormalization was also observed in ab-initio atomistic Monte Carlo (MC) simulations, based on a realistic inter-atomic potential, for graphene at room temperature [10], with exponent values close to the SCSA predictions (see also [13]).

Here we do not attempt any review of the subject but only quote a few recent developments (among many). After its first development and application to polymerized membranes[1, 2], the SCSA method was pushed to the next order (including higher order diagrams in $1/d_c$ expansion) by Gazit [14] who found $\eta = 0.789$, $\eta_u = 0.422$ and $\zeta = 0.605$. The relative stability of these values with the order of expansion may explain why the simpler (first order) SCSA is so accurate. The non perturbative RG (NPRG) method was applied in Ref.19 who found $\eta = 0.849$. A quantum extension of the SCSA was developed in [15] to study ripples in graphene (see also [16] and [17]). Indeed experiments show that the suspended graphene is not perfectly flat but exhibits static ripples [4]. Understanding of the nature of these ripples, their interplay with thermal fluctuations and disorder, and of the statistical properties of the effective gauge fields that they induce for electrons [18] remains unsatisfactory. Finally, the crumpling transition was further studied in a number of works, using NPRG [19] and numerical studies, e.g., see [20] and reference therein, to quote a few.

While there has been much activity and contact between theory and experiments on the study of thermal fluctuations in graphene, the effect of quenched disorder that arises from a variety of graphene lattice defects (e.g. vacancies and interstitials, adatoms, impurities, dislocations, grain boundaries, ripples and electron puddles) [4, 21–24], remains significantly less explored. This is despite of the fact that much of the general theory of fluctuating disordered membranes (detailed here) has long been developed dating back to early 90’s [1, 2, 25–31]. In recent developments the SCSA, and related RG methods, were further used in studying the effect of quenched disorder in graphene, e.g., in [32] and for a peculiar model of long-range disorder in 3D printed artificial membranes [33]. The role of *long-range disorder*, which may result from some of the defects listed above, remains also relatively unexplored in the context of graphene. Here we study it in great details and show that long-range disorder leads to a rich variety of flat glassy phases and to crumpled states, depending on disorder’s strength and range. We hope that our pedagogical exposition and detailed derivations in the present paper will help fill the gap between theory, numerics and experiments on the effect of disorder on graphene and motivate further studies.

B. Motivation and background

1. Membranes

Fluctuating membranes has been a subject of much research over the last three decades [34]. On the theoretical side the interest is motivated by the opportunity to study the interplay between geometry, statistical mechanics and field theory. At the same time these two- and higher-dimensional generalizations of flexible one-dimensional manifolds are ubiquitous in nature and laboratory, and much of the theoretical research activity has been stimulated by the many experimental realizations. Biological membranes as e.g., walls of living cells, are one of the early most extensively studied realizations, which consist of amphiphilic lipid bilayer often with protein networks permeating the membrane and giving it its structural integrity and elasticity. In laboratory much of the effort has been directed to utilize the self-assembling nature of various kind of amphiphilic lipid and surfactant molecules. These molecules when put into an aqueous solution self-assemble into structures of various shapes and topologies, often tens of microns in extent. Some of the studied assemblies include open bilayers and monolayers, spherical, cylindrical and tori topologies, and multi-layered lyotropic microstructures [34].

Generically, these self-assembling membranes are two-dimensional fluids characterized by a vanishing in-plane shear modulus, with constituent molecules free to diffuse within the sheet. These *fluid* membranes are therefore somewhat fragile, and in the presence of fluctuations will often break up into smaller parts or undergo topological transformations. As detailed in Ref.34 their thermal fluctuations and resulting properties are quite distinct from tensionless *elastic* sheets that is our focus here.

The self-assembling membranes have many potential technological applications such as the use of the phospholipid vesicles and tubules for drug encapsulation and delivery, blood substitutes, perfumes, and antifouling paints [35]. Because these applications require stable membranes, many of the experimental efforts have been directed toward cross-polymerizing liquid membranes. Using multipli-bonded phospholipids such as diacetylenic lipids, UV irradiation can be used to activate the bonds and create a *polymerized* membrane with bonds virtually unbreakable on the scale of thermal energies at room-temperature. These two- and higher-dimensional realizations of linear polymers have been the subject of extensive studies dating back to late 1980's[34] and are the focus of our manuscript.

There are many other naturally occurring realizations of polymerized membranes. The inner surface of red blood cells contains the fishnet-like biopolymer spectrin network which can be extracted and studied in isolation from the lipid bilayer [36, 37]. Red blood cells themselves, with the spectrin attached to the lipid cell wall, can also be described by membrane theories, as emphasized by Lipowsky and Girardet [38]. Leibler [39] has suggested that simple “paracrystals” of proteins like tropomyosin provide another example of a biological tethered surface. Inorganic examples of tethered surfaces include graphite oxide sheets in an appropriate solvent [40] and the “rag” sheet-like structures found in MoS₂ [41]. And of course, as discussed above, laboratory realizations of single-atom thin graphene sheets have rekindled a renaissance in the study of electronic and mechanical properties of fluctuating elastic sheets [5, 6]. For other experimental realizations, see Ref. 34.

2. Elastic membrane and its critical “flat” phase

Elastic polymerized membranes, two-dimensional generalizations of linear polymer chains [34, 42], have thus been a focus of a large number of theoretical studies over the course of three decades starting in mid 1980's. Analogously to one-dimensional polymers, membranes are expected to be crumpled at high temperatures [42], though for most physical realizations a membrane crumpling scale (that scales exponentially with a ratio of the bending rigidity to temperature) is astronomically long. On the other hand at low temperature based on simple considerations one may expect that a tensionless membrane will undergo a transition to a “flat phase” in which it is on average flat but with strong fluctuations about a spontaneously selected plane [43].

On the other hand, at a simple-minded, mean-field level a membrane is quite analogous to a ferromagnetic spin system, with the local normals to the membrane playing the role of spins. The “crumpled” and the flat states of a membrane are then the analog of the paramagnetic and ferromagnetic phases, respectively. On the other hand, it is expected that *two*-dimensional systems with *short-range* interactions are forbidden to undergo a transition in which a continuous symmetry is broken spontaneously [44–46], as happens when the $O(3)$ rotational symmetry of the crumpled phase is spontaneously reduced to $O(2)$ symmetry in the flat phase. It is the low-energy spin-wave fluctuations, that are responsible for the destruction of a two-dimensional ordered phase in a conventional $O(N)$ spin system [47]. In fact, this expectation is realized in liquid membranes and in linear polymers, whose flat phase is strictly speaking (though typically difficult to observe) destroyed by thermal conformational fluctuations at any finite temperature in a thermodynamic limit.

In stark qualitative contrast, the flat phase of a *polymerized* membrane was predicted [7] to be *stable* at low temperatures, a highly nontrivial observation in thermodynamic limit, that is seemingly in conflict with Hohenberg-Mermin-Wagner theorems. In polymerized membranes, through the shear modulus coupling of the in-plane and out-of-plane deformations, fluctuations that try to (and do so in a fluid membrane) destabilize the flat phase, instead infinitely stiffen its bending rigidity via a statistical “corrugation” effect [7, 34]. The resulting anomalous elasticity then in fact stabilizes the flat phase against these very same fluctuations, in a spectacular phenomenon of order-from-disorder.

This striking phenomenon was first demonstrated using a simple one-loop self-consistent theory that *assumed* a non-renormalization of in-plane elastic moduli, leading to a roughness exponent $\zeta = 1/2$ and $\eta = 1, \eta_u = 0$ [7]. Later detailed renormalization group calculations [8], controlled by an $\epsilon = 4 - D$ expansion, predicted renormalized elastic constants $\lambda(\mathbf{q}) \sim \mu(\mathbf{q}) \sim q^{\eta_u}$, $\eta_u > 0$, with $\eta_u = 4 - D - 2\eta$, a relation imposed exactly by the underlying rotational invariance. This study found $\eta = 12\epsilon/(24 + d_c)$ ($d_c = d - D$, the codimension of the manifold), leading to $\zeta \approx 1/2$ for physical membranes [8]. A complementary $1/d$ -expansion similarly confirmed the stability and anomalous elasticity of the flat phase and predicted $\zeta \approx 2/d$ for a two-dimensional polymerized membrane [9].

3. Crumpling transition and the crumpled phase

Similar to conventional polymers, the crumpled phase of a membrane is characterized by a radius of gyration R_G , which describes the average size of the crumpled membrane inside the 3-dimensional embedding space. The radius of gyration that characterizes the crumpled phase is predicted to scale as a power of the internal size of the membrane, $R_G(L) \sim L^\nu$ [48–50]. Flory type arguments, which are based on dimensional analysis predict $\nu = (D + 2)/(d + 2)$. This approach had lead to accurate predictions of ν for one-dimensional polymers, but it is not clear how accurate its prediction is for membranes and higher dimensional manifolds.

However, the high-temperature crumpled phase has turned out to be elusive to numerical and experimental realization, because the self-avoiding interaction of a membrane tend to stabilizes the flat phase. At first, a high-temperature crumpled phase has only been seen in computer simulations of the so-called “phantom” membranes, in the absence of self-avoiding interaction, with interactions between nearest neighbor monomers only [51, 52, 54]. The crumpled phase however has subsequently been seen in Monte Carlo simulations of self-avoiding tethered surfaces modeled by impenetrable flexible plaquette. It has also been demonstrated to exist as an intermediate phase between a collapsed and the flat phases of the membrane with finely-tuned attractive interactions [53]. Experimentally investigated graphite oxide sheets [40], MoS₂ structures [41] and red blood cell “ghosts” [37] were also observed to exist in the crumpled phase.

The theory of the crumpling transition [9, 43] started with considering phantom membranes. In mean-field approximation the crumpling transition between the flat and crumpled phases is second-order. However, there are several open problems with the theory. First the renormalization group calculation of Paczuski *et al.* [43] did not find a perturbative critical point for the physical case of $d = 3 < d_c = 219$. Although they interpreted these runaway flows as a fluctuation-driven first-order transition, the explicit demonstration of the order of the transition has remained open. Other related technical issues will be discussed at the end of Section (IV). Secondly, the role of self-avoidance at the crumpling transition remains to be elucidated. Indeed, if $2D - \nu_c d > 0$ self-avoidance should be relevant, where ν_c is the radius of gyration exponent at the transition.

4. Quenched disorder heterogeneity in an elastic membrane

Motivated by a variety of physical realizations, subsequent studies of elastic membranes considered the effects of quenched internal disorder in addition to thermal fluctuations [25, 26]. Various kinds of local random heterogeneities are an almost inevitable feature of real membranes and graphene. Examples of disorder include holes or tears in the polymerized network, variations in the local coordination number and impurities in the form of functional proteins and lipids of odd size incorporated at random into the biological membrane. Partial and random polymerization of self-assembled microstructures will also inadvertently lead to defects in the form of vacancies, interstitials, dislocations and disclinations in a polymerized membrane and graphene sheets [27].

In such elastic membranes most of the defects leading to disorder will relax on much longer time scale than the conformational degrees of freedom of the membrane and can therefore be treated as static, i.e., quenched. In contrast, the annealed (dynamic) disorder can be shown to be unimportant, since it leads to only nonsingular renormalization of the elastic coefficient. Quenched disorder in a membrane leads to a local, random curving and stretching of the sheet even in its zero temperature ground state. Disorder that curves the membrane locally breaks the up-down symmetry of the sheet, while the stretching disorder respects this inversion symmetry [26]. As was first described theoretically

by Nelson and Radzihovsky [26], in the continuum description of a membrane the important effects of disorder can be summarized by a quenched extrinsic curvature and random stress disorders, which are analogous to the random field and random exchange models of the magnetic spin systems, respectively. Vacancies and interstitials introduce local uncorrelated random strains and therefore lead to disorder that has short-range spatial correlations. On the other hand, disclinations, dislocations and grain-boundaries resulting from partially polymerized liquid membranes will lead to local stresses that are power-law correlated and therefore can be modeled by strain and curvature disorder, but with power-law correlations [27].

In the crumpled phase of phantom membranes the disorder leads to a swelling of the membrane but does not modify the size exponent ν [26]. Simple arguments also suggest that disorder will modify the crumpling transition but careful analysis remains to be performed. At nonzero temperature, the effect of disorder on the flat phase were studied extensively and more carefully. Based on renormalization group calculations and expansions in dimensionality it was found that at long wavelengths, short-range weak stress-only disorder does not lead to significant modifications of the properties of pure membranes [26]. At vanishingly small temperatures the disorder becomes important and its effective strength grows at long length scales. At zero temperature the short-range curvature disorder dominates and leads to a new ground state whose roughness is found to scale as $L^{\zeta'}$, analogously to the finite temperature roughness, but now in the statistically rough ground state [28, 29]. This zero-temperature “crinkled” fixed point, was found to be marginally unstable to temperature. The ϵ -expansion of [28] predicted a roughness exponent $\zeta' = 1 - \frac{3}{14}\epsilon \approx 0.571$. The numerical simulation found $\zeta' = 0.81 \pm 0.02$ [29]. As we detail in current manuscript, we extended the SCSA to disordered membranes, and found the zero temperature crinkled phase solution with the ground-state roughness exponent $\zeta' = 0.775$ much closer to the numerical simulation value of Ref.29.

The early theoretical consideration of disordered polymerized membranes was motivated by beautiful experiments on polymerizable lipid vesicles subjected to UV irradiation [55]. Upon partial polymerization the vesicles were observed to undergo what appeared to be a reversible, first-order wrinkling phase transition either spontaneously or upon cooling (depending on experimental conditions). During the transition a spherically symmetric fluctuating vesicle would undergo a shrinking and wrinkling transformation to a raisin glassy structure.

Since, as described above, the short-range disorder was shown to be irrelevant at finite temperatures, the generation and effects of long-range disorder were naturally considered. A simple microscopic model was used to demonstrate that long-range disorder in the form of networks of grain-boundaries and unscreened disclinations will naturally arise in partially polymerized membranes [27]. It was found that unlike short-range disorder, the resulting long-range strains and extrinsic curvature disorders with power-law correlations, with exponents larger than a critical value, lead to an instability of the membrane’s flat phase [2, 27]. The strength and onset of the instability was also estimated from simple extensions of Harris-type arguments. The nature of the resulting phase was investigated theoretically in [30] and was described as a “crumpled glass” with spin glass like order in the membrane normals. Although the detailed nature of this phase remains open the disorder-activated instability predicted by the theory appeared to be a good candidate to explain the wrinkling transition observed in the experiments.

C. Self-consistent screening approximation (SCSA)

Theoretical investigations have led to much progress in qualitative understanding of polymerized membranes, especially of the flat phase where the challenging self-avoiding interaction is believed to be unimportant. Unfortunately, the quantitative predictions of the ϵ - and $1/d$ -expansions are far from the physical dimensions of a two-dimensional membrane embedded in 3d, explaining the lack of accuracy of these approaches. The original attempt at a self-consistent approach failed to obtain an independent set of equations to determine η and η_u , reproducing the rotational symmetry based relation between these exponents [7]. Furthermore, for heterogeneous membranes controlled by quenched disorder even the qualitative questions of the nature of the instability and the resulting phase remained a mystery.

This motivated us in 1992 to study homogeneous [1] and heterogeneous [2] membranes with a Self-Consistent Screening Approximation (SCSA), generalized from the studies of $O(N)$ magnets [67]. As we detail below, this analysis allowed us to perform calculations directly for membranes of physical dimensions (and their arbitrary D, d generalizations) and uniquely determines the relevant exponents. For disorder-free thermal membranes we calculated the roughness exponent and found $\zeta = 0.590$, which fell in the middle of all the known predictions from numerical simulations at the time. The comparison with numerics is summarized in Fig.1. In addition the SCSA prediction for the Poisson ratio, $\sigma = -1/3$, was later confirmed by numerical simulations (see caption of Fig.1). Furthermore, as detailed below, we also extended the SCSA method to describe the crumpling transition in thermal, homogeneous membranes.

In contrast to its original application to the $O(N)$ model, we found that the SCSA is unprecedentedly accurate when applied to the problem of polymerized membranes. As we demonstrated, although uncontrolled (no small systematic expansion parameter), this method encompasses both the ϵ and $1/d$ approximations. Namely, it is exact to first

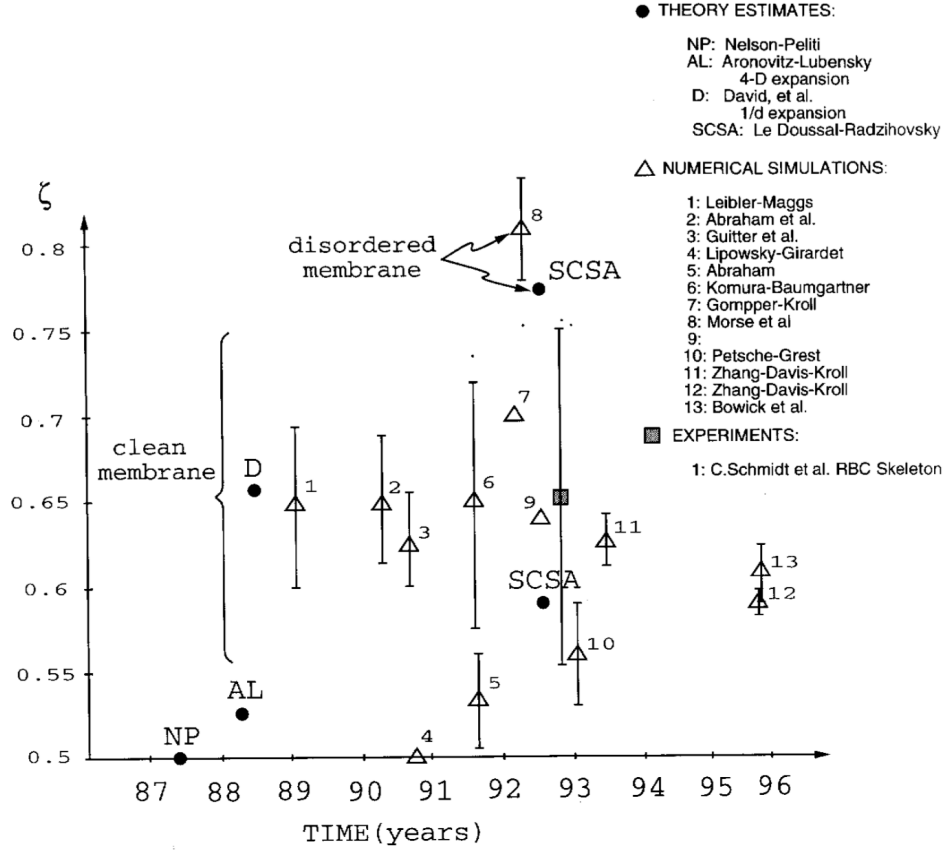


FIG. 1: Universal roughness exponent ζ of a tensionless elastic membrane (with physical dimensions $D = 2$, $d_c = 1$), as a function of the year, in the 1987-1996 range. ζ is also directly related to the anomalous (length-scale-dependent) elasticity exponents $\eta = 2(1 - \zeta)$ and $\eta_u = 4\zeta - 2$. Black dots: theoretical predictions (NP [7], AL [8], D [9], SCSA [1]). Triangles: numerical simulations (with error bars) (1[56], 2[54], 3[57], 4[58], 5[59], 6[60], 7[61], 8[29], 10[62], 11[63], 12[64], 13[65]). Square: experiment on red blood cell cytoskeleton[37]. Note that the SCSA prediction for the Poisson ratio $\sigma = -1/3$ was confirmed in numerical simulations in [66] who obtained $\sigma = -0.32(4)$.

order in ϵ for arbitrary d , exact for $d = D$, and by construction, it is exact in the limit of $d \rightarrow \infty$. Our results thus interpolate between two extreme dimensionalities, and are therefore expected to be substantially more accurate for physical membranes, than the RG perturbative expansions in dimensionalities.

Encouraged by the quantitative success of the SCSA, as we detail below, we extended it to membranes in the presence of short- and long-range disorder [1, 2]. We found a rich phase diagram that describes flat phases of a homogeneous and of a short-range-disordered membrane, previously studied, as well as new wrinkled glassy phases towards which the ordinary flat phase is unstable when long-range disorder is turned on. The SCSA theory thus captures the nature of the new disordered glassy phases and makes quantitatively accurate predictions about their statistical conformations and effective mechanical properties.

D. Outline of the manuscript

In the present manuscript we present the previously unpublished calculational details of our studies of polymerized membranes from the mid 1990s. As discussed in Section I A these results became even more relevant after 2004 with the synthesis of atom-thin graphene sheets. In the next Section II, we review the main properties of the continuum model of an elastic membrane, and describe the mean-field theory, thermal fluctuations and the model for a disordered membrane. In Section III we present the details of the SCSA method and apply it to the calculation of the roughness ζ and anomalous elasticity η, η_u exponents for a homogeneous thermally fluctuating membrane in its flat phase. In Section IV we extend the SCSA method to the study of the crumpling transition of a phantom membrane, from which the lower critical dimension for the finite temperature transition can be calculated. From the lower critical

dimension the roughness exponent for the flat phase can be extracted and we find that it is in complete agreement with one found in Section II. In Section V we derive the effective model for the flat phase in presence of disorder in terms of replicated out-of-plane height fields. We use this model to extend the SCSA equations to the case of the disordered membrane. In Section VI we analyze the SCSA equations for short-range disorder, and obtain the disorder related exponents ζ', η', η'_u . Finally, in Section VII we analyze the SCSA equations for the heterogeneous membrane in presence of long-range disorder, and derive the rich phase diagram containing a variety of glassy wrinkled phases, determined by the range and strength of quenched disorder. We analyzed in detail the properties of these glassy phases.

II. GENERALIZED MODEL OF A POLYMERIZED MEMBRANE

A. Homogeneous membrane: mean-field theory

As will become clear from our analysis, it is useful to study a higher-dimensional generalization of a physical two-dimensional membrane. Without much extra difficulty we will study an elastic D -dimensional manifold of interconnected particles fluctuating in the embedding d -dimensional space. Physically important degrees of freedom are the positions of the constituent particles. At long length-scale, continuum description that we will be interested in here, the discrete network, on scales longer than the typical mesh length a , can be described as a continuous manifold with the internal points labeled by a D -dimensional coordinate \mathbf{x} with components x_α , $\alpha = 1, \dots, D$, and their location in the embedding space specified by a d -dimensional vector $\vec{r}(\mathbf{x})$, with components $r_i(\mathbf{x})$, $i = 1, \dots, d$. We consider the case of positive codimension $d_c = d - D > 0$. Underlying symmetries of the problem impose constraints on the possible local Landau-Ginzburg Hamiltonians that one can write to describe the long wavelength properties of the membrane. The rotational and translational invariances of the embedding space require the effective Hamiltonian to be a local, analytic expansion in the scalar product of a local tangent vector-field $\vec{t}_\alpha(\mathbf{x}) = \partial_\alpha \vec{r}(\mathbf{x})$. For a homogeneous membrane these invariances also exist in the internal space. They restrict the Hamiltonian to a scalar with respect to rotations of the \mathbf{x} coordinate system and require constant coefficients in the Landau-Ginzburg expansion [68, 71].

Focussing our attention on membranes with only local interactions both in the embedding and internal spaces and keeping only terms that are most dominant at long scales, we obtain the Hamiltonian previously used in a number of studies of polymerized membranes [42, 43, 51, 52]

$$\mathcal{F}[\vec{r}] = \int d^D x \left[\frac{1}{2} \kappa (\partial^2 \vec{r})^2 + \frac{1}{2} \tau (\partial_\alpha \vec{r})^2 + u (\partial_\alpha \vec{r} \cdot \partial_\beta \vec{r})^2 + \tilde{v} (\partial_\alpha \vec{r} \cdot \partial_\alpha \vec{r})^2 \right], \quad (1)$$

where the sums over the repeated indices are implied. Upon identifying the tangent vector $\vec{t}_\alpha(\mathbf{x})$ or equivalently the local normal as the order parameter, the above Hamiltonian takes the form of a ϕ^4 -theory typically used in critical phenomena to describe second-order phase transitions. We therefore expect that at least in mean-field theory the membrane will undergo a continuous phase transition.

By minimizing the above Hamiltonian with respect to \vec{r} , we find that for positive values of the reduced temperature τ ($\tau = T - T_c^{MF} > 0$) the order parameter \vec{t}_α vanishes, describing the crumpled phase of the membrane characterized by randomly distributed local normals with zero average. On the other hand for $T < T_c^{MF}$ the bending energy (first term) dominates and the energy is minimized by aligning the local normals. The resulting ordered flat phase spontaneously breaks the full $O(d) \times O(D)$ rotational symmetry of the membrane down to $O(d) \times O(D)/O(D)$. In the flat phase the average tangent is nonzero and in mean-field theory is given by,

$$\vec{r}(\mathbf{x}) = t(x_1, \dots, x_D, 0) \quad , \quad |\vec{t}_\alpha^{MF}| = t = \frac{1}{2} \left[\frac{-\tau}{u + D\tilde{v}} \right]^{1/2}. \quad (2)$$

t is the scalar order parameter of the mean-field theory which vanishes in the high-temperature crumpled phase. In the flat phase it measures the shrinkage factor of the membrane with respect to its internal size L due to its out-of-plane thermal undulations. We observe that the usual mean-field order parameter exponent $\beta = 1/2$ has emerged from Eq. (2). In the flat phase the quartic (u, \tilde{v}) interactions become essential to render the Hamiltonian positive.

It is enlightening to examine the physical origin as well as the geometrical structure of the various terms appearing in the effective Hamiltonian, Eq. (1). The first term represents the bending rigidity of the membrane which arises from the energetic and entropic interactions, e.g., between amphiphilic rod-like lipids in the case of biological membranes, or from carbon-carbon bond stiffness in graphene. This interaction can be derived from a lattice model of locally interacting normals $\vec{n}_\mathbf{x}$, similar to the Heisenberg model of spin systems

$$\mathcal{H}_{\text{bend}} = -\tilde{\kappa} \sum_{\langle \mathbf{x}\mathbf{x}' \rangle} \vec{n}_\mathbf{x} \cdot \vec{n}_{\mathbf{x}'} \quad (3)$$

Ignoring a constant term, generalizing to D -dimensions and taking the continuum limit, we obtain,

$$\mathcal{H}_{\text{bend}} = \frac{1}{2} \kappa \int d^D x (\partial_\alpha \vec{n}(\mathbf{x}))^2, \quad (4)$$

where $\kappa \sim \tilde{\kappa}$ is the bending rigidity modulus. Since the normal is related to the tangent $\partial_\alpha \vec{r}$ by a simple rotation, we obtain the bending rigidity term of Eq.(1). Geometrically this contribution is simply the square of the extrinsic curvature [34, 69], originally proposed by Frolich to describe the oblate shape of red blood cells.

The rest of the terms in the Landau-Ginzburg expansion are the elastic contributions to the membrane energy arising from an expansion of the local nearest neighbor tethering interaction,

$$\mathcal{H}_{\text{el}} = \sum_{\mathbf{x}, \mathbf{e}} V(\vec{r}(\mathbf{x} + \mathbf{e}) - \vec{r}(\mathbf{x})) \quad (5)$$

in powers of the local tangent $\partial_\alpha \vec{r}$ in the continuum limit.

To study the flat phase of the membrane it is convenient to rewrite the effective Hamiltonian Eq.(1) in a slightly different form. By completing the square in the elastic interaction we obtain,

$$\mathcal{F}[\vec{r}] = \int d^D x \left[\frac{1}{2} \kappa (\partial^2 \vec{r})^2 + \mu (u_{\alpha\beta})^2 + \frac{1}{2} \lambda (u_{\alpha\alpha})^2 \right], \quad (6)$$

where μ and λ are known as the Lamé coefficients and are related to the previous coupling constants, $\mu = 4ut^4$, $\lambda = 8\tilde{v}t^4$. $u_{\alpha\beta}$ is the strain tensor related to the membrane metric tensor $\partial_\alpha \vec{r} \cdot \partial_\beta \vec{r}$ inherited from the embedding,

$$u_{\alpha\beta} = \frac{1}{2t^2} (\partial_\alpha \vec{r} \cdot \partial_\beta \vec{r} - t^2 \delta_{\alpha\beta}). \quad (7)$$

The strain tensor measures the local deformation of the membrane relative to the metric of the lowest energy configuration, which for homogeneous (disorder-free) membranes is the dilated flat metric $t^2 \delta_{\alpha\beta}$. In this form it becomes obvious that the total energy is minimized by minimizing the curvature and the elastic terms independently. The curvature term is minimized by any constant tangent vector, while the elastic terms vanish when the metric is precisely the preferred flat metric of the homogeneous membrane, $\partial_\alpha \vec{r} \cdot \partial_\beta \vec{r} = t^2 \delta_{\alpha\beta}$, with the obvious solution,

$$\vec{r}(\mathbf{x}) = t (x_1, x_2, \dots, x_D, 0, 0, \dots, 0). \quad (8)$$

The effects of the fluctuations in the flat phase can be studied by expanding the general conformation of the membrane around this perfectly flat ground state. A general deformation of the membrane that assumes no overhangs is described in the Monge representation,

$$\vec{r}(\mathbf{x}) = t \left((x_\alpha + u_\alpha(\mathbf{x})) \hat{e}_\alpha + \vec{h}(\mathbf{x}) \right), \quad (9)$$

where $u_\alpha(\mathbf{x})$ are the in-plane D phonon displacements, $\vec{h}(\mathbf{x})$ are the d_c out-of-plane membrane undulation modes [70], and the \hat{e}_α form a D -dimensional basis of in plane unit vectors. In this representation the strain tensor becomes,

$$u_{\alpha\beta} = \frac{1}{2} \left(\partial_\alpha u_\beta + \partial_\beta u_\alpha + \partial_\alpha \vec{h} \cdot \partial_\beta \vec{h} + \partial_\alpha u_\gamma \partial_\beta u_\gamma \right), \quad (10)$$

$$\simeq \frac{1}{2} \left(\partial_\alpha u_\beta + \partial_\beta u_\alpha + \partial_\alpha \vec{h} \cdot \partial_\beta \vec{h} \right), \quad (11)$$

where the phonon non-linearity (last term) has been neglected when going from the first line to the second, since it is quite clearly subdominant to $\partial_\alpha u_\beta$ at long wavelengths [7]. Aside from the bending rigidity term the effective Hamiltonian takes on the standard form of elastic energy of an isotropic solid [68, 71]

$$\mathcal{F}[\vec{h}, u_\alpha] = \int d^D x \left[\frac{1}{2} \kappa (\partial^2 \vec{h})^2 + \mu (u_{\alpha\beta})^2 + \frac{1}{2} \lambda (u_{\alpha\alpha})^2 \right]. \quad (12)$$

Note that in the broken symmetry flat phase the underlying embedding-space rotational invariance of the model (1), manifest in (7), is encoded in the non-linear form of $u_{\alpha\beta}$. For instance, this nonlinear form ensures that the (apparent) distortion $u_1^0(x_1, x_2) = x_1(\cos \theta - 1)$, $h^0(x_1, x_2) = x_1 \sin \theta$, corresponding to a rigid rotation of a flat membrane (in e.g., the 1 – 3 plane) consistently gives a vanishing strain, $u_{\alpha\beta}^0 = 0$.

B. Homogeneous membrane: thermal fluctuations

We now consider the effect of thermal fluctuations around the mean-field flat phase, defined by the in-plane phonons u_α and out-of-plane flexural modes \vec{h} . The statistical averages of any observable $O[\vec{h}, u_\alpha]$ are defined from the Gibbs measure

$$\langle O[\vec{h}, u_\alpha] \rangle = \mathcal{Z}^{-1} \int \mathcal{D}u_\alpha \mathcal{D}\vec{h} O[\vec{h}, u_\alpha] e^{-\mathcal{F}[\vec{h}, u_\alpha]/k_B T}. \quad (13)$$

As we already described in the Introduction, the fluctuations in the flat phase have been studied by the methods of renormalization group together with ϵ - and $1/d_c$ -expansions [8, 9], as well as with the SCSA described below [1], with the key result that the flat phase is stable to thermal fluctuations up to the crumpling transition temperature T_c . Surprisingly, the fluctuations actually tend to stabilize the flat phase [7] and lead to the elastic properties that differ remarkably from that of classical theory of local elasticity [71]. As we will show below, in the presence of these fluctuations the membrane is described by a universal (fixed point) renormalized Hamiltonian of the same form as Eq.(12), but with length scale-dependent renormalized elastic moduli, with the bending rigidity diverging as a power law of length scale,

$$\kappa_R(\mathbf{k}) \sim k^{-\eta}, \quad (14)$$

and vanishing Lamé coefficients

$$\mu_R(\mathbf{k}) \sim \lambda_R(\mathbf{k}) \sim k^{\eta_u}. \quad (15)$$

The underlying rotational invariance in the embedding space, that requires that coarse-graining (RG) preserves the full nonlinear form of the strain tensor, Eq.(11), implies the exact relation

$$\eta_u = 4 - D - 2\eta. \quad (16)$$

Thus there is only a single independent universal exponent characterizing the large scale fluctuations of a homogeneous membrane. A related property is the roughness of the membrane due to thermal fluctuations, defined by the root-mean-square fluctuations of the height difference of two distant points on the membrane,

$$\langle (\vec{h}(\mathbf{x}) - \vec{h}(0))^2 \rangle = 2d_c T \int \frac{d^D k}{(2\pi)^D} \frac{1 - e^{i\mathbf{k} \cdot \mathbf{x}}}{\kappa_R(\mathbf{k}) k^4} \sim x^{2\zeta}, \quad \langle h_i(\mathbf{k}) h_j(-\mathbf{k}) \rangle = \frac{T}{\kappa_R(\mathbf{k}) k^4} \delta_{ij} \sim \frac{1}{k^{4-\eta}}, \quad (17)$$

where the Fourier transform is defined in the standard way $\vec{h}(\mathbf{k}) = \int d^D x \vec{h}(\mathbf{x}) e^{-i\mathbf{k} \cdot \mathbf{x}}$, we use units in which the total membrane area is 1 (i.e., $(2\pi)^D \delta^{(D)}(\mathbf{k} - \mathbf{k}) = 1$), and ζ is the out-of-plane roughness exponent, related to η as

$$\zeta = (4 - D - \eta)/2. \quad (18)$$

The in-plane phonon fluctuations also acquire an anomalous dimension, and at large scale have a universal power-law roughness,

$$\langle (u_\alpha(\mathbf{x}) - u_\alpha(0))^2 \rangle \sim x^{2\zeta_u}, \quad \langle u_\alpha(\mathbf{k}) u_\beta(-\mathbf{k}) \rangle \simeq \frac{T}{\mu_R(\mathbf{k}) k^2} P_{\alpha\beta}^T(\mathbf{k}) + \frac{T}{(2\mu_R(\mathbf{k}) + \lambda_R(\mathbf{k})) k^2} P_{\alpha\beta}^L(\mathbf{k}) \sim \frac{1}{k^{2+\eta_u}}, \quad (19)$$

where ζ_u is the in-plane phonon roughness exponent, related to η_u and therefore to the transverse roughness exponent ζ according to

$$\zeta_u = (2 - D + \eta_u)/2 = 2\zeta - 1. \quad (20)$$

It is clear from Eq.(17) that for $\zeta < 1$, while transverse thermal height fluctuations diverge with system size, $h_{rms} \sim L^\zeta$, they remain smaller than membrane's in-plane extent, L , and thus the rotational broken symmetry “flat” phase (though qualitatively quite distinct from its literally flat mean-field $T = 0$ form) is stable to low-temperature thermal fluctuations. Based on Eq.(18), this stability is satisfied in the case of $D = 2$ for $\eta > 0$, driven by the anomalous enhancement of the membrane's bending rigidity, (14) by the very same thermal fluctuations that try (but fail at low temperature) to destabilize the flat phase. This order-from-disorder phenomenon thus circumvents the naive application of the Hohenberg-Mermin-Wagner theorem[44–46], that would otherwise argue for an instability of the two-dimensional flat phase to arbitrarily weak thermal fluctuations.

In the subsequent section we will derive these results, computing the anomalous exponents, by using the SCSA method which encompasses both the ϵ - and $1/d_c$ -expansion results as special limits and as we will argue is therefore significantly more accurate than all the previous dimensional expansions. In the next subsection we describe how the model of a homogeneous membrane of this section can be generalized to treat the effects of quenched internal disorder that appears to be relevant to understanding a variety of experimental systems, as described in the Introduction.

C. Model of a heterogeneous membrane: quenched disorder

The model for a homogeneous membrane can be extended to treat the effects of disorder, as was first done by Nelson and Radzihovsky [25]. They showed that the effect of weak disorder in the high temperature phase is simply to swell the size of the crumpled membrane, without modifying the radius of gyration exponent ν . On the other hand based on $1/d$ -expansion we subsequently argued that strong disorder leads to a transition to crumpled glassy phase in which the membrane is frozen into an isotropic spin-glass like configuration [30]. Here, however, we concentrate on weak quenched disorder and study its effects only in the flat phase.

To understand how disorder modifies the membrane model we return to the effective Hamiltonian of Eq.(6) and first examine the elastic and bending effects. The simplest contribution to disorder will come from a larger or smaller molecule embedded inside the regular crystalline matrix, or vacancies and interstitials in graphene, that will lead to a local compression or dilation. The strain tensor measures the local deformation of the membrane relative to the metric of the lowest energy configuration. For a homogeneous membrane the reference metric $g_{\alpha\beta}^o(\mathbf{x})$ is (aside from a global scaling factor) a flat metric, $\delta_{\alpha\beta}$. However, in the presence of disorder, the reference metric $g_{\alpha\beta}^o(\mathbf{x})$ will be modified to reflect the local deformation of the membrane due to the presence of impurities. In the continuum limit this will lead to a rough membrane even at $T = 0$ and with the ground state described by a non-trivial disorder-dependent conformation. This can be modeled by generalizing the expression for the strain $u_{\alpha\beta}^o$, Eq.(7) to

$$u_{\alpha\beta}(\mathbf{x}) = \frac{1}{2t_o^2}(g_{\alpha\beta}(\mathbf{x}) - g_{\alpha\beta}^o(\mathbf{x})) . \quad (21)$$

One particularly simple example is to choose $g_{\alpha\beta}^o(\mathbf{x}) = \partial_\alpha \vec{r}_o(\mathbf{x}) \cdot \partial_\beta \vec{r}_o(\mathbf{x})$, where $\vec{r}_o(\mathbf{x})$ is a given, random configuration. The elastic energy is not frustrated as it can be perfectly minimized by having $\vec{r}(\mathbf{x})$ conform to $\vec{r}_o(\mathbf{x})$. This is the membrane analog of the Mattis glass model for a non-frustrated random magnet [72] (for a recent realization of this model see [33]). However, this is clearly not the most general case of disorder, since $g_{\alpha\beta}^o(\mathbf{x})$ can be chosen a priori to be an arbitrary local symmetric tensor, in which case the ground state will generically be frustrated.

The deformation will be small if the size of the impurity molecules is not too different from the size of the host molecules. This allows us to model the effects of the random impurities by taking $g_{\alpha\beta}^o(\mathbf{x})$ to be,

$$g_{\alpha\beta}^o(\mathbf{x}) = t_o^2 [\delta_{\alpha\beta} + 2c_{\alpha\beta}(\mathbf{x})] , \quad (22)$$

where $c_{\alpha\beta}(\mathbf{x})$ is proportional to a local stress due to local heterogeneity in impurity concentration.

Inserting the new strain tensor (21) inside Eq.(6) we see that $g_{\alpha\beta}^o(\mathbf{x})$ and therefore $c_{\alpha\beta}(\mathbf{x})$ couple quadratically to the order parameter $\partial_\alpha \vec{r}$. Hence this type of disorder preserves the inversion symmetry of the membrane and therefore can only model the physics of defects symmetrically positioned with respect to the plane of the membrane.

Another, qualitatively distinct type of disorder, which breaks this up-down symmetry is modeled by introducing a local quenched random extrinsic curvature $\vec{f}(\mathbf{x})$ into the bending rigidity term of Eq.(12) [28],

$$\mathcal{F}_d^B[\vec{h}, u_\alpha] = \int d^D x \frac{1}{2} \kappa (\partial^2 \vec{h} - \vec{f}(\mathbf{x}))^2 . \quad (23)$$

Such disorder type is generically induced by, e.g., adatoms in graphene, or asymmetrical proteins embedded in a biological membrane.

Upon expanding the resulting full effective Hamiltonian and dropping the unimportant terms that do not involve the membrane conformational fields, we obtain,

$$\mathcal{F}_d[\vec{h}, u_\alpha] = \int d^D x \left[\frac{1}{2} \kappa (\partial^2 \vec{h})^2 + \mu (u_{\alpha\beta})^2 + \frac{1}{2} \lambda (u_{\alpha\alpha})^2 - \kappa \partial^2 \vec{h} \cdot \vec{f}(\mathbf{x}) - 2\mu u_{\alpha\beta} c_{\alpha\beta}(\mathbf{x}) - \lambda u_{\alpha\alpha} c_{\beta\beta}(\mathbf{x}) \right] . \quad (24)$$

As expected $c_{\alpha\beta}(\mathbf{x})$ disorder acts like the external local random stress due to defects embedded into the membrane lattice. We also observe that the random curvature $\vec{f}(\mathbf{x})$ and random stress $c_{\alpha\beta}(\mathbf{x})$ disorders symmetry-wise are the analogs of the random field [73], and the random T_c (random bond) [74] types of disorders in random magnets, previously extensively studied. In retrospect therefore, the disorder operators in Eq. (24) could have been written down immediately simply from symmetry considerations, and noting that the randomness in the elastic constants leads to irrelevant operators [26, 28] (as long as they remain positive).

For simplicity we take $c_{\alpha\beta}(\mathbf{x})$ and $\vec{f}(\mathbf{x})$ to be quenched Gaussian random fields with zero mean and correlations, [75]

$$\overline{c_{\alpha\beta}(\mathbf{x}) c_{\gamma\delta}(\mathbf{x}')} = \hat{\Delta}_\lambda(\mathbf{x} - \mathbf{x}') \delta_{\alpha\beta} \delta_{\gamma\delta} + \hat{\Delta}_\mu(\mathbf{x} - \mathbf{x}') (\delta_{\alpha\gamma} \delta_{\beta\delta} + \delta_{\alpha\delta} \delta_{\beta\gamma}) , \quad (25)$$

$$\overline{f_i(\mathbf{x}) f_j(\mathbf{x}')} = \delta_{ij} \hat{\Delta}_\kappa(\mathbf{x} - \mathbf{x}') , \quad (26)$$

where overbars denote averages over disorder realizations, and the hat on the correlators is purely for later notational convenience. For uncorrelated disorder coming for example from randomly positioned impurities, $\hat{\Delta}_\lambda(\mathbf{x} - \mathbf{x}')$, $\hat{\Delta}_\mu(\mathbf{x} - \mathbf{x}')$ and $\hat{\Delta}_\kappa(\mathbf{x} - \mathbf{x}')$ can be taken to be short-ranged, proportional to $\delta^{(D)}(\mathbf{x} - \mathbf{x}')$, that is understood to be cutoff at short scales by the disorder correlation length. However, a more general type of disorder, that might arise from unscreened disclination charges, grain-boundaries or possibly frozen-in tilt order will lead to long-range correlated disorder with power-law correlations [27]. We will extensively analyze both of these types of disorders in subsequent sections.

The two point statistics of fluctuations of an observable ϕ in a finite temperature heterogeneous system are determined by a combination of thermal fluctuations and quenched disorder as $\overline{\langle \phi \phi \rangle} = \overline{(\phi - \langle \phi \rangle)^2} + \overline{\langle \phi \rangle^2}$, respectively, where the second term is the sample-to-sample fluctuations of the heterogeneous ground state, while the first connected correlator, $\overline{\langle \phi \phi \rangle}_{conn} \equiv \overline{(\phi - \langle \phi \rangle)^2}$ quantifies thermal fluctuations around this nontrivial background. Accordingly, the roughness of a membrane with quenched disorder in the flat phase is characterized by the correlation function of the difference between out-of-plane height fluctuations at two different points, averaged over realizations of disorder

$$\overline{\langle (\vec{h}(\mathbf{x}) - \vec{h}(0))^2 \rangle} = \overline{\langle (\vec{h}(\mathbf{x}) - \vec{h}(0))^2 \rangle}_{conn} + \overline{\langle \vec{h}(\mathbf{x}) - \vec{h}(0) \rangle^2}. \quad (27)$$

In above equation the “connected” part measures the roughness due to thermal membrane fluctuations about a disorder specific, thermally averaged background configuration $\langle \vec{h}(x) \rangle$. The second contribution quantifies static spatial correlations in membrane roughness purely due to the presence of disorder. At large length scales we expect (and will show) that the two parts of the correlation functions $\delta h_c^{rms}(\mathbf{x})$ and $\delta h^{rms}(\mathbf{x})$ scale independently with length $x = |\mathbf{x}|$, with two possibly different roughness exponents

$$\delta h_c^{rms}(x)^2 = \overline{\langle (\vec{h}(\mathbf{x}) - \vec{h}(0))^2 \rangle}_{conn} \approx A_c x^{2\zeta}, \quad (28)$$

$$\delta h^{rms}(x)^2 = \overline{(\langle \vec{h}(\mathbf{x}) \rangle - \langle \vec{h}(0) \rangle)^2} \approx A x^{2\zeta'}. \quad (29)$$

Aside from a possible buckling transition which might spontaneously break the up-down ($\vec{h}(\mathbf{x}) \rightarrow -\vec{h}(\mathbf{x})$) symmetry of the membrane (which is not likely to occur in the absence of external forces or disorder), for a disorder-free membrane, i.e., for $\vec{f}(\mathbf{x}) = c_{\alpha\beta}(\mathbf{x}) = 0$, the thermally averaged height vanishes, $\langle \vec{h}(\mathbf{x}) \rangle = 0$. We therefore expect the amplitude A of the disconnected component to vanish for a homogeneous (disorder-free) membrane, while the amplitude A_c of the connected part to vanish as $T \rightarrow 0$. We observe then that the flat phase roughness in general is characterized by two independent roughness exponents ζ and ζ' .

It is convenient to define the height-height correlation functions in Fourier space

$$\overline{\langle (h_i(\mathbf{k}) - \langle h_i(\mathbf{k}) \rangle) (h_j(\mathbf{k}') - \langle h_j(\mathbf{k}') \rangle) \rangle} \sim |\mathbf{k}|^{\eta-4} (2\pi)^D \delta(\mathbf{k} + \mathbf{k}'), \quad (30)$$

$$\overline{\langle h_i(\mathbf{k}) \rangle \langle h_j(\mathbf{k}') \rangle} \sim |\mathbf{k}|^{\eta'-4} (2\pi)^D \delta(\mathbf{k} + \mathbf{k}'), \quad (31)$$

where the anomalous exponents η and η' describe singular renormalization of the bending rigidity $\kappa(\mathbf{k})$, Eq.(14) and disorder correlator $\Delta_\kappa(\mathbf{k}) \sim k^{-\eta'}$, respectively (see below). They are related to the roughness exponents according to

$$\zeta = \frac{4 - D - \eta}{2}, \quad \zeta' = \frac{4 - D - \eta'}{2}. \quad (32)$$

One can also study the roughness of the in-plane phonon deformations. As for the out-of plane deformations there is, quite generally, a thermal (connected) and a disorder parts to these fluctuations. The former has the same form as that for the homogeneous membrane in (19), though with disorder potentially modifying and controlling the universal anomalous exponents. The latter, characterizing the ground state zero-temperature phonon roughness, in Fourier space is given by

$$\overline{\langle u_\alpha(\mathbf{k}) \rangle \langle u_\beta(-\mathbf{k}) \rangle} \sim \frac{4\hat{\Delta}_\mu^R(\mathbf{k})}{k^2} P_{\alpha\beta}^T(\mathbf{k}) + \frac{\hat{\Delta}_L^R(\mathbf{k})}{k^2} P_{\alpha\beta}^L(\mathbf{k}) \sim \frac{1}{k^{2+\eta'_u}}, \quad (33)$$

where the anomalous exponent η'_u describes a singular renormalization of the stress disorder variances, with $\hat{\Delta}_L \equiv [4\mu^2(\hat{\Delta}_\lambda + 2\hat{\Delta}_\mu) + (4\mu + D\lambda)\lambda(D\hat{\Delta}_\lambda + 2\hat{\Delta}_\mu)] / (2\mu + \lambda)^2$. In (33) the superscript (and superscript) R indicates that all couplings must be replaced by their renormalized (k -dependent) values - see below for an equivalent explicit expression. In coordinate space in-plane phonon roughness is given by generalization of (19)

$$\overline{\langle (u_\alpha(\mathbf{x}) - u_\alpha(0))^2 \rangle}_{conn} \sim x^{2\zeta_u}, \quad \zeta_u = \frac{2 - D + \eta_u}{2}, \quad (34)$$

$$\overline{\langle u_\alpha(\mathbf{x}) - u_\alpha(0) \rangle \langle u_\alpha(\mathbf{x}) - u_\alpha(0) \rangle} \sim x^{2\zeta'_u}, \quad \zeta'_u = \frac{2 - D + \eta'_u}{2}, \quad (35)$$

where $\eta'_u = 4 - D - 2\eta'$. Anticipating the following sections, it is useful to give the phonon propagator in terms of the independent renormalized couplings $\tilde{\mu}(\mathbf{k})$, $\tilde{b}(\mathbf{k})$, $\tilde{\Delta}_\mu(\mathbf{k})$, $\tilde{\Delta}_b(\mathbf{k})$ since these are the ones which obey, within SCSA, multiplicative renormalization (see (195)-(198)). Note that the tilde label indicates exactly the same thing as the R subscript, i.e., it denotes renormalized couplings. Let us start by rewriting (19) by expressing $\tilde{\lambda}(\mathbf{k})$ as a function of $\tilde{b}(\mathbf{k})$ and $\tilde{\mu}(\mathbf{k})$. In presence of disorder this gives the following formula for the disorder average of the connected (i.e., the thermal part) of the fluctuations

$$\overline{\langle u_\alpha(\mathbf{k}) u_\beta(-\mathbf{k}) \rangle}_{\text{conn}} \simeq \frac{TP_{\alpha\beta}^T(\mathbf{k})}{\tilde{\mu}(\mathbf{k})k^2} + \left(\frac{D}{\tilde{\mu}(\mathbf{k})} - \frac{\tilde{b}(\mathbf{k})}{\tilde{\mu}(\mathbf{k})^2} \right) \frac{TP_{\alpha\beta}^L(\mathbf{k})}{2(D-1)k^2}. \quad (36)$$

To obtain the corresponding formula for the disorder part of the fluctuations, i.e., the off-diagonal component of the replica phonon propagator, one can simply replace each term in this expression by its corresponding replica matrix, as parameterized in (162), and then take the off-diagonal part, while performing the needed replica matrix multiplications and inversions, according to the rules described in (155)-(156). This leads to

$$\overline{\langle u_\alpha(\mathbf{k}) \rangle \langle u_\beta(-\mathbf{k}) \rangle} \simeq \frac{\tilde{\Delta}_\mu(\mathbf{k}) P_{\alpha\beta}^T(\mathbf{k})}{\tilde{\mu}(\mathbf{k})^2 k^2} + \left((D\tilde{\mu}(\mathbf{k}) - 2\tilde{b}(\mathbf{k}))\tilde{\Delta}_\mu(\mathbf{k}) + \tilde{\mu}(\mathbf{k})\tilde{\Delta}_b(\mathbf{k}) \right) \frac{P_{\alpha\beta}^L(\mathbf{k})}{2(D-1)\tilde{\mu}(\mathbf{k})^3 k^2}, \quad (37)$$

which, one can check is precisely equivalent to the above expression (33). Our aim in subsequent sections is to compute the universal thermal and disorder roughness exponents ζ and ζ' , and related exponents, characterizing the power-law rough critical phases for various types of disorder in the presence of thermal fluctuations.

III. SCSA OF HOMOGENEOUS MEMBRANE IN THE FLAT PHASE

A. Background

We now return to the model of a homogeneous polymerized membrane and study its flat phase using the method of the Self-Consistent Screening Approximation (SCSA), first introduced by Bray [67] in the context of the critical $O(N)$ model. In the following sections we will extend the methods developed here to treat the crumpling transition of phantom membranes and to study disordered membranes. The idea behind SCSA is that instead of performing a perturbative expansion (in nonlinear couplings, ϵ or $1/d_c$) one can study a particularly-truncated closed set of integral Dyson equations satisfied by the correlation functions. These are built by elevating the $1/d_c$ -expansion into a set of self-consistent equations. Although generally quite intractable, as we will show, these integral equations can be solved analytically in closed form in the long wavelength limit using the fact that theory is critical and correlation obey simple isotropic scaling forms.

The first pioneering attempt at this problem was by Nelson and Peliti (NP) [7] who introduced a simplified truncation of Dyson equations involving a renormalized bending rigidity $\kappa_R(\mathbf{k})$. Their self-consistent treatment in $D = 2$ predicted $\kappa_R(\mathbf{k}) \sim k^{-1}$, i.e., $\eta = 1$. Perturbatively, their approximation amounts to a partial resummation of a class of one-loop Feynman graphs for the renormalized height correlator. Their study crucially neglected the nontrivial renormalization of the Lamé coefficients, $\mu_R(\mathbf{k})$ and $\lambda_R(\mathbf{k})$, which arises because the in-plane stresses can also be relaxed by 'soft' out-of-plane displacements. As a result, curvature fluctuations soften these in-plane elastic constants, thereby screening the phonon-mediated nonlinearities. This was first appreciated by Toner (in an unpublished work) and explicitly calculated by Aronowitz-Lubensky (AL) who showed through a detailed one-loop RG calculation that at long wavelength the renormalized Lamé coefficients acquire a non-trivial universal wavevector dependence $\mu_R(\mathbf{k}) \sim k^{\eta_u}$ and $\lambda_R(\mathbf{k}) \sim k^{\eta_u}$, and obtained the exponents η_u and η to accuracy $O(\epsilon = 4 - D)$ in a dimensional expansion. This was complemented by a $1/d_c$ -expansion calculation by David, et al. [9], predicting $\eta = 2/d_c + O(1/d_c^2)$ in $D = 2$.

Significant discrepancies between these methods and numerical simulations, associated with the physical dimensionality $D = 2$, $d = 3$ being far away from the expansion points $D = 4$ and $d_c = +\infty$, respectively, motivated us to introduce a more accurate, self-consistent method, the SCSA, which takes into account the physics of screening neglected in NP. Using the SCSA we derived and solved analytically [1] *two independent* integral equations for the correlator of the d_c -component out-of-plane fluctuations and for the renormalized elastic interaction, which determine the renormalized moduli $\kappa_R(\mathbf{k})$, $\mu_R(\mathbf{k})$, and $\lambda_R(\mathbf{k})$.

We note three important properties of the SCSA applied to the membrane problem. First, the SCSA is *exact* by construction for large codimension $d_c = d - D$ to first order in $1/d_c$ and arbitrary D . Second, in the opposite extreme limit of $d_c = 0$ it gives $\eta = (4 - D)/2$ which is also the *exact* result since clearly $\eta_u = 0$ for $d = D$ and the two exponents are related according to (16). This second property is special to the problem of a polymerized membrane, contrasting the $O(N)$ model where the SCSA is not exact for $N = 0$. Thus, the SCSA approximation as a function

of d_c is tightly constrained by these two extremes. Finally, we find that our SCSA results are also *exact* to first order in $\epsilon = 4 - D$, for arbitrary d_c , a feature again special to the membrane problem, arising from the Ward identities associated with the rotational invariance in the embedding space. Hence, since within a single analysis the SCSA reproduces all previously known exact limits [8, 9], we expect it to be considerably more accurate for the physical membrane predictions. It includes the physics of the lower- as well as of the upper-critical dimension, and summarizes all the information contained in a one-loop calculation. These properties are at the heart of its successful agreement with numerics and experiments, as discussed in the Introduction.

B. Effective model for the out-of-plane height fluctuations

We now use SCSA to study thermal fluctuations of a homogeneous membrane described by the coarse-grained Hamiltonian $\mathcal{F}[\vec{h}, u_\alpha]$, given by Eqs.(12) and (11) in terms of the height $\vec{h}(\mathbf{x})$ and phonon $u_\alpha(\mathbf{x})$ fields. Because in-plane phonon modes $u_\alpha(\mathbf{x})$ appear only linearly and quadratically, it is convenient to integrate them out exactly [7, 26] and obtain an effective Hamiltonian $\mathcal{F}_{eff}[\vec{h}] = \mathcal{F}[\vec{h}, 0] + \delta\mathcal{F}[\vec{h}]$ for the height fluctuations $\vec{h}(\mathbf{x})$. From Eqs.(12) and (11) the coupling of the phonon field to the height field can be written as

$$\mathcal{F}_{u-h} = - \int d^D x u_\gamma A_{\alpha\beta\gamma}(\partial) \partial_\alpha \vec{h} \cdot \partial_\beta \vec{h}, \quad (38)$$

where $A_{\alpha\beta\gamma}(\mathbf{k}) = \frac{\lambda}{2} \delta_{\alpha\beta} i k_\gamma + \frac{\mu}{2} (i k_\alpha \delta_{\beta\gamma} + i k_\beta \delta_{\alpha\gamma})$. Integrating over the in-plane phonon field u_γ using the harmonic Hamiltonian

$$\mathcal{F}_u[u_\alpha] \equiv \mathcal{F}[0, u_\alpha] = \frac{1}{2} \int_k u_\alpha(-\mathbf{k}) k^2 [\mu P_{\alpha\beta}^T(\mathbf{k}) + (2\mu + \lambda) P_{\alpha\beta}^L(\mathbf{k})] u_\beta(\mathbf{k}), \quad (39)$$

with $P_{\alpha\beta}^T(\mathbf{k}) = \delta_{\alpha\beta} - k_\alpha k_\beta / k^2$ and $P_{\alpha\beta}^L(\mathbf{k}) = k_\alpha k_\beta / k^2$ the transverse and longitudinal projection operators, leads to

$$\delta\mathcal{F} = - \frac{1}{2} \int_k A_{\alpha\beta\gamma}(\mathbf{k}) A_{\alpha'\beta'\gamma'}(-\mathbf{k}) \langle u_\gamma(\mathbf{k}) u_{\gamma'}(-\mathbf{k}) \rangle_0 \times (\partial_\alpha \vec{h} \cdot \partial_\beta \vec{h})(\mathbf{k}) (\partial_{\alpha'} \vec{h} \cdot \partial_{\beta'} \vec{h})(-\mathbf{k}), \quad (40)$$

where we defined $\int_k = \int \frac{d^D k}{(2\pi)^D}$ and $\langle \dots \rangle_0$ denotes the average with respect to (39). Hence we obtain the following height-only effective Hamiltonian,

$$\mathcal{F}_{eff}[\vec{h}] = \frac{1}{2} \kappa \int d^D x (\partial^2 \vec{h})^2 + \frac{1}{4d_c} \int d^D x \left[\mu \left(P_{\alpha\delta}^T \partial_\alpha \vec{h} \cdot \partial_\beta \vec{h} \right) \left(P_{\beta\gamma}^T \partial_\gamma \vec{h} \cdot \partial_\delta \vec{h} \right) + \frac{\mu\lambda}{2\mu + \lambda} \left(P_{\alpha\beta}^T \partial_\alpha \vec{h} \cdot \partial_\beta \vec{h} \right)^2 \right], \quad (41)$$

where here and below the summation over the repeated indices is implied and $P_{\alpha\beta}^T$ is the transverse projection operator $P_{\alpha\beta}^T = \delta_{\alpha\beta} - \partial_\alpha \partial_\beta / \partial^2$. For later convenience in implementing the SCSA we have extracted a factor $1/d_c$ from the interaction by redefining the Lamé coefficients, $\mu \rightarrow \mu/d_c$, $\lambda \rightarrow \lambda/d_c$. We note that for physical membranes, with $d_c = 1$ this rescaling leaves the elastic moduli unchanged. The effective Hamiltonian above describes the physics of a polymerized membrane purely in terms of the height fluctuations field $\vec{h}(\mathbf{x})$. Note that there is an implicit short length scale cutoff a and correspondingly an ultraviolet momentum cutoff $\Lambda \sim 2\pi/a$ (e.g., in graphene, set by the lattice constant in real space and the size of the first Brillouin zone in reciprocal space), that we will always consider a shorter than any other length scale in the problem.

We note that for $D = 2$, $P^T(\partial)_{\alpha\beta} = (\hat{z} \times \partial)_\alpha (\hat{z} \times \partial)_\beta$ and $\mathcal{F}_{eff}[\vec{h}]$ simplifies considerably, reducing to

$$\mathcal{F}_{eff}[\vec{h}] = \frac{1}{2} \kappa \int d^2 x (\partial^2 \vec{h})^2 + \frac{K_0}{8d_c} \int d^2 x \left(P_{\alpha\beta}^T \partial_\alpha \vec{h} \cdot \partial_\beta \vec{h} \right)^2, \quad (42)$$

where $K_0 = \frac{4\mu(\mu+\lambda)}{(2\mu+\lambda)}$ is the Young's modulus, the only combination of elastic coefficients that characterizes the strength of the out-of-plane non-linearities. However for the general theoretical analysis, we will keep D arbitrary below, working with $\mathcal{F}_{eff}[\vec{h}]$, Eq.(41).

The resulting effective nonlocal interaction has an interesting geometrical interpretation. It can be rewritten as the long-range interaction between local Gaussian curvatures mediated by the in-plane phonons, an interpretation that is physically appealing [7]. In the absence of surface tension or external forces acting on the membrane the effective Hamiltonian above has the form of the $O(d_c) \times O(D)$ invariant ϕ^4 -theory, exactly at criticality ("mass" terms exactly zero). This massless property of the theory is preserved by the renormalization (coarse-graining) because the effective

Hamiltonian describes the theory of the interacting Goldstone modes $\partial_\alpha \vec{h}$ coming from the spontaneously broken $O(d)$ rotational symmetry in the embedding space. The “criticality” is strictly imposed by this nonlinearly realized rotational invariance.

The renormalization of the two transverse tensor parts of the quartic interaction in Eq.(41) determines the two independent renormalized Lamé coefficients $\mu_R(\mathbf{k})$, $\lambda_R(\mathbf{k})$, that characterize fluctuating membrane’s anomalous flat phase. However, as we will see below, while the amplitudes are independently renormalized, the rotational invariance imposes the same power-law wavevector dependence in these renormalized elastic moduli. It is convenient to work in Fourier space where $\mathcal{F}_{eff}[\vec{h}(\mathbf{k})]$ is expressed in terms of the Fourier transform of the height fields, $\vec{h}(\mathbf{k}) = \int d^D x \vec{h}(\mathbf{x}) e^{-i\mathbf{k}\cdot\mathbf{x}}$, and is given by

$$\mathcal{F}_{eff}[\vec{h}(\mathbf{k})] = \frac{\kappa}{2} \int_k k^4 |\vec{h}(\mathbf{k})|^2 + \frac{1}{4d_c} \int_{k_1, k_2, k_3} R_{\alpha\beta, \gamma\delta}(\mathbf{q}) k_{1\alpha} k_{2\beta} k_{3\gamma} k_{4\delta} \vec{h}(\mathbf{k}_1) \cdot \vec{h}(\mathbf{k}_2) \vec{h}(\mathbf{k}_3) \cdot \vec{h}(\mathbf{k}_4), \quad (43)$$

with $\mathbf{q} = \mathbf{k}_1 + \mathbf{k}_2$ and $\mathbf{k}_1 + \mathbf{k}_2 + \mathbf{k}_3 + \mathbf{k}_4 = \mathbf{0}$. The four-point coupling is a fourth-order tensor $R_{\alpha\beta, \gamma\delta}(\mathbf{q})$ that is transverse to \mathbf{q} , and, from (41), reads

$$R_{\alpha\beta, \gamma\delta}(\mathbf{q}) = \mu A_{\alpha\beta, \gamma\delta}(\mathbf{q}) + \frac{\mu\lambda}{2\mu + \lambda} B_{\alpha\beta, \gamma\delta}(\mathbf{q}), \quad (44)$$

where,

$$A_{\alpha\beta, \gamma\delta}(\mathbf{q}) = \frac{1}{2} (P_{\alpha\gamma}^T(\mathbf{q}) P_{\beta\delta}^T(\mathbf{q}) + P_{\alpha\delta}^T(\mathbf{q}) P_{\beta\gamma}^T(\mathbf{q})), \quad (45)$$

$$B_{\alpha\beta, \gamma\delta}(\mathbf{q}) = P_{\alpha\beta}^T(\mathbf{q}) P_{\gamma\delta}^T(\mathbf{q}), \quad (46)$$

with the longitudinal part having been eliminated through the phonon integration. Note that because a uniform strain tensor has $D(D+1)/2$ independent components, the integration over the $\mathbf{q} = 0$ in-plane phonons eliminates all corresponding non-linearities, hence the mode $\mathbf{q} = 0$ is *excluded* from the wavevector summation in the quartic nonlinearity (43) [7, 34].

A product of two transverse operators, $P_{\alpha\beta}^T(\mathbf{q}) P_{\gamma\delta}^T(\mathbf{q})$, together with two inequivalent tensors obtained by permutations of indices, form a complete basis for a space of transverse fourth rank tensors. The membrane’s effective quartic interaction tensors, $A_{\alpha\beta, \gamma\delta}(\mathbf{q})$ and $B_{\alpha\beta, \gamma\delta}(\mathbf{q})$ thus form a two-dimensional, reducible representation of this two-dimensional vector space. Because of the reducibility of the representation the two coupling coefficients of the two transverse operators in Eq.(41) do not renormalize independently, with each feeding into the renormalization of the other. This occurs because the corresponding tensors $A_{\alpha\beta, \gamma\delta}(\mathbf{q})$ and $B_{\alpha\beta, \gamma\delta}(\mathbf{q})$ are not mutually orthogonal. Indeed, using the following notation for the product of two tensors, $(A \star B)_{\alpha\beta, \gamma\delta} = A_{\alpha\beta, \rho\sigma} B_{\rho\sigma, \gamma\delta}$ we see that $A \star A = A$, $A \star B = B \star A = B$ and $B \star B = (D-1)B$. Instead of working in this two-dimensional space of coupling constants it is more convenient to transform to an independently renormalizable set, i.e., an irreducible representation. This can be accomplished by introducing two new tensors $M_{\alpha\beta, \gamma\delta}(\mathbf{q})$ and $N_{\alpha\beta, \gamma\delta}(\mathbf{q})$ that are mutually orthogonal projectors under the tensor multiplication (i.e., $M \star M = M$, $N \star N = N$ and $M \star N = N \star M = 0$) and are a linear combination of $A_{\alpha\beta, \gamma\delta}(\mathbf{q})$ and $B_{\alpha\beta, \gamma\delta}(\mathbf{q})$,

$$N_{\alpha\beta, \gamma\delta}(\mathbf{q}) = \frac{1}{D-1} P_{\alpha\beta}^T(\mathbf{q}) P_{\gamma\delta}^T(\mathbf{q}), \quad (47)$$

$$M_{\alpha\beta, \gamma\delta}(\mathbf{q}) = \frac{1}{2} (P_{\alpha\gamma}^T(\mathbf{q}) P_{\beta\delta}^T(\mathbf{q}) + P_{\alpha\delta}^T(\mathbf{q}) P_{\beta\gamma}^T(\mathbf{q})) - N_{\alpha\beta, \gamma\delta}(\mathbf{q}). \quad (48)$$

The corresponding new elastic coupling constants are also linearly related to the old ones,

$$\mu = \mu, \quad (49)$$

$$b = \frac{\mu(2\mu + D\lambda)}{2\mu + \lambda}. \quad (50)$$

The elastic constant μ is the usual shear modulus and b the D-dimensional generalization of Young’s modulus, proportional to the bulk modulus of a D-dimensional solid. It is physically reasonable that the bulk and shear moduli renormalize independently, as we find here mathematically.

In terms of these new tensors and coupling constants the vertex $R_{\alpha\beta, \gamma\delta}(\mathbf{q})$ of Eq. (44) becomes

$$R_{\alpha\beta, \gamma\delta}(\mathbf{q}) = \mu M_{\alpha\beta, \gamma\delta}(\mathbf{q}) + b N_{\alpha\beta, \gamma\delta}(\mathbf{q}). \quad (51)$$

In $D = 2$, since $P_{\alpha\beta}^T(\mathbf{q}) = q_\alpha^T q_\beta^T$, where $q_\alpha^T = \epsilon_{\alpha\gamma} q_\gamma$, one sees that the tensor $M_{\alpha\beta, \gamma\delta}(\mathbf{q})$ identically vanishes. This is consistent with the above observation that a single elastic constant, the Young modulus $K_0 = 2b$, characterizes the elastic non-linearities of a two-dimensional sheet.

C. Derivation of the SCSA equations for a homogeneous membrane

The height fluctuations in the flat phase are described by the Hamiltonian (43). It is the sum of the quadratic bending energy part and the quartic elastic nonlinearities, encoding membrane's in-plane elasticity. In the absence of non-linearities (setting $\mu = \lambda = 0$) the fluctuations of the height are Gaussian, with the correlator in Fourier space given by

$$\langle h_i(\mathbf{k}) h_j(\mathbf{k}') \rangle_0 = \delta_{ij} G_0(\mathbf{k}) (2\pi)^D \delta(\mathbf{k} + \mathbf{k}') , \quad G_0(\mathbf{k}) = \frac{T}{\kappa k^4}. \quad (52)$$

This leads to the harmonic roughness exponent $\zeta = (2 - D)/2$, that implies the absence of flat phase order in $D = 2$, consistent with conventional wisdom based on the Hohenberg-Mermin-Wagner theorems[44–46]. To deal with the quartic nonlinearity, schematically $R(\vec{h} \cdot \vec{h})^2$, we study, as usual, the perturbation theory in powers of the coupling constant, here the tensor $R_{\alpha\beta,\gamma\delta}(\mathbf{q})$, around the quadratic theory. Each term in the expansion is represented by a Feynman diagram (see Fig. 2), where the bare propagator $G_0(\mathbf{k})$ is represented by a solid line, and the quartic nonlinearity $(\vec{h} \cdot \vec{h})^2$ with interaction vertex, $R_{\alpha\beta,\gamma\delta}(\mathbf{q})$ by a dotted line joining the two pairs of fields $\vec{h} \cdot \vec{h}$ on each side.

We aim to calculate the correlator of the height field \vec{h} fluctuations

$$\langle h_i(\mathbf{k}) h_j(-\mathbf{k}) \rangle = \delta_{ij} G(\mathbf{k}) (2\pi)^D \delta(\mathbf{k} + \mathbf{k}') \quad , \quad G(\mathbf{k}) = \frac{T}{\kappa_R(\mathbf{k}) k^4} = \frac{T}{\kappa k^4 + \sigma_c(\mathbf{k})} , \quad (53)$$

where $G(\mathbf{k})$ is the propagator dressed by thermal fluctuations in the presence of non-linearities. For convenience we have introduced the self-energy $\sigma_c(\mathbf{k})$ which is the correction to the bare propagator.

In addition to the self-energy there are also corrections to the quartic non-linearities. To construct the SCSA equations, which will determine both the propagator and the renormalized interaction vertex $\tilde{R}_{\alpha\beta,\gamma\delta}(\mathbf{q})$, it is useful to recall the exact analysis in the limit of large d_c (a $1/d_c$ -expansion). Since for each internal loop of unconstrained d_c -component height fields, there is a factor d_c , the dominant set of diagrams which correct the four point vertex $R_{\alpha\beta,\gamma\delta}(\mathbf{q})$ for $d_c = +\infty$ form a geometric series of so-called polarization (or RPA) bubbles, which can be resummed exactly. These are depicted in Fig. 2 and represent screening of the elastic interactions by out-of-plane fluctuations. This is equivalent to introducing a Hubbard-Stratonovich field χ to decouple the quartic interaction and formally integrate over \vec{h} leading [76, 77] to a $\text{Tr} \ln(G_0^{-1} + \chi)$ term in the action.

The self-energy is then determined exactly to first order in $1/d_c$ by a single sunset diagram involving the screened interaction $\tilde{R}_{\alpha\beta,\gamma\delta}(\mathbf{q})$, illustrated in Fig. 2. In the figure the double solid line denotes the renormalized propagator, $G(\mathbf{k})$, the dotted line the bare interaction vertex $R_{\alpha\beta,\gamma\delta}(\mathbf{q})$ and the wiggly line represents the “screened” interaction $\tilde{R}_{\alpha\beta,\gamma\delta}(\mathbf{q})$, dressed by the vacuum polarization bubbles. The resulting expression would obviously lead to exponents and other physical quantities that diverge as $d_c \rightarrow 0$ and therefore are not expected to be accurate at the physical value of $d_c = 1$. The SCSA corrects this deficiency by self-consistently replacing all the bare \vec{h} propagators by the corresponding renormalized propagator, (53). The resulting closed set of two SCSA integral equations, corresponding to Fig. 2, is given by

$$\kappa_R(\mathbf{k}) k^4 = \kappa k^4 + \frac{2}{d_c} k_\alpha k_\beta k_\gamma k_\delta \int_{\mathbf{q}} \tilde{R}_{\alpha\beta,\gamma\delta}(\mathbf{q}) G(\mathbf{k} - \mathbf{q}) , \quad (54)$$

$$\tilde{R}_{\alpha\beta,\gamma\delta}(\mathbf{q}) = R_{\alpha\beta,\gamma\delta}(\mathbf{q}) - R_{\alpha\beta,\gamma_1\gamma_2}(\mathbf{q}) \Pi_{\gamma_1\gamma_2,\delta_1\delta_2}(\mathbf{q}) \tilde{R}_{\delta_1\delta_2,\gamma\delta}(\mathbf{q}) , \quad (55)$$

where

$$\Pi_{\alpha\beta,\gamma\delta}(\mathbf{q}) = \frac{1}{T} \int_{\mathbf{p}} p_\alpha p_\beta p_\gamma p_\delta G(\mathbf{p}) G(\mathbf{q} - \mathbf{p}) \quad (56)$$

is the vacuum polarization bubble, that encodes screening of the long-scale in-plane elasticity by short-scale out-of-plane fluctuations. We note that the Dyson equation for the self-energy contains an additional “tadpole” diagram contribution (which is usually dominant, i.e., $O(1)$ in the $1/d_c$ -expansion, and corresponds to a shift in the critical point). Here this term is strictly absent, since it involves zero momentum transfer for which $R(\mathbf{q} = 0) = 0$ (since the zero mode is excluded, as remarked above). This is a reflection of the general principle that precludes generation of a mass for a Goldstone mode, that in this case corresponds to absence of surface tension for free boundary conditions in the flat phase.

The resulting SCSA equations therefore amount to a partial resummation of the $1/d_c$ -expansion based on the result correct only to first order in $1/d_c$. Although a priori this approximation is uncontrolled, in retrospect it is expected to be quite accurate given the properties of the SCSA described in the Introduction and in the beginning of this section.

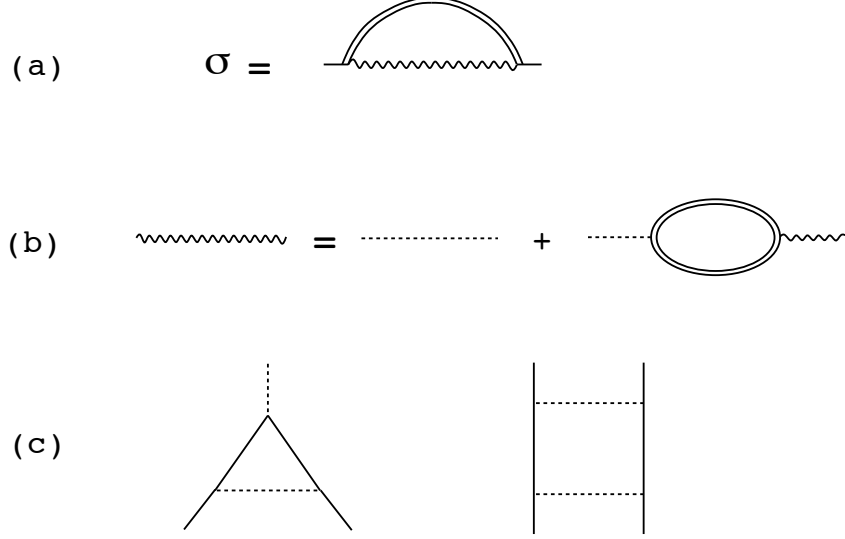


FIG. 2: Graphical representation of the SCSA: (a) self-energy correction, (54) to the out-plane-fluctuations propagator, that determines the renormalized bending rigidity, enhanced by fluctuations, (b) screened quartic elastic nonlinearity, (55), that determines the renormalized in-plane elastic moduli, softened by fluctuations, (c) UV finite vertex and polarization diagram, neglected in SCSA.

Let us now simplify the above equations using the symmetries of the theory. It can be verified that the dressed interaction has the same tensorial form as the bare one

$$\tilde{R}_{\alpha\beta,\gamma\delta}(\mathbf{q}) = \mu_R(\mathbf{q})M_{\alpha\beta,\gamma\delta}(\mathbf{q}) + b_R(\mathbf{q})N_{\alpha\beta,\gamma\delta}(\mathbf{q}) , \quad (57)$$

but with renormalized shear $\mu_R(\mathbf{q})$ and bulk-like moduli $b_R(\mathbf{q})$. To determine them we now study the polarization bubble. From its definition the tensor $\Pi_{\alpha\beta,\gamma\delta}(q)$ is the sum of a symmetric component $\Pi_{\alpha\beta,\gamma\delta}^{sym}(\mathbf{q}) = TI(\mathbf{q})S_{\alpha\beta,\gamma\delta}$ proportional to the fully symmetric tensor $S_{\alpha\beta,\gamma\delta} = \delta_{\alpha\beta}\delta_{\gamma\delta} + \delta_{\alpha\gamma}\delta_{\beta\delta} + \delta_{\alpha\delta}\delta_{\beta\gamma}$ with

$$I(\mathbf{q}) = \frac{1}{(D-1)(D+1)T^2} \int_p (p_\alpha P_{\alpha\beta}^T(\mathbf{q})p_\beta)^2 G(\mathbf{p})G(\mathbf{q}-\mathbf{p}), \quad (58)$$

and a longitudinal component where some of tensor indices are carried by q_α . Clearly, from Eqs.(44) and (45), because of the transverse structure of the vertex $R_{\alpha\beta,\gamma\delta}(\mathbf{q})$, only the symmetric component $\Pi_{\alpha\beta,\gamma\delta}^{sym}(\mathbf{q})$ contributes. Equation (55) can then be easily solved since in the subspace spanned by $M_{\alpha\beta,\gamma\delta}(\mathbf{q})$ and $N_{\alpha\beta,\gamma\delta}(\mathbf{q})$ we have

$$N_{\alpha\beta,\gamma_1\gamma_2}(\mathbf{q}) S_{\gamma_1\gamma_2,\gamma_3\gamma_4} N_{\gamma_3\gamma_4,\gamma\delta}(\mathbf{q}) = (D+1)N_{\alpha\beta,\gamma\delta}(\mathbf{q}) , \quad (59)$$

$$M_{\alpha\beta,\gamma_1\gamma_2}(\mathbf{q}) S_{\gamma_1\gamma_2,\gamma_3\gamma_4} M_{\gamma_3\gamma_4,\gamma\delta}(\mathbf{q}) = 2M_{\alpha\beta,\gamma\delta}(\mathbf{q}) , \quad (60)$$

$$M_{\alpha\beta,\gamma_1\gamma_2}(\mathbf{q}) S_{\gamma_1\gamma_2,\gamma_3\gamma_4} N_{\gamma_3\gamma_4,\gamma\delta}(\mathbf{q}) = N_{\alpha\beta,\gamma_1\gamma_2}(\mathbf{q}) S_{\gamma_1\gamma_2,\gamma_3\gamma_4} M_{\gamma_3\gamma_4,\gamma\delta}(\mathbf{q}) = 0 . \quad (61)$$

Using the above orthogonal projection relations inside Eq. (55), and the form (57) for $\tilde{R}_{\alpha\beta,\gamma\delta}(\mathbf{q})$ we obtain the equations for the renormalized shear and bulk-like moduli,

$$\mu_R(\mathbf{q}) = \frac{\mu}{1 + 2TI(\mathbf{q})\mu} , \quad (62)$$

$$b_R(\mathbf{q}) = \frac{b}{1 + (D+1)TI(\mathbf{q})b} . \quad (63)$$

Using Eqs. (57) inside Eq. (54) we obtain,

$$\kappa_R(\mathbf{k}) = \kappa + \frac{2T}{d_c} \int_q \frac{b_R(\mathbf{q}) + (D-2)\mu_R(\mathbf{q})}{D-1} \frac{\left(\hat{k}_\alpha P_{\alpha\beta}^T(\mathbf{q})\hat{k}_\beta\right)^2}{\kappa_R(\mathbf{k}-\mathbf{q})|\mathbf{k}-\mathbf{q}|^4} . \quad (64)$$

We note again that for $D = 2$ the renormalized bending rigidity is determined by the Young modulus $K_0(\mathbf{q}) = 2b_R(\mathbf{q})$ alone, consistent with (42).

The closed set of Eqs. (62), (64), (58), (53) constitute the SCSA equations for an homogeneous membrane of internal dimension D , in embedding dimension d . They determine the out-of-plane propagator $G(\mathbf{k})$, i.e. the wave-vector dependent renormalized bending rigidity $\kappa_R(\mathbf{k})$ and the renormalized elastic moduli $\mu_R(\mathbf{q})$ and

$$b_R(\mathbf{q}) = \frac{\mu_R(\mathbf{q})(2\mu_R(\mathbf{q}) + D\lambda_R(\mathbf{q}))}{2\mu_R(\mathbf{q}) + \lambda_R(\mathbf{q})}. \quad (65)$$

D. Analysis of the SCSA equations for a homogeneous membrane

The SCSA equations above predict the full non-trivial momentum dependence of the elastic moduli of the homogeneous fluctuating membrane. There are two main regimes corresponding to large and small q , respectively.

For sufficiently large $q \gg q_{\text{nl}}$, where q_{nl} is determined below, we expect that perturbation theory converges and that $G(\mathbf{k}) \approx G_0(\mathbf{k})$. In this regime, from Eq. (58), we see that $I(\mathbf{q}) \sim 1/(\kappa^2 q^{4-D})$ for $D < 4$, hence from Eqs. (62), (64) the thermal fluctuation corrections to the elastic moduli are small and are given by

$$\frac{b_R(\mathbf{q}) - b}{b} \sim -\frac{bT}{\kappa^2 q^{4-D}}, \quad (66)$$

$$\frac{\kappa_R(\mathbf{k}) - \kappa}{\kappa} \sim \frac{bT}{d_c \kappa^2 k^{4-D}}. \quad (67)$$

This high q regime extends down to q_{nl} defined by the above dimensionless corrections being small compared to unity, which is given by

$$q_{\text{nl}} \sim \left(\frac{bT}{\kappa^2} \right)^{1/(4-D)}, \quad (68)$$

the analog of Ginzburg criterion in critical phenomena[78]. We note that $q_{\text{nl}} \rightarrow 0$ for small temperature and/or large κ , with the nontrivial strong-fluctuation regime below q_{nl} squeezed out in this stiff regime limit. For $q \ll q_{\text{nl}}$ we expect that the effect of non-linearities become important and the system crosses over to the so-called universal anomalous elasticity regime which we now study.

We now study the regime of small wavevector q . Anticipating that the solution will describe a critical fixed point, with power-law correlations, we search a solution for the height-height correlation function, equivalently the propagator $G(\mathbf{k})$, as a power of k ,

$$G(\mathbf{k}) = \frac{T}{\kappa_R(\mathbf{k})k^4} \simeq T Z_\kappa^{-1} k^{-4+\eta} \quad , \quad \kappa_R(\mathbf{k}) \simeq Z_\kappa k^{-\eta}, \quad (69)$$

where Z_κ is an amplitude, which in the present case will be non-universal, and η determines the universal roughness exponent through Eq.(18). Substituting this ansatz into Eq.(58) we find that the vacuum polarization integral diverges as

$$I(\mathbf{q}) \simeq \frac{1}{(D^2 - 1)Z_\kappa^2} \int_p \frac{(p_\alpha P_{\alpha\beta}^T(\mathbf{q})p_\beta)^2}{|\mathbf{p}|^{4-\eta}|\mathbf{p} + \mathbf{q}|^{4-\eta}} = \frac{\Pi(\eta, D)}{(D^2 - 1)Z_\kappa^2} q^{-\eta_u}, \quad (70)$$

with

$$\eta_u = 4 - D - 2\eta \quad (71)$$

the anomalous exponent of the in-plane phonons modes, and in the second equality in (70) we have set the short scale cutoff $a \rightarrow 0$ since the integral is ultraviolet convergent. For future use we have defined

$$\Pi(\eta, \eta', D) = \int_p \frac{(p_\alpha P_{\alpha\beta}^T(\hat{\mathbf{q}})p_\beta)^2}{|\mathbf{p}|^{4-\eta}|\mathbf{p} + \hat{\mathbf{q}}|^{4-\eta'}} \quad , \quad \Pi(\eta, D) = \Pi(\eta, \eta, D), \quad (72)$$

and the integral is calculated in the Appendix B, with the amplitude $\Pi(\eta, D)$ found to be

$$\Pi(\eta, D) = (D^2 - 1) \frac{\Gamma(2 - \eta - D/2)\Gamma(D/2 + \eta/2)\Gamma(D/2 + \eta/2)}{4(4\pi)^{D/2}\Gamma(2 - \eta/2)\Gamma(2 - \eta/2)\Gamma(D + \eta)}. \quad (73)$$

Substituting Eq.(70) into Eqs.(62) and assuming $\eta_u > 0$, (i.e., that we are looking for a self-consistent solution with $\eta < (4 - D)/2$, to be checked a posteriori), we find for $q \ll q_{nl}$ that the $I(\mathbf{q})$ terms in the denominators in Eqs.(62) dominate, giving

$$\mu_R(\mathbf{q}) \simeq \frac{1}{2TI(\mathbf{q})} \sim \frac{(D^2 - 1)Z_\kappa^2}{2T\Pi(\eta, D)} q^{\eta_u}, \quad (74)$$

and similarly for $b_R(\mathbf{q})$ leading to the small q behavior of the renormalized elastic constants

$$\mu_R(\mathbf{q}) \simeq Z_\mu q^{\eta_u} \quad , \quad Z_\mu = \frac{(D^2 - 1)Z_\kappa^2}{2T\Pi(\eta, D)}, \quad (75)$$

$$b_R(\mathbf{q}) \simeq Z_b q^{\eta_u} \quad , \quad Z_b = \frac{(D - 1)Z_\kappa^2}{T\Pi(\eta, D)}. \quad (76)$$

Using the SCSA equation (64) for $\kappa_R(\mathbf{q})$ we obtain

$$\kappa_R(\mathbf{k}) = \kappa + \left(\frac{2T}{d_c} \frac{Z_b + (D - 2)Z_\mu}{(D - 1)Z_\kappa} \int_q \frac{\left(\hat{k}_\alpha P_{\alpha\beta}^T(\mathbf{q}) \hat{k}_\beta \right)^2 |\mathbf{q}|^{\eta_u}}{|\hat{\mathbf{k}} - \mathbf{q}|^{4-\eta}} \right) k^{-\eta}. \quad (77)$$

For future use we define

$$\Sigma(\eta, \eta', D) = \int_q \frac{(\hat{k}_\alpha P_{\alpha\beta}^T(\hat{\mathbf{q}}) \hat{k}_\beta)^2 |\mathbf{q}|^{4-D-2\eta}}{|\hat{\mathbf{k}} + \mathbf{q}|^{4-\eta'}} \quad , \quad \Sigma(\eta, D) := \Sigma(\eta, \eta, D), \quad (78)$$

and the integral is calculated in the Appendix B, with the amplitude $\Sigma(\eta, D)$ found to be

$$\Sigma(\eta, D) = \frac{(D^2 - 1)\Gamma(\eta/2)\Gamma(D/2 + \eta/2)\Gamma(2 - \eta)}{4(4\pi)^{D/2}\Gamma(2 - \eta/2)\Gamma(D/2 + \eta)\Gamma(D/2 + 2 - \eta/2)}. \quad (79)$$

We now note that the second term in (77) dominates at small k leading to $\kappa_R(\mathbf{q}) \simeq Z_\kappa k^{-\eta}$ consistent with the ansatz. Hence the solution is self-consistent.

Substituting Z_b and Z_μ into (77) we find that, crucially, the amplitude Z_κ cancel out. The remaining equality gives a transcendental equation, depending only d_c and D , determines the exponent $\eta(D, d_c)$, that is therefore universal,

$$\frac{D(D - 1)}{d_c} \frac{\Sigma(\eta, D)}{\Pi(\eta, D)} = 1. \quad (80)$$

More explicitly, this equation reads

$$D(D - 1) \frac{\Gamma(2 - \eta)\Gamma(2 - \frac{\eta}{2})\Gamma(\frac{\eta}{2})\Gamma(D + \eta)}{\Gamma(-\frac{D}{2} - \eta + 2)\Gamma(\frac{1}{2}(D - \eta + 4))\Gamma(\frac{D}{2} + \eta)\Gamma(\frac{D + \eta}{2})} = d_c. \quad (81)$$

Analysis of the left hand side shows that there is a unique solution continuously related to $\eta = 0$ for either $d_c = +\infty$ or $D = 4$, which we call $\eta(D, d_c)$.

For membranes of physical dimensionality $D = 2$ and arbitrary d_c , we can explicitly solve Eq. (81) and we obtain for $\eta(D = 2, d_c)$

$$\eta(D = 2, d_c) = \frac{4}{d_c + \sqrt{16 - 2d_c + d_c^2}}, \quad (82)$$

with the corresponding values for $\eta_u = 2 - 2\eta$ and $\zeta = 1 - \frac{\eta}{2}$ obtained from the rotational identity, Eq. (71), and from Eq. (18), respectively. Thus for physical membranes $D = 2$, $d = 1$ we obtain

$$\eta = \frac{4}{1 + \sqrt{15}} \approx 0.821, \quad (83)$$

$$\eta_u = \frac{2}{7}(9 - 2\sqrt{15}) \approx 0.358, \quad (84)$$

$$\zeta = \frac{1}{7}(8 - \sqrt{15}) \approx 0.590. \quad (85)$$

E. Discussion of the SCSA predictions for a homogeneous membrane

We can now examine various limiting approximations of our SCSA result. For the membranes of large codimension we can expand the solution of (81) in powers of $1/d_c$ obtaining,

$$\eta(D, d_c) = \frac{8}{d_c} \left(\frac{D-1}{D+2} \right) \frac{\Gamma[D]}{\Gamma[\frac{D}{2}]^3 \Gamma[2 - \frac{D}{2}]} + O\left(\frac{1}{d_c^2}\right), \quad (86)$$

$$\eta(D=2, d_c) = \frac{2}{d_c} + O\left(\frac{1}{d_c^2}\right). \quad (87)$$

This result agrees with the findings of Refs. 8, 9. As discussed above, this limiting property was expected from the construction of the SCSA, built on $1/d_c$ -expansion.

Expansion of the solution of (81) to first order in $\epsilon = 4 - D$ gives

$$\eta(D = 4 - \epsilon, d_c) = \frac{\epsilon}{2 + d_c/12}, \quad (88)$$

which is also in agreement with the result of Ref. 8, exact to $O(\epsilon)$ for all d_c . This is not a general property of SCSA. Here it can be traced to the fact that the vertex diagram (c) in Fig. 2 is *convergent*, due to the structure of the theory. Because of the transverse projectors in (47) one can always extract one power of external momentum from each external \vec{h} legs. As a result the only counter-terms needed are for two-point functions. This special property can be traced to a Ward identities based on the underlying embedding-space rotational invariance. The results of the two-loop calculation are in progress, and already indicate that the SCSA is not exact, with the deviations appearing at the two-loop order. [79]

We also observe from (81) that the solution for $d_c = 0$ is $\eta(D, d_c = 0) = \frac{4-D}{2}$, i.e., $\eta_u = 0$, which is the exact result for $d_c = 0$, as discussed in previous section.

Thus, as advertised, the SCSA is indeed *exact* in three distinct complementary limits. These strong constraints are at the heart of its quantitative accuracy in the physical dimension.

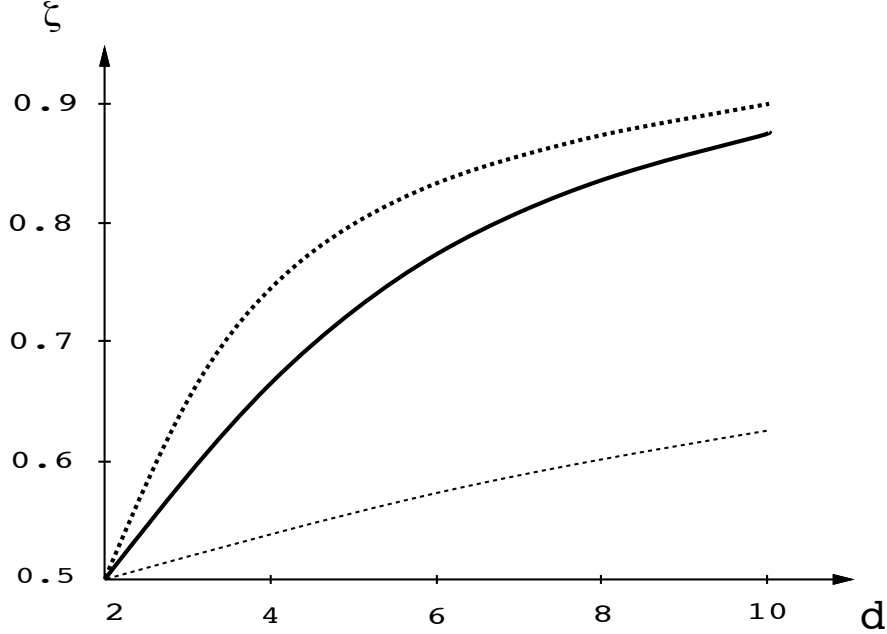


FIG. 3: A roughness ζ as a function of embedding dimension, d for two-dimensional ($D=2$) elastic membranes. The solid curve is the SCSA result, Eq.(82). The long-dashed-short-dashed curve is the $O(\epsilon)$ result, setting $\epsilon = 2$. The dashed curve corresponds to $\eta = 2/d$ chosen (somewhat arbitrarily) in Ref.8, 9 as a possible interpolation to finite d (asymptotic to the solid curve for $d \rightarrow \infty$).

The present method also gives interesting predictions for the lower-critical dimension $D_{lc}(d_c)$ for orientational order, i.e., order in $\nabla \mathbf{h}$. The fluctuations of the latter can be calculated as

$$\langle (\nabla h)^2 \rangle \sim T \int_q \frac{q^2}{Z_\kappa q^{4-\eta}} \sim T L^{2-D-\eta}, \quad (89)$$

which is found to diverge with system size L for $D < D_{lc}$ determined by the equation

$$2 - \eta(D_{lc}, d_c) = D_{lc}. \quad (90)$$

From (81) one easily finds that this equation is equivalent to $d_c = D_{lc}(D_{lc} - 1)/(2 - D_{lc})$. Thus, we find the lower-critical dimension as a function of d_c to be

$$D_{lc}(d_c) = \frac{1}{2}(1 - d_c + \sqrt{d_c^2 + 6d_c + 1}). \quad (91)$$

In particular for $d_c = 1$ we find $D_{lc} = \sqrt{2}$. We also observe that $D_{lc}(d_c)$ increases from $D_{lc} = 1$ for $d_c = 0$, to $D_{lc} = 2$ when $d_c \rightarrow \infty$. On the other hand if one keeps the embedding dimension d fixed, solving $2 - \eta(D_{lc}, d - D_{lc}) = D_{lc}$ gives $D_{lc} = 3/2$ for $d = 3$. Hence in either case, the flat phase of a physical two-dimensional membrane, that spontaneously breaks a continuous rotational symmetry, is thus stable and is in fact stabilized by thermal fluctuations (through renormalization of its elastic moduli), thus evading the Hohenberg-Mermin-Wagner-Coleman theorems [44–46], thereby exhibiting the aforementioned order-from-disorder phenomenon.

Similarly, one can ask how the anomalous thermal fluctuations affect the in-plane translational order, i.e., in the u_α fields, by calculating the exponent of the Debye-Waller factor

$$\langle (u_\alpha)^2 \rangle \sim T \int_q \frac{1}{Z_b q^{2+\eta_u}} \sim T L^{2\zeta_u}, \quad \zeta_u = \frac{2 - D + \eta_u}{2}, \quad (92)$$

using (19). Hence we find that the fluctuations in the in-plane positions of the atoms diverge for $D < D_u$ where D_u is determined by the equation $2 + \eta_u(D_u, d_c) = D_u$. By virtue of Ward identity $\eta_u = 4 - D - 2\eta$, (16), this is equivalent to $\eta(D_u) = 3 - D_u$, and from (81) we obtain that $D_u = 2.24$ for $d_c = 1$. Hence, for physical membranes the quasi-long-range positional order of a flat two-dimensional crystal is made unstable by out-of-plane fluctuations. It suggests that dislocations in a crystalline membrane at finite temperature cost a finite energy and if so, will always unbind at sufficient long scales (which of course can be very large depending on the core energy determined by the bond strength). Strictly speaking, it therefore precludes the existence of a crystalline fluctuating membrane in the thermodynamic dynamic. For the idealized case of permanent bonds the length at which this occurs becomes infinite.

Another related mechanism for proliferation of dislocations was analyzed by Nelson and Seung (NS) [31], who showed that at $T = 0$ above a scale $R_b^0 \sim 122 \frac{\kappa}{K_0 a}$ a dislocation will buckle out of plane, lowering its energy to a finite value. At finite temperature, our analysis shows that this estimate holds only for temperature such that $R_b^0 \ll L_{nl}$, where $L_{nl} \sim 1/q_{nl} \sim \kappa/\sqrt{K_0 T}$ is the length scale beyond which anomalous elasticity sets in, as the system crosses over to the non-trivial fixed point of the thermal membrane studied above. At higher temperature, the renormalization of the bending rigidity and the Young modulus by thermal fluctuations must be taken into account, and one finds the thermally-modified estimate,

$$R_b \sim R_b^0 \left(\frac{R_b^0}{L_{nl}} \right)^\delta, \quad (93)$$

with $\delta = \eta - \eta_u/(1 - \eta + \eta_u) \approx 0.862$. We find $R_b^0/L_{nl} = 122\sqrt{T/(K_0 a^2)}$ (which is ≈ 4.3 in graphene at room temperature $T = 1/40$ eV, using the standard parameters $a = 1.4\text{\AA}$, $a^2 K_0 = 20\text{eV}$, $\kappa = 1\text{eV}$). This demonstrates that the effective buckling length (beyond which dislocations unbind by buckling) at finite temperature grows as almost the square of the NS length (valid at $T = 0$, at the Gaussian fixed point). Hence temperature has actually a stabilizing affect on in-plane order at intermediate scale. At longer scales, in principle, dislocations unbind and lead to a hexatic fluctuating membrane[7], whose flat phase is expected to be unstable to out-of-plane fluctuations. However, in the idealized case of a tethered membrane, and even in graphene, whose covalent carbon bonds are much more energetic than the relevant thermal energy, dislocation core energies are very large and for finite size membrane the flat phase remains stable with properties discussed here.

Let us now comment on the values of the amplitudes Z_κ , Z_μ and Z_b in (69), (75). Although each of them is non-universal one can form two universal ratio from them, respectively

$$\frac{2TZ_b}{Z_\kappa^2} = \frac{2(D-1)}{\Pi(\eta, D)}, \quad (94)$$

$$\frac{2Z_b}{Z_\mu} = \frac{4}{D+1}. \quad (95)$$

For the physical membrane, $D = 2$, we find $2TZ_b/Z_\kappa^2 \approx 11.23$ and $2Z_b/Z_\mu = 4/3$. Examining further the elastic properties of a membrane from our SCSA solution we find from Eqs. (62), that in the long wavelength limit $\frac{\lambda_R(\mathbf{q})}{\mu_R(\mathbf{q})} \simeq -\frac{2}{D+2}$. Hence the membrane is described by a negative universal Poisson ratio,

$$\sigma_R(\mathbf{q}) = \frac{\lambda_R(\mathbf{q})}{2\mu_R(\mathbf{q}) + (D-1)\lambda_R(\mathbf{q})} = -\frac{1}{3}. \quad (96)$$

Although at first this result seems counterintuitive, it has a nice physical interpretation. A regular solid in the absence of thermal fluctuations is characterized by a positive Poisson ratio because when it is stretched in one direction it must contract in the other to minimize large density changes. However, as we have seen, a two-dimensional tensionless membrane in the presence of thermal fluctuations exhibits wild out-of-plane fluctuations. On average it therefore occupies a smaller projected area with the shrinkage factor determined by the scalar order parameter t , Eq. (2). If we stretch such a membrane in one direction we necessarily suppress its transverse fluctuations and therefore the membrane stretches in all in-plane directions, corresponding to a negative Poisson ratio.

We note that the SCSA equations admit two other, peculiar, fixed points. Indeed from (62) the choice of a zero bulk modulus $b = 0$ leads to $b_R(\mathbf{q}) = 0$, and is a solution of the SCSA equations at the limit of mechanical stability of the elastic manifold. Similarly, the choice $\mu = 0$ in (62) with $b \neq 0$, leads to another solution, with $\mu_R(\mathbf{q}) = 0$. It corresponds to anomalous elasticity of a nematic elastomer[80], studied extensively in Ref.81, 82. As is easily seen by inserting into (64), the equation for the associated exponent η is obtained by multiplying the left hand side of (81) by $(D+1)(D-2)/(D(D-1))$ for the first one ($b = 0$) and $2/(D(D-1))$ for the second one ($\mu = 0$). Hence we find

$$\eta(D, d_c; b = 0) = \eta(D, \frac{D(D-1)}{(D-2)(D+1)}d_c), \quad (97)$$

$$\eta(D, d_c; \mu = 0) = \eta(D, \frac{D(D-1)}{2}d_c), \quad (98)$$

where $\eta(D, d_c)$ is the standard SCSA solution analyzed above. For the first, fully compressible $b = 0$ fixed point in $D = 3$ we find $\eta = 0.446$. Since $\eta \rightarrow 0$ as $D \rightarrow 2^+$, we conclude that $D_{lc} = 2$ for this fixed point, which corresponds to a membrane fine tuned to the edge of its mechanical stability. The second, $\mu = 0$ fixed point gives, for $D = 2$ and $d_c = 1$, $\eta(2, 1; \mu = 0) = \eta(2, 1) = \frac{4}{1+\sqrt{15}} \approx 0.821$, the same value as for the standard SCSA fixed point. It is in principle possible to realize a vanishing shear modulus in a nematic elastomer membrane.[81] However, it remains to be further studied whether the neglected in-plane phonon nonlinearities (that have been shown to be irrelevant at the Gaussian fixed point) remain irrelevant at the present SCSA fixed point.[81]

Finally, one can ask about properties of a membrane in presence of a finite, but small tension and compression, i.e., slightly off-criticality. Here we will not reanalyze this buckling transition via the SCSA calculation, but will use the scaling relations derived in Ref. 9, 83 to predict the buckling critical exponents within our SCSA for the η, η_u exponents. There are various ways to study deviations from the critical tensionless, rotational invariant membrane. One is to put the membrane under stress, without breaking the embedding-space rotational invariance, by adding to the free energy (6) the term

$$\delta\mathcal{F} = \tau \int d^D x (\partial_\alpha u_\alpha + \frac{1}{2} \partial_\alpha \vec{h} \cdot \partial_\alpha \vec{h}), \quad (99)$$

which leads to the change $\kappa q^4 \rightarrow \kappa q^4 + \tau q^2$ in the quadratic part of the free energy (42) for the out-of-plane height modes. For $\tau > 0$ the membrane is stretched, while for $\tau < 0$ it tends to buckle. Alternatively, one can use constrained boundary conditions, imposing a projected area $(tL)^D$ for the membrane, where t is different from the spontaneous equilibrium value $t_{sp}(T) < 1$. As argued in [9] this generates a tension, with $\tau_R \sim t - t_{sp}(T)$, where τ_R is the renormalized value of the tension. Finally, one can set $\tau_R = 0$, but introduce a linear term $\delta\mathcal{F} = -f \int d^D x \partial_\alpha u_\alpha$, which explicitly breaks rotational invariance (as a frame would do).

It is shown in [9, 83] that this leads to a finite internal correlation length, which diverges as $\xi \sim \tau_R^{-\nu}$, in the tensionless limit, and to $t - t_{sp}(T) \sim f^{1/\delta}$, where the two exponents ν and δ are given by

$$\frac{1}{\nu} = D - 2 + \eta, \quad \delta = (2 - \eta)\nu. \quad (100)$$

Combining these with our SCSA values for the η exponent leads to $\nu = \frac{1}{4}(1 + \sqrt{15}) = 1.2182$, and $\delta = \frac{1}{2}(\sqrt{15} - 1) = 1.4365$, for a physical membrane. Note that the theory of Ref. 9, 83 also predicts $t \sim f^{1/\delta}$ at $T = T_c$, where T_c is the crumpling transition temperature. It would be interesting to extend the SCSA calculation to derive (and confirm) these results from first principles, and also to obtain a better description of the buckled state at $\tau_R < 0$.

IV. THE CRUMPLING TRANSITION

A. Derivation of the SCSA equations

In this Section we analyze the crumpling transition using the SCSA. We focus at the critical point, and thus tune all the parameters to sit exactly at criticality. We will thus determine the only exponent at criticality, the exponent η (see below). Calculation of the other independent exponent (e.g. ν) requires an independent calculation. Because the crumpling transition occurs at nonzero temperature, for convenience in this section we work in units in which $T = 1$. We start from the isotropic theory for a polymerized phantom membrane tuned at its critical crumpling point [42, 43, 51, 52]. The Hamiltonian is given by

$$\mathcal{F}[\vec{r}] = \int d^D x \left[\frac{\kappa}{2} (\partial^2 \vec{r})^2 + \frac{\mu_0}{4d} (\partial_\alpha \vec{r} \cdot \partial_\beta \vec{r})^2 + \frac{\lambda_0}{8d} (\partial_\alpha \vec{r} \cdot \partial_\alpha \vec{r})^2 \right], \quad (101)$$

where, as compared to (1), we have denoted $u = \frac{\mu_0}{4d}$ and $\tilde{v} = \frac{\lambda_0}{8d}$, where we have used subscripts to distinguish the coefficients of the anharmonic terms from the true Lamé coefficients in the flat phase. Equation (101) can be rewritten in terms of Fourier components, in a form analogous to (43)

$$\mathcal{F}[\vec{r}] = \frac{\kappa}{2} \int_k k^4 |\vec{r}(\mathbf{k})|^2 + \frac{1}{4d} \int_{\mathbf{k}_1, \mathbf{k}_2, \mathbf{k}_3} R_{\alpha\beta, \gamma\delta}(\mathbf{q}) k_{1\alpha} k_{2\beta} k_{3\gamma} k_{4\delta} \vec{r}(\mathbf{k}_1) \cdot \vec{r}(\mathbf{k}_2) \vec{r}(\mathbf{k}_3) \cdot \vec{r}(\mathbf{k}_4), \quad (102)$$

with $\mathbf{q} = \mathbf{k}_1 + \mathbf{k}_2$ and $\mathbf{k}_1 + \mathbf{k}_2 + \mathbf{k}_3 + \mathbf{k}_4 = \mathbf{0}$, and we use \int_k to denote $\int d^D k / (2\pi)^D$. Note that we work exactly at the crumpling transition point where the renormalized quadratic term has been tuned to and kept at zero. The bare four-point fourth order tensorial interaction has the form:

$$R_{\alpha\beta, \gamma\delta} = \frac{\mu_0}{2} (\delta_{\alpha\gamma} \delta_{\beta\delta} + \delta_{\alpha\delta} \delta_{\beta\gamma}) + \frac{\lambda_0}{2} \delta_{\alpha\beta} \delta_{\gamma\delta}. \quad (103)$$

This parameterization is insufficient to express the renormalized $\tilde{R}_{\alpha\beta, \gamma\delta}(\mathbf{q})$ (i.e., after dressing by the vacuum polarization bubbles), since the momentum \mathbf{q} can carry indices and tensors, for instance, $q_\alpha q_\beta \delta_{\gamma\delta}$ can appear. The most general parameterization that we will need, in terms of the irreducible representations under tensor multiplication, which is defined as $R'' = R' * R$, i.e., $R''_{\alpha\beta, \gamma\delta} = R'_{\alpha\beta, \alpha'\beta'} R_{\alpha'\beta', \gamma\delta}$, is :

$$R = \sum_{i=1}^5 w_i W_i, \quad (104)$$

in terms of five "elastic constants" w_i and five "projectors" W_i , $i = 1, \dots, 5$, defined as

$$(W_3)_{\alpha\beta, \gamma\delta}(\mathbf{q}) = \frac{1}{D-1} P_{\alpha\beta}^T P_{\gamma\delta}^T, \quad (W_5)_{\alpha\beta, \gamma\delta}(\mathbf{q}) = P_{\alpha\beta}^L P_{\gamma\delta}^L, \quad (105)$$

$$(W_4)_{\alpha\beta, \gamma\delta}(\mathbf{q}) = (W_{4a})_{\alpha\beta, \gamma\delta}(\mathbf{q}) + (W_{4b})_{\alpha\beta, \gamma\delta}(\mathbf{q}), \quad (106)$$

$$(W_{4a})_{\alpha\beta, \gamma\delta}(\mathbf{q}) = \frac{1}{\sqrt{D-1}} P_{\alpha\beta}^T P_{\gamma\delta}^L, \quad (W_{4b})_{\alpha\beta, \gamma\delta}(\mathbf{q}) = \frac{1}{\sqrt{D-1}} P_{\alpha\beta}^L P_{\gamma\delta}^T, \quad (107)$$

$$(W_2)_{\alpha\beta, \gamma\delta}(\mathbf{q}) = \frac{1}{2} (P_{\alpha\gamma}^T P_{\beta\delta}^L + P_{\alpha\delta}^T P_{\beta\gamma}^L + P_{\alpha\gamma}^L P_{\beta\delta}^T + P_{\alpha\delta}^L P_{\beta\gamma}^T), \quad (108)$$

$$W_1(\mathbf{q}) = \frac{1}{2} (\delta_{\alpha\gamma} \delta_{\beta\delta} + \delta_{\alpha\delta} \delta_{\beta\gamma}) - W_3(\mathbf{q}) - W_5(\mathbf{q}) - W_2(\mathbf{q}), \quad (109)$$

where $P_{\alpha\beta}^T = \delta_{\alpha\beta} - q_\alpha q_\beta / q^2$ and $P_{\alpha\beta}^L = q_\alpha q_\beta / q^2$ are the standard transverse and longitudinal projection operators associated to \mathbf{q} . The first two projectors W_1, W_2 are mutually orthogonal and orthogonal to the other three. Note that while R , being symmetric, can be expressed in terms of the symmetric tensors W_i , $i = 1, \dots, 5$, we will need at some intermediate stages of the calculations some products (such as $\Pi * R$ see below), which are not symmetric. Hence we introduced W_4^a and W_4^b , which together with W_i , $i = 1, 2, 3$ and W_5 make the representation complete under tensor multiplication. The rules for the tensor multiplication $T'' = T' * T$ of the more general tensors $T = \sum_{i=1}^3 w_i W_i + w_{4a} W_{4a} + w_{4b} W_{4b} + w_5 W_5$ and $T' = \sum_{i=1}^3 w'_i W_i + w'_{4a} W_{4a} + w'_{4b} W_{4b} + w'_5 W_5$ are then

$$w''_1 = w'_1 w_1, \quad w''_2 = w'_2 w_2, \quad \begin{pmatrix} w''_3 & w''_{4a} \\ w''_{4b} & w''_5 \end{pmatrix} = \begin{pmatrix} w'_3 & w'_{4a} \\ w'_{4b} & w'_5 \end{pmatrix} \begin{pmatrix} w_3 & w_{4a} \\ w_{4b} & w_5 \end{pmatrix}, \quad (110)$$

with $T'' = \sum_{i=1}^3 w_i'' W_i + w_{4a}'' W_{4a} + w_{4b}'' W_{4b} + w_5'' W_5$. For the tensor $R_{\alpha\beta,\gamma\delta}$, which belongs to the space of tensors which are symmetric under $\alpha \leftrightarrow \beta$, under $\gamma \leftrightarrow \delta$ and under $(\alpha, \beta) \leftrightarrow (\gamma, \delta)$ (let us call this symmetry \mathcal{S}) the five couplings in (104) are sufficient, and their bare values (so that (104) reproduces (103)) are given by

$$w_1 = w_2 = \mu_0, \quad w_3 = \frac{1}{2}(D-1)\lambda_0 + \mu_0, \quad w_4 = \frac{1}{2}\sqrt{D-1}\lambda_0, \quad w_5 = \frac{1}{2}\lambda_0 + \mu_0. \quad (111)$$

Note that the two eigenvalues of the matrix formed by the w_i , $i = 3, 4, 5$, are then μ_0 , and $\mu_0 + \frac{1}{2}D\lambda$.

For the crumpling transition the SCSA equations now take the form:

$$\mathcal{G}(\mathbf{k})^{-1} - \kappa k^4 =: \sigma(\mathbf{k}) = \frac{2}{d} \int_q k_\alpha (k_\beta - q_\beta) (k_\gamma - q_\gamma) k_\delta \tilde{R}_{\alpha\beta,\gamma\delta}(\mathbf{q}) \mathcal{G}(\mathbf{k} - \mathbf{q}), \quad (112)$$

$$\tilde{R}(\mathbf{q}) = R(\mathbf{q}) - R(\mathbf{q}) \Pi(\mathbf{q}) \tilde{R}(\mathbf{q}), \quad (113)$$

where $\mathcal{G}(\mathbf{k})$ is the propagator of the \vec{r} field, i.e., $\langle r_i(\mathbf{k}) r_j(\mathbf{k}') \rangle = \mathcal{G}(\mathbf{k}) (2\pi)^D \delta(\mathbf{k} + \mathbf{k}') \delta_{ij}$, and in the second line tensor-product notation is implied. The complete Dyson equation for the self-energy contains an additional UV divergent "tadpole" diagram contribution, which scales as k^2 . The integral in (112) also contains a component that scales as k^2 at small k . Both contributions have been subtracted by the shift in a critical point. This is a standard procedure when dealing with a critical theory, where a parameter (distance to crumpling transition parameters) must be tuned.

The vacuum polarization tensor is also a symmetric tensor (with the symmetry \mathcal{S} defined above)

$$\Pi_{\alpha\beta,\gamma\delta}(\mathbf{q}) = \frac{1}{4} \int_p (p_\alpha (q_\beta - p_\beta) + p_\beta (q_\alpha - p_\alpha)) (p_\gamma (q_\delta - p_\delta) + p_\delta (q_\gamma - p_\gamma)) \mathcal{G}(\mathbf{p}) \mathcal{G}(\mathbf{q} - \mathbf{p}). \quad (114)$$

Hence it can be written as

$$\Pi(\mathbf{q}) = \sum_{i=1}^5 \pi_i(\mathbf{q}) W_i(\mathbf{q}), \quad (115)$$

where the $\pi_i(\mathbf{q})$ are "polarization bubble" integrals in the W_i basis. The renormalized interaction $\tilde{R}(\mathbf{q})$ also exhibits \mathcal{S} symmetry, and can thus be written as

$$\tilde{R}(\mathbf{q}) = \sum_{i=1}^5 \tilde{w}_i(\mathbf{q}) W_i(\mathbf{q}), \quad (116)$$

where the renormalized couplings $\tilde{w}_i(\mathbf{q})$ read

$$\tilde{w}_1(\mathbf{q}) = \frac{w_1}{1 + w_1 \pi_1(\mathbf{q})}, \quad \tilde{w}_2(\mathbf{q}) = \frac{w_2}{1 + w_2 \pi_2(\mathbf{q})}, \quad (117)$$

$$\begin{pmatrix} \tilde{w}_3(\mathbf{q}) & \tilde{w}_4(\mathbf{q}) \\ \tilde{w}_4(\mathbf{q}) & \tilde{w}_5(\mathbf{q}) \end{pmatrix} = \begin{pmatrix} w_3 & w_4 \\ w_4 & w_5 \end{pmatrix} \left(\begin{pmatrix} 1 & 0 \\ 0 & 1 \end{pmatrix} + \begin{pmatrix} \pi_3(\mathbf{q}) & \pi_4(\mathbf{q}) \\ \pi_4(\mathbf{q}) & \pi_5(\mathbf{q}) \end{pmatrix} \begin{pmatrix} w_3 & w_4 \\ w_4 & w_5 \end{pmatrix} \right)^{-1}. \quad (118)$$

Note that in this section we denote with $\tilde{w}_i(\mathbf{q})$ the renormalized couplings. Substituting the form (116) in (112) we obtain

$$\sigma(\mathbf{k}) = \frac{2}{d} \sum_{i=1,5} \int_q \tilde{w}_i(\mathbf{q}) \mathcal{G}(\mathbf{k} - \mathbf{q}) k_\alpha (k_\beta - q_\beta) (W_i)_{\alpha\beta,\gamma\delta}(\mathbf{q}) k_\gamma (k_\delta - q_\delta), \quad (119)$$

which allows us to obtain $\kappa_R(\mathbf{q})$ (after the subtraction of the k^2 term). The above equations form a closed set of SCSA equations for the five renormalized elastic coupling constants, together with the renormalized bending rigidity.

B. Analysis and results

We now analyze the SCSA equations for the crumpling transition, following closely the analysis in the previous section for the flat phase. To solve these equations at the critical point, we use the long wavelength form of the

critical propagator, $\mathcal{G}(\mathbf{k}) = Z_\kappa^{-1}/k^{4-\eta}$. The $\pi_i(\mathbf{q})$ are integrals similar to the ones studied for the flat phase, and are calculated in the Appendix C. They diverge for small q as:

$$\pi_i(\mathbf{q}) \simeq Z_\kappa^{-2} a_i(\eta, D) q^{-(4-D-2\eta)}. \quad (120)$$

For the amplitudes $a_i(\eta, D)$ we find

$$\begin{aligned} a_1 &= 2A, \quad a_2 = A \frac{2(2-\eta)}{D+\eta-2}, \quad a_3 = A(D+1), \quad a_4 = A\sqrt{D-1}(D+2\eta-3), \\ a_5 &= \frac{A}{D-2+\eta}(-22+31D-10D^2+D^3+43\eta-32D\eta+5D^2\eta-24\eta^2+8D\eta^2+4\eta^3), \end{aligned} \quad (121)$$

with

$$A = \frac{\Pi(\eta, D)}{D^2-1}, \quad (122)$$

where the “polarization bubble” integral, $\Pi(\eta, D)$ is defined in (72),(73) and derived in Appendix B.

To compute the self-energy we define the amplitudes $b_i(\eta, D)$ through:

$$\int_q q^{4-D-2\eta} |\mathbf{k}-\mathbf{q}|^{-(4-\eta)} k_\alpha(k_\beta-q_\beta) (W_i)_{\alpha\beta,\gamma\delta}(\mathbf{q}) k_\gamma(k_\delta-q_\delta) = b_i(\eta, D) k^{4-\eta}. \quad (123)$$

The explicit calculation in the Appendix C gives

$$\begin{aligned} b_1 &= B(D-2)(D+1), \quad b_2 = -B \frac{(D-1)(D^2-4+2\eta)}{D-2+\eta}, \quad b_3 = B(D+1), \\ b_4 &= 2B\sqrt{D-1}(2\eta-3), \quad b_5 = \frac{B}{D-2+\eta}(-22+15D-2D^2+43\eta-16D\eta-24\eta^2+4D\eta^2+4\eta^3), \end{aligned} \quad (124)$$

where

$$B = \frac{\Sigma(\eta, D)}{D^2-1}, \quad (125)$$

with $\Sigma(\eta, D)$ defined in (78),(79) and derived in Appendix B.

In the limit $\mathbf{q} \rightarrow 0$ we find

$$\tilde{w}_1(\mathbf{q}) \simeq \frac{1}{\pi_1(\mathbf{q})}, \quad \tilde{w}_2(\mathbf{q}) \simeq \frac{1}{\pi_2(\mathbf{q})}, \quad (126)$$

$$\begin{pmatrix} \tilde{w}_3(\mathbf{q}) & \tilde{w}_4(\mathbf{q}) \\ \tilde{w}_4(\mathbf{q}) & \tilde{w}_5(\mathbf{q}) \end{pmatrix} \simeq \begin{pmatrix} \pi_3(\mathbf{q}) & \pi_4(\mathbf{q}) \\ \pi_4(\mathbf{q}) & \pi_5(\mathbf{q}) \end{pmatrix}^{-1}. \quad (127)$$

Substituting Eqs.(118),(122),(125) into (119) we see that factors of Z_κ cancel and we find the self-consistent equation:

$$\frac{d}{2} = \sum_{i=1,2} \frac{b_i(\eta, D)}{a_i(\eta, D)} + \frac{b_3(\eta, D)a_5(\eta, D) - b_4(\eta, D)a_4(\eta, D) + b_5(\eta, D)a_3(\eta, D)}{a_3(\eta, D)a_5(\eta, D) - a_4(\eta, D)^2}. \quad (128)$$

Putting everything together, after considerable simplifications, the equation determining the crumpling transition exponent $\eta = \eta_{cr}(D, d)$ is found to be:

$$d = \frac{D(D+1)(D-4+\eta)(D-4+2\eta)(2D-3+2\eta)\Gamma[\frac{1}{2}\eta]\Gamma[2-\eta]\Gamma[\eta+D]\Gamma[2-\frac{1}{2}\eta]}{2(2-\eta)(5-D-2\eta)(D+\eta-1)\Gamma[\frac{1}{2}D+\frac{1}{2}\eta]\Gamma[2-\eta-\frac{1}{2}D]\Gamma[\eta+\frac{1}{2}D]\Gamma[\frac{1}{2}D+2-\frac{1}{2}\eta]}, \quad (129)$$

which in $D=2$ reduces to finding the root of a cubic equation

$$d = \frac{24(\eta-1)^2(2\eta+1)}{(\eta-4)\eta(2\eta-3)}. \quad (130)$$

For $d=3$ and $D=2$ we find

$$\eta_{cr}(2, 3) = 0.5352.. \quad (131)$$

At the crumpling transition the radius of gyration of the membrane scales as

$$\langle (\vec{r}(L) - \vec{r}(0))^2 \rangle = R_G^2 \quad , \quad R_G \sim L^{\nu_G} \quad , \quad \nu_G = \frac{4 - D - \eta_{cr}}{2} \quad , \quad (132)$$

which leads for $d = 3$, $D = 2$ to the radius of gyration exponent and the Hausdorff dimension, respectively,

$$\nu_G = 0.7324 \quad , \quad d_H = D/\nu_G = 2.7308. \quad (133)$$

To compare our prediction with the result of the $1/d$ -expansion we expand it to lowest order in $1/d$,

$$\begin{aligned} \eta_{cr}(D, d) &\simeq \frac{C(D)}{d} + O(1/d^2) \quad , \quad \text{where} \\ C(D) &= \frac{(D-4)^2(2D-3)\Gamma(D+2)}{2(5-D)(D-1)\Gamma(2-\frac{D}{2})\Gamma(\frac{D}{2}+2)\Gamma(\frac{D}{2})^2} \quad , \end{aligned} \quad (134)$$

which can be shown to coincide with that of Ref. 8. We can also expand our SCSA prediction in $\epsilon = 4 - D$, finding

$$\eta_{cr}(D, d) \simeq \frac{25}{3d}(4-D)^3 + O((4-D)^3), \quad (135)$$

though it cannot be checked against a previous ϵ -expansion as η_{cr} was neglected in Ref. 43, consistent with its vanishing to $O(\epsilon)$.

It is also interesting to determine the embedding dimension $d_u(D)$ above which self-avoidance is *irrelevant* for the membrane *at* the crumpling transition. The self-avoiding membrane interaction, that we have so far neglected, is proportional to $\int d^D x d^D x' \delta^{(d)}(\vec{r}(x) - \vec{r}(x'))$. Hence by power counting it scales as $L^{2D-d\nu_G}$ with membrane's internal dimension L . It is thus expected to be irrelevant when

$$d > 2D/\nu_G = 4D/(4-D-\eta_{cr}(D, d)) \quad \Leftrightarrow \quad \text{self-avoidance irrelevant.} \quad (136)$$

Solving this equation, using (130), for $D = 2$ amounts to solving the following equation for η :

$$d_u(2) = \frac{8}{2-\eta} = \frac{24(\eta-1)^2(2\eta+1)}{(\eta-4)\eta(2\eta-3)}. \quad (137)$$

There are four roots with only physical one given by $\eta = 0.3956$. Hence we find

$$d_u(2) = 4.986. \quad (138)$$

This shows that for a physical membrane, $d = 3$, self-avoidance is *relevant* at the crumpling transition. Indeed the scaling dimension of the self-avoiding interaction of a physical membrane is $2D - d\nu_G = 4 - 3\nu_G = 1.803$, namely, strongly relevant at long scales.

One can also obtain the lower-critical dimension $D_{lc,cr}(d)$ for the crumpling transition, defined by $2 - \eta(D_{lc,cr}, d) = D_{lc,cr}$, when the correction to the critical temperature is driven to negative infinity. From (129) we find the equation $d = D_{lc,cr}/(2 - D_{lc,cr})$, or, equivalently, $D_{lc,cr}(d) = 2d/(1+d)$. Since $d = D/(2-D)$ is equivalent to $d_c = D(D-1)/(2-D)$ we find that the lower-critical dimensions of both the crumpling transition and the flat phase (see (90)) fixed points are identical. Although originating from an approximation on different theories, and resulting from a priori very different calculations, we find $D_{lc}(d_c + D_{lc}(d_c)) = D_{lc}(d_c)$, for arbitrary d_c , which shows that the SCSA is quite consistent.

To first order in ϵ from the above result, (122), neglecting $\eta = O(\epsilon^3)$, we find

$$a_1 = a_2 = 2A \quad , \quad a_3 = 5A \quad , \quad a_4 = \sqrt{3}A \quad , \quad a_5 = 3A \quad , \quad (139)$$

where

$$A = \frac{1}{192\pi^2\epsilon}. \quad (140)$$

Using expression (120) for $\pi_i(\mathbf{q}) \sim a_i$ and (127) we see that to this order, near $D = 4$,

$$\tilde{w}_1(\mathbf{q}) \simeq \tilde{w}_2(\mathbf{q}) \simeq \frac{Z_\kappa^2 q^{\epsilon-2\eta}}{2A} \quad (141)$$

$$\begin{pmatrix} \tilde{w}_3(\mathbf{q}) & \tilde{w}_4(\mathbf{q}) \\ \tilde{w}_4(\mathbf{q}) & \tilde{w}_5(\mathbf{q}) \end{pmatrix} \simeq \frac{Z_\kappa^2 q^{\epsilon-2\eta}}{A} \begin{pmatrix} \frac{1}{4} & -\frac{1}{4\sqrt{3}} \\ -\frac{1}{4\sqrt{3}} & \frac{5}{12} \end{pmatrix}. \quad (142)$$

Remarkably, comparing with (111), or equivalently computing $\tilde{R}(\mathbf{q})$ in (116) we see that (to this lowest order in ϵ) the renormalized vertex recovers the tensor structure in (103), parameterizable by only two renormalized Lamé moduli (as in the bare theory with local elasticity), with

$$\tilde{\mu}_0(\mathbf{q}) = 96\pi^2 \epsilon Z_\kappa^2 q^{\epsilon-2\eta} = -3\tilde{\lambda}_0(\mathbf{q}). \quad (143)$$

These renormalized moduli agree *exactly* with those derived from the $d \rightarrow \infty$ limit of the fixed-point couplings at the crumpling transition critical point, studied to lowest-order in ϵ -expansion in Ref. 43 (after a correction to their constant K_4 , taking it to be $S_4/(2\pi)^4 = 1/(8\pi^2)$ rather than $1/(2\pi^2)$). However, in contrast to this ϵ -expansion (valid near $D = 4$), that found a fluctuation-driven first-order transition when extended to a physical membrane ($D = 2$ and $d = 3 < 219$), our SCSA analysis predicts a continuous crumpling transition, that survives in a physical membrane, as in other applications of SCSA.[84]

Based on the above ratio of the renormalized long wavelength moduli $\tilde{\lambda}_0(\mathbf{q})/\tilde{\mu}_0(\mathbf{q}) \simeq -1/3$, (found to hold to leading order in ϵ in the limit of large d) we predict a negative universal Poisson ratio at the crumpling transition of a phantom membrane near the upper critical dimension

$$\tilde{\sigma}_c(\mathbf{q}) = \frac{\tilde{\lambda}_0(\mathbf{q})}{2\tilde{\mu}_0(\mathbf{q}) + \tilde{\lambda}_0(\mathbf{q})} \Big|_{D \simeq 4, d \rightarrow +\infty} = -\frac{1}{5}. \quad (144)$$

V. FLAT PHASE OF AN ELASTIC MEMBRANE WITH QUENCHED DISORDER

We now turn our study to a flat phase of a heterogeneous elastic membrane. Motivated by the quantitative success of the SCSA when applied to a disorder-free homogeneous membrane, here we extend this calculation method to a treatment of a membrane with quenched disorder. This will complement earlier studies of Ref.[26, 28] using the renormalization group, controlled by an ϵ -expansion.

A. Effective flat-phase model of a heterogeneous elastic membrane

We recall the model of a disordered membrane introduced in Section II C. It is defined by free energy Eq.(24)

$$\mathcal{F}[\vec{h}, u_\alpha] = \int d^D x \left[\frac{1}{2} \kappa (\partial^2 \vec{h})^2 + \mu (u_{\alpha\beta})^2 + \frac{1}{2} \lambda (u_{\alpha\alpha})^2 - \kappa \partial^2 \vec{h} \cdot \vec{f}(\mathbf{x}) - 2\mu u_{\alpha\beta} c_{\alpha\beta}(\mathbf{x}) - \lambda u_{\alpha\alpha} c_{\beta\beta}(\mathbf{x}) \right], \quad (145)$$

with random zero-mean Gaussian stress and curvature disorder, fully characterized by the correlators Eq.(25)

$$\overline{c_{\alpha\beta}(\mathbf{x}) c_{\gamma\delta}(\mathbf{x}')} = \hat{\Delta}_\lambda(\mathbf{x} - \mathbf{x}') \delta_{\alpha\beta} \delta_{\gamma\delta} + \hat{\Delta}_\mu(\mathbf{x} - \mathbf{x}') (\delta_{\alpha\gamma} \delta_{\beta\delta} + \delta_{\alpha\delta} \delta_{\beta\gamma}), \quad (146)$$

$$\overline{f_i(\mathbf{x}) f_j(\mathbf{x}')} = \delta_{ij} \hat{\Delta}_\kappa(\mathbf{x} - \mathbf{x}'). \quad (147)$$

As for the homogeneous membrane in Sec.III it is useful to integrate out the in-plane phonon degrees of freedom $u_\alpha(\mathbf{x})$, that can be done exactly as they appear only linearly and quadratically in the free energy above. We thereby obtain the extension of the effective free energy in Eq.(41) to disordered membranes

$$\mathcal{F}[\vec{h}] = \int d^D x \left\{ \frac{1}{2} \kappa (\partial^2 \vec{h})^2 + \frac{1}{4} \left[\mu \left(P_{\alpha\delta}^T \partial_\alpha \vec{h} \cdot \partial_\beta \vec{h} \right) \left(P_{\beta\gamma}^T \partial_\gamma \vec{h} \cdot \partial_\delta \vec{h} \right) + \frac{\mu\lambda}{2\mu + \lambda} \left(P_{\alpha\beta}^T \partial_\alpha \vec{h} \cdot \partial_\beta \vec{h} \right)^2 \right] \right\}, \quad (148)$$

$$- \kappa \partial^2 \vec{h} \cdot \vec{f}(\mathbf{x}) - \left[\mu \left(P_{\alpha\delta}^T \partial_\alpha \vec{h} \cdot \partial_\beta \vec{h} \right) \left(P_{\beta\gamma}^T c_{\gamma\delta}(\mathbf{x}) \right) + \frac{\mu\lambda}{2\mu + \lambda} \left(P_{\alpha\beta}^T \partial_\alpha \vec{h} \cdot \partial_\beta \vec{h} \right) \left(P_{\gamma\delta}^T c_{\gamma\delta}(\mathbf{x}) \right) \right] \Bigg\}. \quad (149)$$

A system with quenched disorder is characterized by a distribution function of physical observables. Averages of an observable over possible realizations of disorder will be very close to its typical value if the corresponding distribution function is narrowly distributed. It turns out that the distribution function for the free energy density has a vanishing variance in the thermodynamic limit, while the partition function \mathcal{Z} is widely distributed. Therefore in a quenched disordered system, like the membrane considered here, the average and also sample representative, typical free energy is given by

$$F = -T \ln \overline{\mathcal{Z}[\vec{f}(\mathbf{x}), c_{\alpha\beta}(\mathbf{x})]}, \quad (150)$$

rather than by a logarithm of the disorder-average of the partition function $\ln \bar{\mathcal{Z}}$, as it would be for an annealed form of disorder. In above equations the overbar denotes the average over disorder realizations. The difficulty in computing the average of $\ln \mathcal{Z}$ can be handled in the standard way using the replica ‘trick’ [85] (although there are alternative methods [27]). Using the identity

$$\ln \mathcal{Z} = \lim_{n \rightarrow 0} \frac{\mathcal{Z}^n - 1}{n}, \quad (151)$$

and assuming the validity of the interchange of the thermodynamic and $n \rightarrow 0$ limits, we reduce a difficult average over a logarithm into an average of an n -replicated theory represented by \mathcal{Z}^n . In the replicated theory described by n height fields $\vec{h}_a(\mathbf{x})$, ($a = 1, 2, \dots, n$), the effective averages over disorder fields $\vec{f}(\mathbf{x})$ and $c_{\alpha\beta}(\mathbf{x})$ (which couple linearly) can now be easily performed. The effective replicated free energy takes the form of a critical (massless) $O(d_c) \times O(N)$ symmetric theory, with a nonlocal, tensor quartic interaction, generalizing Eq.(43) to a disordered membrane[1, 26]

$$\mathcal{F}_{eff}^r[\vec{h}_\alpha(\mathbf{k})] = \frac{1}{2} \int_k \kappa_{ab}(\mathbf{k}) k^4 \vec{h}_\alpha^a(\mathbf{k}) \cdot \vec{h}_\beta^b(-\mathbf{k}) + \frac{1}{4d_c} \int_{k_1, k_2, k_3} R_{\alpha\beta, \gamma\delta}^{ab}(\mathbf{q}) k_{1\alpha} k_{2\beta} k_{3\gamma} k_{4\delta} \vec{h}_a(\mathbf{k}_1) \cdot \vec{h}_a(\mathbf{k}_2) \vec{h}_b(\mathbf{k}_3) \cdot \vec{h}_b(\mathbf{k}_4), \quad (152)$$

with $\mathbf{q} = \mathbf{k}_1 + \mathbf{k}_2$ and $\mathbf{k}_1 + \mathbf{k}_2 + \mathbf{k}_3 + \mathbf{k}_4 = \mathbf{0}$, and sum over repeated indices is implied throughout. As in the pure case we have rescaled uniformly by a factor $1/d_c$ all quartic terms (which is immaterial for $d_c = 1$) in order to obtain a well defined large d_c limit. Let us now describe the different terms in (152). For convenience we define

$$\Delta_\kappa(\mathbf{q}) = \kappa^2 \hat{\Delta}_\kappa(\mathbf{q}) \quad , \quad \Delta_\mu(\mathbf{q}) = 4\mu^2 \hat{\Delta}_\mu(\mathbf{q}) \quad , \quad \Delta_\lambda(\mathbf{q}) = 4\mu^2 \hat{\Delta}_\lambda(\mathbf{q}). \quad (153)$$

The replica matrix $\kappa_{ab}(\mathbf{k})$ is the bending rigidity analog in the replicated theory and has the form,

$$\kappa_{ab}(\mathbf{k}) = \kappa \delta_{ab} - \frac{\Delta_\kappa(\mathbf{k})}{T} J_{ab}, \quad (154)$$

where J_{ab} is an $n \times n$ matrix with all entries equal to 1. Here we will only be interested in the replica symmetric solutions, with all correlators invariant under permutation of replica indices. In this subspace all the replica matrices can be represented as a two component supervector, with the first and second component being the coefficients of δ_{ab} and J_{ab} , respectively. In this notation

$$\kappa_{ab}(\mathbf{k}) = \left(\kappa, -\frac{\Delta_\kappa(\mathbf{k})}{T} \right). \quad (155)$$

Using the definition in terms of the original matrices in replica space, the replica matrix product $u_{ab}u_{bc}$ and the replica matrix inversion in the new vector space is easily defined and in the $n \rightarrow 0$ limit is given by,

$$u_{ad}v_{db} = (u_c, u)(v_c, v) = (u_c v_c, uv_c + u_c v), \quad (156)$$

$$(u^{-1})_{ab} = (u_c, u)^{-1} = (1/u_c, -u/u_c^2). \quad (157)$$

The bare four-point coupling tensor $R_{\alpha\beta, \gamma\delta}^{ab}(\mathbf{q})$ is an n -replica generalization of the quartic interaction of the pure membrane, Eq.(44) to the disordered case,

$$R_{\alpha\beta, \gamma\delta}^{ab}(\mathbf{q}) = \frac{1}{2} \mu_{ab}(\mathbf{q}) (P_{\alpha\gamma}^T(\mathbf{q}) P_{\beta\delta}^T(\mathbf{q}) + P_{\alpha\delta}^T(\mathbf{q}) P_{\beta\gamma}^T(\mathbf{q})) + \rho_{ab}(\mathbf{q}) P_{\alpha\beta}^T(\mathbf{q}) P_{\gamma\delta}^T(\mathbf{q}), \quad (158)$$

where in our notation the replicated elastic moduli tensors are

$$\mu_{ab}(\mathbf{q}) = \left(\mu, -\frac{1}{T} \Delta_\mu(\mathbf{q}) \right), \quad (159)$$

$$\rho_{ab}(\mathbf{q}) = \left(\frac{\mu\lambda}{2\mu + \lambda}, -\frac{\lambda(4\mu + (D+1)\lambda)}{T(2\mu + \lambda)^2} \Delta_\mu(\mathbf{q}) - \frac{1}{2T} \left(\frac{2\mu + D\lambda}{2\mu + \lambda} \right)^2 \Delta_\lambda(\mathbf{q}) \right). \quad (160)$$

B. The SCSA equations for the heterogeneous membrane

We next present the SCSA equations for the flat phase of an elastic membrane with quenched internal disorder using the effective replicated free energy $\mathcal{F}_{eff}^r[\vec{h}_\alpha(\mathbf{k})]$, (152), derived above. As for the disorder-free case it is more

convenient to work in the orthogonal representation of tensors $M_{\alpha\beta,\gamma\delta}(\mathbf{q})$ and $N_{\alpha\beta,\gamma\delta}(\mathbf{q})$ defined in Eq.(47). In terms of these the quartic interaction becomes,

$$R_{\alpha\beta,\gamma\delta}^{ab}(\mathbf{q}) = \mu_{ab}M_{\alpha\beta,\gamma\delta}(\mathbf{q}) + b_{ab}N_{\alpha\beta,\gamma\delta}(\mathbf{q}) , \quad (161)$$

where,

$$\mu_{ab}(\mathbf{q}) = \left(\mu , -\frac{1}{T}\Delta_\mu(\mathbf{q}) \right) , \quad (162)$$

$$b_{ab}(\mathbf{q}) = \left(b , -\frac{1}{T}\Delta_b(\mathbf{q}) \right) , \quad (163)$$

$$= \left(\frac{\mu(2\mu + D\lambda)}{2\mu + \lambda} , -\frac{1}{2T} \left(\frac{2\mu + D\lambda}{2\mu + \lambda} \right)^2 [2\Delta_\mu(\mathbf{q}) + (D-1)\Delta_\lambda(\mathbf{q})] \right) , \quad (164)$$

which defines $\Delta_b(\mathbf{q}) := \frac{1}{2} \left(\frac{2\mu + D\lambda}{2\mu + \lambda} \right)^2 (2\Delta_\mu(\mathbf{q}) + (D-1)\Delta_\lambda(\mathbf{q}))$.

As described in Sec. II C the roughness of the membrane in the flat phase is determined by two correlation functions of the height-field, $\vec{h}(\mathbf{k})$,

$$\overline{\langle h^i(\mathbf{k})h^j(\mathbf{k}') \rangle} - \overline{\langle h^i(\mathbf{k}) \rangle} \overline{\langle h^j(\mathbf{k}') \rangle} = G_\kappa(\mathbf{k})\delta_{ij}(2\pi)^D\delta^{(D)}(\mathbf{k} + \mathbf{k}') , \quad (165)$$

$$\overline{\langle h^i(\mathbf{k}) \rangle} \overline{\langle h^j(\mathbf{k}') \rangle} = G_\Delta(\mathbf{k})\delta_{ij}(2\pi)^D\delta^{(D)}(\mathbf{k} + \mathbf{k}') , \quad (166)$$

where the first connected correlation function describes thermal roughness and the thermally disconnected piece corresponds to zero temperature roughness due to disorder. It is easy to show that in the replicated theory in our notation the two components of the replicated correlator

$$\lim_{n \rightarrow 0} \langle h_a^i(\mathbf{k})h_b^j(\mathbf{k}') \rangle = G_{ab}(\mathbf{k})\delta_{ij}(2\pi)^D\delta^{(D)}(\mathbf{k} + \mathbf{k}') , \quad (167)$$

$$= (G_\kappa(\mathbf{k}) , G_\Delta(\mathbf{k}))\delta_{ij}(2\pi)^D\delta^{(D)}(\mathbf{k} + \mathbf{k}') , \quad (168)$$

correspond to the correlators defined in Eqs.(165),(166). For these correlators one can define the renormalized bending rigidity $\tilde{\kappa}(\mathbf{k})$ and renormalized curvature disorder $\tilde{\Delta}_\kappa(\mathbf{k})$ as follows

$$G_\kappa(\mathbf{k}) = \frac{T}{\tilde{\kappa}(\mathbf{k})k^4} , \quad G_\Delta(\mathbf{k}) = \frac{\tilde{\Delta}_\kappa(\mathbf{k})}{\tilde{\kappa}(\mathbf{k})^2k^4} . \quad (169)$$

For notational convenience, in this Section and the next two, we will denote the renormalized parameters (obtained from SCSA) with a tilde, instead of the subscript R as in the previous sections, but these denote the same quantities, e.g., $\tilde{\kappa}(\mathbf{q}) = \kappa_R(\mathbf{q})$.

To study the physics of the flat phase of a disordered membrane we set up two coupled tensor integral equations for the renormalized propagator $G_{ab}(\mathbf{k})$ and the renormalized four point interaction $\tilde{R}_{\alpha\beta,\gamma\delta}^{ab}(q)$, generalizing the SCSA method to the replicated theory. The $1/d_c$ -expansion for the quartic vertex and two-point height correlator, when made self-consistent, gives

$$T(G^{-1})_{ab}(\mathbf{k}) = \kappa_{ab}(\mathbf{k})k^4 + \frac{2}{d_c}k_\alpha k_\beta k_\gamma k_\delta \int_q \tilde{R}_{\alpha\beta,\gamma\delta}^{ab}(\mathbf{q})G_{ab}(\mathbf{k} - \mathbf{q}) , \quad (170)$$

$$\tilde{R}_{\alpha\beta,\gamma\delta}^{ab}(\mathbf{q}) = R_{\alpha\beta,\gamma\delta}^{ab}(\mathbf{q}) - R_{\alpha\beta,\gamma_1\gamma_2}^{ac}(\mathbf{q})\hat{\Pi}_{\gamma_1\gamma_2,\gamma_3\gamma_4}^{cd}(\mathbf{q})\tilde{R}_{\gamma_3\gamma_4,\gamma\delta}^{db}(\mathbf{q}) , \quad (171)$$

where we have defined the replicated polarization bubble matrix

$$\hat{\Pi}_{\alpha\beta,\gamma\delta}^{ab}(\mathbf{q}) = \frac{1}{T} \int_p p_\alpha p_\beta p_\gamma p_\delta G_{ab}(\mathbf{p})G_{ab}(\mathbf{q} - \mathbf{p}) , \quad (172)$$

which in our compact two component notation reads

$$\left(\Pi_1^{\alpha\beta,\gamma\delta}(\mathbf{q}) , \Pi_2^{\alpha\beta,\gamma\delta}(\mathbf{q}) \right) = \frac{1}{T} \int_p p_\alpha p_\beta p_\gamma p_\delta (G_\kappa(\mathbf{p})G_\kappa(\mathbf{q} - \mathbf{p}) + G_\kappa(\mathbf{p})G_\Delta(\mathbf{q} - \mathbf{p}) \quad (173)$$

$$+ G_\kappa(\mathbf{q} - \mathbf{p})G_\Delta(\mathbf{p}) , G_\Delta(\mathbf{p})G_\Delta(\mathbf{q} - \mathbf{p})) , \quad (174)$$

Note that the sum over repeated indices is implied except for the equation (172) for $\hat{\Pi}_{\alpha\beta,\gamma\delta}^{ab}(\mathbf{q})$, where indices a, b are not summed.

As for the homogeneous membrane, $\hat{\Pi}_{\alpha\beta,\gamma\delta}^{ab}(\mathbf{q})$ has a following tensor structure (see Appendix A, for more details)

$$\hat{\Pi}_{\alpha\beta,\gamma\delta}^{ab}(\mathbf{q}) = \hat{\Pi}_{ab}^{sym}(\mathbf{q}) S_{\alpha\beta,\gamma\delta} + \hat{\Pi}_{ab}^{long1}(\mathbf{q}) (\delta_{\alpha\beta} q_\gamma q_\delta + \delta_{\gamma\delta} q_\alpha q_\beta) + \hat{\Pi}_{ab}^{long2}(\mathbf{q}) q_\alpha q_\beta q_\gamma q_\delta, \quad (175)$$

where

$$S_{\alpha\beta,\gamma\delta} = \delta_{\alpha\beta} \delta_{\gamma\delta} + \delta_{\alpha\gamma} \delta_{\beta\delta} + \delta_{\alpha\delta} \delta_{\beta\gamma} \quad (176)$$

is a fully symmetric tensor previously defined. Because the quartic interaction is a transverse projector in indices $\alpha, \beta, \gamma, \delta$ upon tensor multiplication in Eq.(171) only the symmetric part of $\hat{\Pi}_{\alpha\beta,\gamma\delta}^{ab}(\mathbf{q})$ survives

$$\hat{\Pi}_{ab}^{sym}(\mathbf{q}) = (\Pi_1^{sym}(\mathbf{q}), \Pi_2^{sym}(\mathbf{q})), \quad (177)$$

$$= (T\Pi_{\kappa\kappa}(\mathbf{q}) + 2\Pi_{\kappa\Delta}(\mathbf{q}), \frac{1}{T}\Pi_{\Delta\Delta}(\mathbf{q})), \quad (178)$$

where we have defined the integrals

$$\Pi_{nm}(\mathbf{q}) = \frac{1}{(D^2 - 1)T^{a_{n,m}}} \int_p (p_\alpha P_{\alpha\beta}^T(\mathbf{q}) p_\beta)^2 G_n(\mathbf{p}) G_m(\mathbf{q} - \mathbf{p}), \quad (179)$$

with $n, m = \kappa, \Delta$ and the $a_{n,m}$ are chosen as $a_{\kappa,\kappa} = 2$, $a_{\Delta,\kappa} = a_{\kappa,\Delta} = 1$ and $a_{\Delta,\Delta} = 0$, so that the $\Pi_{nm}(\mathbf{q})$ have well defined $T = 0$ limits.

Using the above results together with the orthogonality property of tensors $M_{\alpha\beta,\gamma\delta}(\mathbf{q})$ and $N_{\alpha\beta,\gamma\delta}(\mathbf{q})$ from which the quartic vertex is composed, we find again that the renormalized interaction can be written as

$$\tilde{R}_{\alpha\beta,\gamma\delta}^{ab}(\mathbf{q}) = \tilde{\mu}_{ab}(\mathbf{q}) M_{\alpha\beta,\gamma\delta}(\mathbf{q}) + \tilde{b}_{ab}(\mathbf{q}) N_{\alpha\beta,\gamma\delta}(\mathbf{q}), \quad (180)$$

where

$$\tilde{\mu}_{ab}(\mathbf{q}) = \left(\tilde{\mu}(\mathbf{q}), -\frac{1}{T} \tilde{\Delta}_\mu(\mathbf{q}) \right), \quad (181)$$

$$\tilde{b}_{ab}(\mathbf{q}) = \left(\tilde{b}(\mathbf{q}), -\frac{1}{T} \tilde{\Delta}_b(\mathbf{q}) \right), \quad (182)$$

and $\tilde{\mu}(\mathbf{q})$ and $\tilde{b}(\mathbf{q})$ are the renormalized shear and bulk moduli (denoted by $\mu_R(\mathbf{q})$ and $b_R(\mathbf{q})$ in the previous sections) and $\tilde{\Delta}_\mu(\mathbf{q})$ and $\tilde{\Delta}_b(\mathbf{q})$ are the associated renormalized disorder variances. To determine these renormalized couplings we note that the tensor equation (171) is then equivalent to two independent replica matrix equations for $\tilde{\mu}_{ab}(\mathbf{q})$ and $\tilde{b}_{ab}(\mathbf{q})$

$$\tilde{\mu}_{ab}(\mathbf{q}) = \left(\hat{1} + 2 \hat{\mu}(\mathbf{q}) \cdot \hat{\Pi}^{sym}(\mathbf{q}) \right)_{ac}^{-1} \mu_{cb}, \quad (183)$$

$$\tilde{b}_{ab}(\mathbf{q}) = \left(\hat{1} + (D + 1) \hat{b}(\mathbf{q}) \cdot \hat{\Pi}^{sym}(\mathbf{q}) \right)_{ac}^{-1} b_{cb}, \quad (184)$$

where the hat denotes replica matrices, and replica matrix multiplication and inversion are implied.

We now use the multiplication and inversion rules that hold within our replica symmetric subspace, Eq.(156), to further reduce the above two matrix equations to four scalar equations for $\tilde{\mu}(\mathbf{q})$, $\tilde{b}(\mathbf{q})$, $\tilde{\Delta}_\mu(\mathbf{q})$ and $\tilde{\Delta}_b(\mathbf{q})$ (whose bare

values are defined in Eq.(162)). Beginning with $\tilde{\mu}_{ab}(\mathbf{q})$ we obtain

$$\tilde{\mu}_{ab}(\mathbf{q}) = \left(\tilde{\mu}(\mathbf{q}), -\frac{1}{T} \tilde{\Delta}_\mu(\mathbf{q}) \right), \quad (185)$$

$$= \left(1 + 2\mu \Pi_1^{sym}(\mathbf{q}), 2\mu \Pi_2^{sym}(\mathbf{q}) - \frac{2}{T} \Delta_\mu(\mathbf{q}) \Pi_1^{sym}(\mathbf{q}) \right)^{-1} \cdot \left(\mu, -\frac{1}{T} \Delta_\mu(\mathbf{q}) \right), \quad (186)$$

$$= \left(\frac{1}{1 + 2\mu \Pi_1^{sym}(\mathbf{q})}, -\frac{2\mu \Pi_2^{sym}(\mathbf{q}) - \frac{2}{T} \Delta_\mu(\mathbf{q}) \Pi_1^{sym}(\mathbf{q})}{(1 + 2\mu \Pi_1^{sym}(\mathbf{q}))^2} \right) \cdot \left(\mu, -\frac{1}{T} \Delta_\mu(\mathbf{q}) \right), \quad (187)$$

$$= \left(\frac{\mu}{1 + 2\mu \Pi_1^{sym}(\mathbf{q})}, -\frac{\frac{1}{T} \Delta_\mu}{1 + 2\mu \Pi_1^{sym}(\mathbf{q})} - \frac{2\mu^2 \Pi_2^{sym}(\mathbf{q}) - 2\mu \frac{1}{T} \Delta_\mu(\mathbf{q}) \Pi_1^{sym}(\mathbf{q})}{(1 + 2\mu \Pi_1^{sym}(\mathbf{q}))^2} \right), \quad (188)$$

$$= \left(\frac{\mu}{1 + 2\mu [T\Pi_{\kappa\kappa}(\mathbf{q}) + 2\Pi_{\kappa\Delta}(\mathbf{q})]}, -\frac{1}{T} \frac{\Delta_\mu + 2\mu^2 T\Pi_{\Delta\Delta}(\mathbf{q})}{(1 + 2\mu [T\Pi_{\kappa\kappa}(\mathbf{q}) + 2\Pi_{\kappa\Delta}(\mathbf{q})])^2} \right). \quad (189)$$

Identical manipulations give,

$$\tilde{b}_{ab}(\mathbf{q}) = \left(\tilde{b}(\mathbf{q}), -\frac{1}{T} \tilde{\Delta}_b(\mathbf{q}) \right), \quad (190)$$

$$= \left(\frac{b}{1 + (D+1)b [T\Pi_{\kappa\kappa}(\mathbf{q}) + 2\Pi_{\kappa\Delta}(\mathbf{q})]}, -\frac{1}{T} \frac{\Delta_b + (D+1)b^2 \Pi_{\Delta\Delta}(\mathbf{q})}{(1 + (D+1)b [T\Pi_{\kappa\kappa}(\mathbf{q}) + 2\Pi_{\kappa\Delta}(\mathbf{q})])^2} \right). \quad (191)$$

Having determined the renormalized four-point coupling constants we turn to Eq.(170) to determine the two components of the propagator, $G_\kappa(\mathbf{k})$ and $G_\Delta(\mathbf{k})$, which will in turn determine the roughness exponents ζ and ζ' , respectively. Using the index permutation symmetry of the tensor $k_\alpha k_\beta k_\gamma k_\delta$ and the definition of $\tilde{R}_{\alpha\beta,\gamma\delta}^{ab}(\mathbf{q})$ in terms of $\tilde{\mu}_{ab}(\mathbf{q})$ and $\tilde{b}_{ab}(\mathbf{q})$ inside the second term on the right-hand side of Eq.(170), we find,

$$k_\alpha k_\beta k_\gamma k_\delta \tilde{R}_{\alpha\beta,\gamma\delta}^{ab}(\mathbf{q}) = (k_\alpha P_{\alpha\beta}^T(\mathbf{q}) k_\beta)^2 \left[\frac{D-2}{D-1} \tilde{\mu}_{ab}(\mathbf{q}) + \frac{1}{D-1} \tilde{b}_{ab}(\mathbf{q}) \right]. \quad (192)$$

Substituting this result into Eq.(170), and inverting $G_{ab}(\mathbf{k})$ on the right-hand side we obtain two self-consistent scalar equations for $G_\kappa(\mathbf{k})$ and $G_\Delta(\mathbf{k})$. These, together with their definition in (169) give

$$\begin{aligned} \tilde{\kappa}(\mathbf{k}) = & \kappa + \frac{2}{d_c} \int_q (\hat{k}_\alpha P_{\alpha\beta}^T(\mathbf{q}) \hat{k}_\beta)^2 \left\{ \left[\frac{D-2}{D-1} \tilde{\mu}(\mathbf{q}) + \frac{1}{D-1} \tilde{b}(\mathbf{q}) \right] \left[\frac{T}{\tilde{\kappa}(\mathbf{k}-\mathbf{q})(\mathbf{k}-\mathbf{q})^4} + \frac{\tilde{\Delta}_\kappa(\mathbf{k}-\mathbf{q})}{\tilde{\kappa}(\mathbf{k}-\mathbf{q})^2(\mathbf{k}-\mathbf{q})^4} \right] \right. \\ & \left. - \left[\frac{D-2}{D-1} \tilde{\Delta}_\mu(\mathbf{q}) + \frac{1}{D-1} \tilde{\Delta}_b(\mathbf{q}) \right] \frac{1}{\tilde{\kappa}(\mathbf{k}-\mathbf{q})(\mathbf{k}-\mathbf{q})^4} \right\}, \end{aligned} \quad (193)$$

$$\tilde{\Delta}_\kappa(\mathbf{k}) = \Delta_\kappa(\mathbf{k}) + \frac{2}{d_c} \int_q (\hat{k}_\alpha P_{\alpha\beta}^T(\mathbf{q}) \hat{k}_\beta)^2 \left[\frac{D-2}{D-1} \tilde{\Delta}_\mu(\mathbf{q}) + \frac{1}{D-1} \tilde{\Delta}_b(\mathbf{q}) \right] \frac{\tilde{\Delta}_\kappa(\mathbf{k}-\mathbf{q})}{\tilde{\kappa}(\mathbf{k}-\mathbf{q})^2(\mathbf{k}-\mathbf{q})^4}. \quad (194)$$

Recalling the second set of SCSA equations (obtained above)

$$\tilde{\mu}(\mathbf{q}) = \frac{\mu}{1 + 2\mu [T\Pi_{\kappa\kappa}(\mathbf{q}) + 2\Pi_{\kappa\Delta}(\mathbf{q})]}, \quad (195)$$

$$\tilde{b}(\mathbf{q}) = \frac{b}{1 + (D+1)b [T\Pi_{\kappa\kappa}(\mathbf{q}) + 2\Pi_{\kappa\Delta}(\mathbf{q})]}, \quad (196)$$

$$\tilde{\Delta}_\mu(\mathbf{q}) = \frac{\Delta_\mu(\mathbf{q}) + 2\mu^2 \Pi_{\Delta\Delta}(\mathbf{q})}{(1 + 2\mu [T\Pi_{\kappa\kappa}(\mathbf{q}) + 2\Pi_{\kappa\Delta}(\mathbf{q})])^2}, \quad (197)$$

$$\tilde{\Delta}_b(\mathbf{q}) = \frac{\Delta_b(\mathbf{q}) + (D+1)b^2 \Pi_{\Delta\Delta}(\mathbf{q})}{(1 + (D+1)b [T\Pi_{\kappa\kappa}(\mathbf{q}) + 2\Pi_{\kappa\Delta}(\mathbf{q})])^2}, \quad (198)$$

and the three polarization bubbles,

$$\Pi_{\kappa\kappa}(\mathbf{q}) = \frac{1}{(D^2 - 1)} \int_p (p_\alpha P_{\alpha\beta}^T(\mathbf{q}) p_\beta)^2 \frac{1}{\tilde{\kappa}(\mathbf{p}) p^4 \tilde{\kappa}(\mathbf{q} - \mathbf{p}) |\mathbf{q} - \mathbf{p}|^4}, \quad (199)$$

$$\Pi_{\kappa\Delta}(\mathbf{q}) = \frac{1}{(D^2 - 1)} \int_p (p_\alpha P_{\alpha\beta}^T(\mathbf{q}) p_\beta)^2 \frac{\tilde{\Delta}_\kappa(\mathbf{p})}{\tilde{\kappa}(\mathbf{p})^2 p^4 \tilde{\kappa}(\mathbf{q} - \mathbf{p}) |\mathbf{q} - \mathbf{p}|^4}, \quad (200)$$

$$\Pi_{\Delta\Delta}(\mathbf{q}) = \frac{1}{(D^2 - 1)} \int_p (p_\alpha P_{\alpha\beta}^T(\mathbf{q}) p_\beta)^2 \frac{\tilde{\Delta}_\kappa(\mathbf{p}) \tilde{\Delta}_\kappa(\mathbf{q} - \mathbf{p})}{\tilde{\kappa}(\mathbf{p})^2 p^4 \tilde{\kappa}(\mathbf{q} - \mathbf{p})^2 |\mathbf{q} - \mathbf{p}|^4}, \quad (201)$$

equations (193), (194), (195)-(198), (199) form a closed set of SCSA equations for a heterogeneous membrane. They reduce to the homogeneous SCSA equations, Eqs. (62), (64), (58), (53) for $\Delta_\kappa(\mathbf{k}) = \Delta_\mu(\mathbf{k}) = \Delta_b(\mathbf{k}) = 0$.

One important remark which can be made immediately from these equations is that curvature disorder, i.e., a non-zero $\Delta_\kappa(\mathbf{k})$, generates a non-zero $\tilde{\Delta}_\kappa(\mathbf{k})$, hence a non-zero $\Pi_{\Delta\Delta}(\mathbf{q})$, which in turn generates a non-zero stress disorder, $\tilde{\Delta}_\mu(\mathbf{q}) > 0$ and $\tilde{\Delta}_b(\mathbf{q}) > 0$, even if stress disorder is absent in the bare model (i.e., even if we take $\Delta_\mu(\mathbf{q}) = \Delta_b(\mathbf{q}) = 0$). Hence the three types of disorders must be considered simultaneously. Note, however, that the converse is not true. Namely, curvature disorder is *not* generated by stress-only disorder, protected by the up-down, $\vec{h} \rightarrow -\vec{h}$ symmetry. Thus, the case of stress-only disorder, $\Delta_\kappa(\mathbf{q}) = 0$ is special and requires a separate discussion, as we do below.

VI. ANALYSIS OF THE SCSA EQUATIONS FOR THE HETEROGENEOUS MEMBRANE WITH SHORT-RANGE DISORDER

We begin by studying the problem of short-range disorder, characterized by three bare (curvature and two stress) disorder variances, that are \mathbf{q} independent at long scales,

$$\Delta_\kappa(\mathbf{q}) = \Delta_\kappa, \quad \Delta_\mu(\mathbf{q}) = \Delta_\mu, \quad \Delta_\lambda(\mathbf{q}) = \Delta_\lambda. \quad (202)$$

In principle the SCSA integral equations can be solved numerically, to obtain the full q dependence of the height correlators $G_\kappa(\mathbf{k})$, $G_\Delta(\mathbf{k})$ and phonon correlators, on all the microscopic parameters, $\mu, \lambda, \kappa, \Delta_\kappa(\mathbf{q}), \Delta_\mu(\mathbf{q}), \Delta_\lambda(\mathbf{q}), T$ and \mathbf{k} . Again, as in the homogeneous case, in the large and small q regimes we can explore the asymptotics analytically.

A. Perturbative regime of short length, large $q \gg q_{\text{nl}}$ scales

Because of the complexity of the SCSA equations (195)-(198) there are number of crossover momentum scales, to which we will generically refer as q_{nl} . For sufficiently large $q \gg q_{\text{nl}}$, where q_{nl} is determined below, we expect that perturbation theory converges and that the correlators are approximately equal to the bare, Gaussian fixed point propagators

$$G_\kappa(\mathbf{k}) \approx G_\kappa^0(\mathbf{k}) = \frac{T}{\kappa k^4}, \quad (203)$$

$$G_\Delta(\mathbf{k}) \approx G_\Delta^0(\mathbf{k}) = \frac{\Delta_\kappa(k)}{\kappa^2 k^4}, \quad (204)$$

for short-range disorder, $\Delta_\kappa(k) = \Delta_\kappa$, characterized by the roughness exponents $\zeta = \zeta' = (4 - D)/2$.

In this regime from the denominator of Eqs.(196) and from (199), we see that the correction to the bulk modulus at $T = 0$ (coming from the screening by frozen out-of-plane undulations is given by

$$\frac{\tilde{b}(\mathbf{q}) - b}{b} \sim - \frac{b \Delta_\kappa}{\kappa^3 q^{4-D}}. \quad (205)$$

$$(206)$$

The perturbation theory for a heterogeneous membrane at $T = 0$ remains convergent when such correction to the above Gaussian fixed point description remain small. For the case of physical interest $D < 4$, this regime extends down to $q_{\text{nl},\Delta}$, given by

$$q_{\text{nl},\Delta} \sim \left(\frac{b \Delta_\kappa}{\kappa^3} \right)^{1/(4-D)}, \quad (207)$$

to be contrasted with the thermal nonlinear crossover wavevector in Eq.(66), which we can now denote $q_{\text{nl},T}$ to differentiate it from $q_{\text{nl},\Delta}$. We note that $q_{\text{nl},\Delta}$ reassuringly vanishes in the large κ , small Δ_κ limit, corresponding to a stiff and/or homogeneous membrane. The nonlinear ($T = 0$, disorder-driven) crossover wavevector scale for the shear modulus is of the same form but with the bulk modulus, b replaced by μ .

Finally, comparing the two terms in the numerators of Eqs.(197), (198) and (199) one finds that the corrections to the bare stress disorder Δ_b due to the curvature disorder remains small as long as

$$\frac{b^2 \Delta_\kappa^2}{\kappa^4 q^{4-D}} \ll \Delta_b, \quad (208)$$

hence there is a distinct length scale, q_Δ^{-1} , above which they cannot be neglected. The characteristic wavevector is

$$q_\Delta \sim \left(\frac{b^2 \Delta_\kappa^2}{\kappa^4 \Delta_b} \right)^{1/(4-D)}, \quad (209)$$

where we recall that $2b = K_0$ is the Young modulus for a physical membrane $D = 2$. There is a similar condition and wavevector associated to Δ_μ .

B. Non-perturbative regime of long-length, small $q \ll q_{\text{nl}}$ scales

We now study the non-perturbative regime of wavevectors smaller than q_{nl} , where the system crosses over to a nontrivial, fluctuations and nonlinearity-controlled fixed point. At these long scales the solutions to the SCSA equations are universal, independent of the microscopic parameters and can be obtained analytically. Anticipating, as in the case of a homogeneous membrane, that the solution describes a critical fixed point, we search for a height-height correlator, the propagator $G(\mathbf{k})$, that, for small k is a power-law in k

$$G_\kappa(\mathbf{k}) = \frac{T}{\tilde{\kappa}(\mathbf{k}) k^4} \simeq T Z_\kappa^{-1} k^{-4+\eta} \quad , \quad \tilde{\kappa}(\mathbf{k}) \simeq Z_\kappa k^{-\eta}, \quad (210)$$

$$G_\Delta(\mathbf{k}) = \frac{\tilde{\Delta}_\kappa(\mathbf{k})}{\tilde{\kappa}(\mathbf{k})^2 k^4} \simeq Z_\Delta^{-1} k^{-4+\eta'} \quad , \quad \tilde{\Delta}_\kappa(\mathbf{k}) \simeq Z_{\Delta_\kappa} k^{\eta'-2\eta}, \quad (211)$$

where Z_κ and Z_Δ are thermal and disorder non-universal amplitudes, with $Z_\Delta^{-1} = Z_{\Delta_\kappa}/Z_\kappa^2$. The universal exponents η and η' also determine (via (32)) the scaling of the roughness of the membrane due to temperature and disorder, respectively, (see also Eqs. (28) and (167)), with exponents

$$\zeta = 2 - D/2 - \eta/2 \quad , \quad \zeta' = 2 - D/2 - \eta'/2. \quad (212)$$

We note that G_κ vanishes at $T = 0$, while G_Δ remains non-zero, vanishing for a homogeneous membrane, $\Delta_\kappa = \Delta_\mu = \Delta_\lambda = 0$.

Using the above Ansatz (210), (211), in the long wavelength limit we can now compute the three polarization ‘‘bubbles’’, defined in Eq.(179). The details of the calculation are presented in Appendix B, with the result (72)

$$\begin{aligned} \Pi_{\kappa\kappa}(\mathbf{q}) &= \frac{1}{D^2 - 1} Z_\kappa^{-2} q^{2\eta-4+D} \Pi(\eta, D), \quad \text{for } \eta < \frac{4-D}{2}, \\ \Pi_{\kappa\Delta}(\mathbf{q}) &= \frac{1}{D^2 - 1} Z_\kappa^{-1} Z_\Delta^{-1} q^{\eta+\eta'-4+D} \Pi(\eta, \eta', D), \quad \text{for } \eta + \eta' < 4 - D, \\ \Pi_{\Delta\Delta}(\mathbf{q}) &= \frac{1}{D^2 - 1} Z_\Delta^{-2} q^{2\eta'-4+D} \Pi(\eta', D), \quad \text{for } \eta' < \frac{4-D}{2}, \end{aligned} \quad (213)$$

where, from (214)

$$\Pi(\eta, \eta', D) = (D^2 - 1) \frac{\Gamma(2 - \frac{\eta+\eta'}{2} - \frac{D}{2}) \Gamma(\frac{D}{2} + \frac{\eta}{2}) \Gamma(\frac{D}{2} + \frac{\eta'}{2})}{4(4\pi)^{D/2} \Gamma(2 - \frac{\eta}{2}) \Gamma(2 - \frac{\eta'}{2}) \Gamma(D + \frac{\eta+\eta'}{2})} \quad , \quad \Pi(\eta, D) = \Pi(\eta, \eta, D). \quad (214)$$

We note that the result given for each integral $\Pi_{ij}(\mathbf{q})$ in (213) holds only when the corresponding integral is *divergent* at small q , as indicated there by exponent inequalities. When the above exponent inequality does not hold, the corresponding integral is convergent and equal to a finite number at $q = 0$, which depends on the full q -dependence

of $G_\kappa(\mathbf{q})$ and $G_\Delta(\mathbf{q})$ and cannot be expressed simply through the small q behaviors of the propagators. The condition for all three $\Pi_{ij}(\mathbf{q})$ in (213) to diverge as $\mathbf{q} \rightarrow 0$ is thus given by

$$\eta, \eta' < \frac{4-D}{2}, \quad (215)$$

and will be found to hold in most (but not all) cases, that we will check a posteriori.

We now insert results in (213) into equations (195)-(198) for the renormalized elastic moduli and disorder variances. We observe that different solutions emerge depending on which of the polarization bubbles dominates in the denominator of the renormalized coupling constants in (195)-(198). From Eqs.(213) we see that there are three cases which are possible *a priori* (assuming all bare couplings non-zero):

1. $\eta < \eta'$, then $T\Pi_{\kappa\kappa}(\mathbf{q}) \gg \Pi_{\kappa\Delta}(\mathbf{q})$ as $\mathbf{q} \rightarrow 0$, corresponding to a *temperature dominated fixed point*.
2. either $T = 0$, or $\eta' < \eta$ for any T , then, in both cases $T\Pi_{\kappa\kappa}(\mathbf{q}) \ll \Pi_{\kappa\Delta}(\mathbf{q})$ as $\mathbf{q} \rightarrow 0$, corresponding to a *disorder-dominated fixed point*.
3. $\eta' = \eta$, then $T\Pi_{\kappa\kappa}(\mathbf{q}) \sim \Pi_{\kappa\Delta}(\mathbf{q})$ as $\mathbf{q} \rightarrow 0$, a *marginal fixed point*, meaning that *both disorder and temperature play a role*. Its $T = 0$ limit is also called marginal when $\eta' = \eta$, as an infinitesimal temperature would play a role (in fact, as discussed below, it is even marginally relevant in the present case, meaning that any infinitesimal temperature eventually flows to the thermal fixed point).

We will now examine all three cases to determine which actually occur as self-consistent solutions of above SCSA equations.

1. Disorder-dominant, $T = 0$, short-range correlated disordered fixed point

We start with the case 2,

(i) $\eta' < \eta$ for arbitrary T

(ii) $T = 0$ with a weaker assumption on η, η' (which turns out to be $\eta' < 2\eta$, as seen below).

The two cases can be studied simultaneously since in both one can neglect $T\Pi_{\kappa\kappa}(\mathbf{q})$ compared to $\Pi_{\kappa\Delta}(\mathbf{q})$ in the denominator of the renormalized coupling constants. We assume that

$$\eta + \eta' < 4 - D, \quad (216)$$

so that $\Pi_{\kappa\Delta}(\mathbf{q})$ and $\Pi_{\Delta\Delta}(\mathbf{q})$ diverge and thus dominate at small q , checking this assumption a posteriori. From Eqs. (195)-(198) and (213) we find at small q

$$\left(\tilde{\mu}(\mathbf{q}), \tilde{\Delta}_\mu(\mathbf{q}) \right) \simeq \left(\frac{1}{4\Pi_{\kappa\Delta}(\mathbf{q})}, \frac{\Pi_{\Delta\Delta}(\mathbf{q})}{8\Pi_{\kappa\Delta}(\mathbf{q})^2} \right), \quad (217)$$

$$\simeq (D^2 - 1) \left(\frac{Z_\kappa Z_\Delta}{4\Pi(\eta, \eta', D)} q^{4-D-\eta-\eta'}, \frac{Z_\kappa^2 \Pi(\eta', D)}{8\Pi(\eta, \eta', D)^2} q^{4-D-2\eta} \right), \quad (218)$$

$$\left(\tilde{b}(\mathbf{q}), \tilde{\Delta}_b(\mathbf{q}) \right) \simeq \frac{2}{D+1} \left(\tilde{\mu}(\mathbf{q}), \tilde{\Delta}_\mu(\mathbf{q}) \right). \quad (219)$$

Inserting these expressions into the equations (193), (194) and utilizing the integral

$$\Sigma(\eta, \eta', D) := \int_q \frac{(\hat{k}_\alpha P_{\alpha\beta}^T(\hat{\mathbf{q}}) \hat{k}_\beta)^2 |\mathbf{q}|^{4-D-2\eta}}{|\hat{\mathbf{k}} + \mathbf{q}|^{4-\eta'}}, \quad (220)$$

defined in Eq.(78) and calculated in the Appendix B,

$$\Sigma(\eta, \eta', D) = \frac{(D^2 - 1) \Gamma(2 - \eta) \Gamma\left(\frac{D}{2} + \frac{\eta'}{2}\right) \Gamma\left(\eta - \frac{\eta'}{2}\right)}{4(4\pi)^{D/2} \Gamma\left(2 - \frac{\eta'}{2}\right) \Gamma\left(\frac{D}{2} + \eta\right) \Gamma\left(\frac{D}{2} - \eta + \frac{\eta'}{2} + 2\right)}, \quad \Sigma(\eta, D) := \Sigma(\eta, \eta', D), \quad (221)$$

we obtain the self-consistency equations

$$Z_\kappa k^{-\eta} = \kappa + \frac{D(D-1)}{4d_c} \left[\frac{2Z_\kappa}{\Pi(\eta, \eta', D)} \Sigma\left(\frac{\eta+\eta'}{2}, \eta', D\right) k^{-\eta} - \frac{Z_\kappa \Pi(\eta', D)}{\Pi(\eta, \eta', D)^2} \Sigma(\eta, D) k^{-\eta} \right], \quad (222)$$

$$\frac{Z_\kappa^2}{Z_\Delta} k^{-2\eta+\eta'} = \Delta_\kappa + \frac{D(D-1)}{4d_c} \frac{Z_\kappa^2 \Pi(\eta', D)}{Z_\Delta \Pi(\eta, \eta', D)^2} \Sigma(\eta, \eta', D) k^{-2\eta+\eta'}. \quad (223)$$

In the first line, we have dropped the first correction term to κ in (193) (either subdominant, or absent in the present case). We now assume $\eta' < 2\eta$ at this disorder-controlled fixed point, which is implied by $\eta' < \eta$ for case (i) and added as an assumption for case (ii). Then we can safely neglect the bare value Δ_κ in Eq.(223). Canceling out the remaining factors of powers of k and nonuniversal amplitudes, we obtain two equations implicitly determining η and η' as a function of D, d_c ,

$$1 = \frac{D(D-1)}{4d_c} \left[\frac{2\Sigma(\frac{\eta+\eta'}{2}, \eta', D)}{\Pi(\eta, \eta', D)} - \frac{\Pi(\eta', D)\Sigma(\eta, D)}{\Pi(\eta, \eta', D)^2} \right], \quad (224)$$

$$1 = \frac{D(D-1)}{4d_c} \frac{\Pi(\eta', D)\Sigma(\eta, \eta', D)}{\Pi(\eta, \eta', D)^2}. \quad (225)$$

These equations can be solved using the definitions of the functions $\Pi(\eta, \eta', D)$ and $\Sigma(\eta, \eta', D)$ in (214) and (221). As is easily checked numerically, or via a series expansion in small η, η' , the only solution continuously related to $\eta = \eta' = 0$ at $d_c = +\infty$ is a *marginal* disorder dominated fixed point, i.e., with

$$\eta = \eta'. \quad (226)$$

Hence, for short-range disorder, there are no disorder dominated fixed point with $\eta' < \eta$, case (i) above, and the only solution we find within SCSA is a $T = 0$ fixed point, i.e., the case (ii) above (with, $\eta' = \eta < 2\eta$ consistent with our assumptions). As discussed below, this SCSA solution corresponds to the $T = 0$ fixed point which was obtained in Ref. [28] using renormalization group methods, controlled in an expansion in $\epsilon = 4 - D$. As for the homogeneous membrane, the present method is expected to be more accurate in the physical dimension.

For $\eta = \eta'$, we find that both equations reduce to the same, simpler equation,

$$1 = \frac{D(D-1)}{4d_c} \frac{\Sigma(\eta, D)}{\Pi(\eta, D)}. \quad (227)$$

Comparing with (80) we see that this is exactly the same equation as the one for the homogeneous membrane with d_c replaced by $4d_c$, hence we find the remarkable result at the $T = 0$ disorder-dominated fixed point [86]

$$\eta'_{\text{dis}}(D, d_c) = \eta_{\text{dis}}(D, d_c) = \eta_{\text{pure}}(D, 4d_c), \quad (228)$$

which holds within the SCSA for any D, d_c . Here and below we add the subscript pure to denote all exponents of the thermal fixed point of the homogeneous, i.e. pure, flat phase studied in Section (III). It also implies for the thermal and disorder roughness exponents

$$\zeta'_{\text{dis}}(D, d_c) = \zeta_{\text{dis}}(D, d_c) = \zeta_{\text{pure}}(D, 4d_c). \quad (229)$$

Note that at $T = 0$, strictly only the disorder-driven roughness is non-zero, i.e., the minimum energy configuration $h_{\text{min}}(x)$ is rough with exponent ζ'

$$\overline{(h_{\text{min}}(x) - h_{\text{min}}(0))^2} \sim |x|^{2\zeta'}. \quad (230)$$

However, the fact that we find $\zeta = \zeta'$ means that, for infinitesimal temperature $T > 0$, the thermal fluctuations and the disorder fluctuations scale with the same exponent. This is the sense in which the temperature is marginal at this fixed point. This marginality of temperature, in an RG sense, with thermal crossover exponent $\phi_T = 0$, was also observed in [28], consistent with the SCSA result above. We defer the discussion of whether the temperature is marginally relevant, or marginally irrelevant to the next section.

Let us now give more details on this $T = 0$ fixed point. For a $D = 2$ membrane the expression simplifies to

$$\eta_{\text{dis}}(D = 2, d_c) = \frac{1}{d_c + \sqrt{1 - \frac{1}{2}d_c + d_c^2}}, \quad (231)$$

and in the physical dimensions $D = 2$, $d_c = 1$ we find

$$\eta'_{\text{dis}} = \eta_{\text{dis}} = \frac{2}{2 + \sqrt{6}} \approx 0.449, \quad (232)$$

$$\zeta'_{\text{dis}} = \zeta_{\text{dis}} = 2 - \sqrt{\frac{3}{2}} \approx 0.775. \quad (233)$$

We thus predict that a heterogeneous membrane, characterized by short-range quenched disorder, exhibits a wrinkled ground state ($T = 0$) that is qualitatively rougher than a homogeneous membrane at finite temperature.

As we discussed for a homogeneous membrane, the SCSA is exact to leading order in the $1/d_c$ -expansion for any D , and also to leading order in the $\epsilon = 4 - D$ expansion for any d_c . The same applies here for a disordered membrane. Expanding our result around $D = 4$ we find

$$\eta_{\text{dis}}(D = 4 - \epsilon, d_c) = \frac{\epsilon}{2 + d_c/3} \quad (234)$$

for any d_c , in agreement with the $O(\epsilon)$ result of Ref.[28]. Expanding now our solution for large codimension, in powers of $1/d_c$, we obtain

$$\eta_{\text{dis}}(D, d_c) = \frac{2}{d_c} \left(\frac{D-1}{D+2} \right) \frac{\Gamma[D]}{\Gamma[\frac{D}{2}]^3 \Gamma[2 - \frac{D}{2}]} + O\left(\frac{1}{d_c^2}\right), \quad (235)$$

$$\eta_{\text{dis}}(D = 2, d_c) = \frac{1}{2d_c} + O\left(\frac{1}{d_c^2}\right), \quad (236)$$

an *exact* result, which, to our knowledge, is new. Finally the result for $d_c = 0$, $\eta_{\text{dis}} = (4 - D)/2$ is also exact. It is the limiting case for our starting assumption (216), which is thus verified for all $d_c > 0$.

Similar to our discussion for a homogeneous membrane we compute the lower critical dimension D_{lc} of the $T = 0$ disorder fixed point. Since $\eta = \eta'$, it reduces to a single equation $2 - \eta_{\text{dis}}(D_{lc}, d_c) = D_{lc}$ and using (228) we find

$$D_{lc}(d_c) = \frac{1}{2}(1 - 4d_c + \sqrt{16d_c^2 + 24d_c + 1}), \quad (237)$$

$$D_{lc}(1) = \frac{1}{2}(-3 + \sqrt{41}) \approx 1.70, \quad (238)$$

while we recall that $D_{lc} = 1.41$ for a homogeneous membrane.

We can now study the renormalized elastic moduli and random stress variances at this $T = 0$ fixed point. From (217) and $\eta' = \eta$, we see that they share the same screening exponent $\eta_u = \eta'_u$, where $\eta'_u = 4 - D - 2\eta'$, giving

$$\tilde{\mu}(\mathbf{q}) \simeq Z_\mu q^{\eta_u}, \quad \tilde{b}(\mathbf{q}) \simeq Z_b q^{\eta_u}, \quad \tilde{\Delta}_\mu(\mathbf{q}) \simeq Z_{\Delta_\mu} q^{\eta_u}, \quad \tilde{\Delta}_b(\mathbf{q}) \simeq Z_{\Delta_b} q^{\eta_u}, \quad (239)$$

where here

$$\eta_u = 4 - D - 2\eta \approx_{\substack{D=2 \\ d_c=1}} 1.101. \quad (240)$$

The roughness of the in-plane-phonon deformations at this $T = 0$ fixed point is given by

$$\overline{(u_\alpha(\mathbf{x}) - u_\alpha(0))(u_\alpha(\mathbf{x}) - u_\alpha(0))} \sim x^{2\zeta'_u}, \quad \zeta'_u = \frac{2 - D + \eta'_u}{2} \approx_{\substack{D=2 \\ d_c=1}} 0.55. \quad (241)$$

since here $\eta = \eta'$.

Above, we have introduced the amplitudes Z_μ , Z_b , Z_{Δ_μ} and Z_{Δ_b} , which, together with Z_κ and Z_{Δ_κ} , defined in (210),

$$\tilde{\kappa}(\mathbf{k}) \simeq Z_\kappa k^{-\eta}, \quad \tilde{\Delta}_\kappa(\mathbf{k}) \simeq Z_{\Delta_\kappa} k^{\eta' - 2\eta} = Z_{\Delta_\kappa} k^{-\eta}, \quad (242)$$

form a set of six a priori non-universal amplitudes for the disordered membrane. The fixed point, however, is characterized by four universal amplitude ratios. From (217) we find

$$\frac{2Z_b Z_{\Delta_\kappa}}{Z_\kappa^3} = \frac{4Z_{\Delta_b}}{Z_\kappa^2} = \frac{D-1}{\Pi(\eta, D)} \approx_{\substack{D=2 \\ d_c=1}} 13.706, \quad (243)$$

$$\frac{2Z_b}{Z_\mu} = \frac{2Z_{\Delta_b}}{Z_{\Delta_\mu}} = \frac{4}{D+1}. \quad (244)$$

Following the analysis and discussion in Sec.III D we see that the Poisson ratio is also $\tilde{\sigma}(\mathbf{q}) = -1/3$ for the disordered membrane at this fixed point.

We can now address the question of the anomalous strain response to a stress for a heterogeneous membrane. This is an extension to the disordered case of the theory of the so-called buckling transition mentioned in the pure case around Eq.(99). Here we will simply give a “back of the envelope” derivation (that can be made precise by the RG matching procedure) of the anomalous exponent $1/\delta$, that relates the strain and the stress. Denoting $\varepsilon \equiv \partial u$ the strain and σ the applied stress, one has, schematically $\varepsilon \sim \frac{1}{\mu_R(q_\sigma)} \sigma \sim \frac{\sigma}{\mu} q_\sigma^{-\eta_u}$, where q_σ is the cutoff wave-vector induced by the applied stress σ . The latter is determined by balancing curvature energy against the stress energy of the height fields (the last term in (99) with σ playing the role of τ), $\kappa_R(q_\sigma) q_\sigma^4 \sim \sigma q_\sigma^2$. This gives $q_\sigma \sim \sigma^{1/(2-\eta)}$. Hence we find a *universal anomalous* nonlinear strain-stress relation for arbitrary small stress σ (cut off only by $\sigma_{NL} \sim 1/L^{2-\eta}$ due to membrane’s finite extent, L), $\varepsilon \sim \sigma^{1/\delta}$, with $\delta^{-1} = 1 - \frac{\eta_u}{2-\eta}$. Using $\eta_u = 4 - D - 2\eta$, this reproduces (100).

For a homogeneous (disorder-free) membrane in physical dimension $D = 2$, $d = 1$ we find a *universal* nonlinear strain-stress relation with $\eta = \eta_{\text{pure}}(D = 2, d_c = 1) = 4/(1 + \sqrt{15})$, controlled by the thermal fixed point, with

$$\varepsilon \sim \sigma^{\frac{\eta}{2-\eta}} \sim \sigma^{0.6961}. \quad (245)$$

For a randomly heterogeneous membrane at the $T = 0$ fixed point we replace the exponent $\eta = \eta_{\text{pure}}(D = 2, d_c = 1)$ by $\eta = \eta' = \eta_{\text{dis}}(D = 2, d_c = 1) = \eta_{\text{pure}}(D = 2, 4) = 2/(2 + \sqrt{6})$, leading to a universal anomalous strain-stress relation for the disordered membrane

$$\varepsilon \sim \sigma^{\frac{\eta_{\text{dis}}}{2-\eta_{\text{dis}}}} \sim \sigma^{0.2899}, \quad (246)$$

corresponding to an exponent $\delta = 3.4495$.

Finally let us note that we have assumed generic disorder with $\Delta_\kappa > 0$. The case of disorder $\Delta_\kappa = 0$, symmetric under $\vec{h} \rightarrow -\vec{h}$ is more delicate at $T = 0$, and, as was discussed in [26] leads to runaway RG flows near $D = 4$. One possibility is that the resulting flow to strong stress-only disorder leads to a spontaneous breaking of the $\vec{h} \rightarrow -\vec{h}$ symmetry (or more generally of the $O(d_c)$ symmetry). Such a scenario may further lead to a crumpled spin-glass like order in the normals, as was explored in [30]. Here, within the flat phase, and from our SCSA equations, we see a strong tendency towards such symmetry breaking, since even a very small $\Delta_\kappa > 0$, at very large scale, eventually leads to the $T = 0$ fixed point studied above.

2. Search for a $T > 0$ marginal fixed point

We now explore case 3, that is $\eta' = \eta$ and $T > 0$, i.e., we search for a marginal glass fixed point. We assume again that $\eta = \eta' < \frac{4-D}{2}$, so that all $\Pi_{ij}(\mathbf{q})$ integrals diverge and dominate at small q .

From Eqs. (195) and (213) we find at small q

$$\left(\tilde{\mu}(\mathbf{q}), \tilde{\Delta}_\mu(\mathbf{q}) \right) \simeq \left(\frac{1}{2(T\Pi_{\kappa\kappa}(\mathbf{q}) + 2\Pi_{\kappa\Delta}(\mathbf{q}))}, \frac{\Pi_{\Delta\Delta}(\mathbf{q})}{2(T\Pi_{\kappa\kappa}(\mathbf{q}) + 2\Pi_{\kappa\Delta}(\mathbf{q}))^2} \right), \quad (247)$$

$$\simeq \frac{(D^2 - 1)q^{4-D-2\eta}}{2\Pi(\eta, D)} \left(\frac{1}{TZ_\kappa^{-2} + 2Z_\Delta^{-1}Z_\kappa^{-1}}, \frac{Z_\Delta^{-2}}{(TZ_\kappa^{-2} + 2Z_\Delta^{-1}Z_\kappa^{-1})^2} \right), \quad (248)$$

$$\left(\tilde{b}(\mathbf{q}), \tilde{\Delta}_b(\mathbf{q}) \right) \simeq \frac{2}{D+1} \left(\tilde{\mu}(\mathbf{q}), \tilde{\Delta}_\mu(\mathbf{q}) \right). \quad (249)$$

Substituting these expressions into Eqs.(193), (194), we obtain the self-consistency equations

$$Z_\kappa k^{-\eta} = \kappa + \frac{D(D-1)}{d_c} \left[\frac{TZ_\kappa^{-1} + Z_\Delta^{-1}}{TZ_\kappa^{-2} + 2Z_\Delta^{-1}Z_\kappa^{-1}} - \frac{Z_\Delta^{-2}Z_\kappa^{-1}}{(TZ_\kappa^{-2} + 2Z_\Delta^{-1}Z_\kappa^{-1})^2} \right] \frac{\Sigma(\eta, D)}{\Pi(\eta, D)} k^{-\eta}, \quad (250)$$

$$\frac{Z_\kappa^2}{Z_\Delta} k^{-\eta} = \Delta_\kappa + \frac{D(D-1)}{d_c} \frac{Z_\Delta^{-3}}{(TZ_\kappa^{-2} + 2Z_\Delta^{-1}Z_\kappa^{-1})^2} \frac{\Sigma(\eta, D)}{\Pi(\eta, D)} k^{-\eta}. \quad (251)$$

Identifying the leading terms, we now obtain the equations

$$1 = \frac{D(D-1)}{d_c} \frac{\Sigma(\eta, D)}{\Pi(\eta, D)} \left[\frac{a_T + a_\Delta}{a_T + 2a_\Delta} - \frac{a_\Delta^2}{(a_T + 2a_\Delta)^2} \right], \quad (252)$$

$$1 = \frac{D(D-1)}{d_c} \frac{\Sigma(\eta, D)}{\Pi(\eta, D)} \frac{a_\Delta^2}{(a_T + 2a_\Delta)^2}, \quad (253)$$

where we have defined the thermal and disorder (positive) amplitudes

$$a_T = T Z_\kappa^{-2} \quad , \quad a_\Delta = Z_\Delta^{-1} Z_\kappa^{-1}. \quad (254)$$

Clearly for these two equation to have a solution requires

$$\frac{2a_\Delta^2}{(a_T + 2a_\Delta)^2} = \frac{a_T + a_\Delta}{a_T + 2a_\Delta} \rightarrow a_T(a_T + 3a_\Delta) = 0. \quad (255)$$

Hence the only physical case of positive amplitudes when a solution exists is

$$a_T = 0 \quad \rightarrow \quad T = 0, \quad (256)$$

which is the zero-temperature solution studied in the previous section.

This analysis shows that within the SCSA, there is no finite-temperature $T > 0$ marginal case solution $\eta = \eta'$. The only solution with $\eta = \eta'$ is the $T = 0$ fixed point. This excludes, within SCSA, a scenario with a line of fixed points with continuously varying T . This is also an indication that (at least within SCSA), the temperature is *marginally relevant* at the $T = 0$ fixed point. Indeed, since we also know that the thermal fixed point is stable to disorder (as analyzed in the next section)[26], if instead temperature was irrelevant (i.e., the flow of temperature was towards $T = 0$), there would be a genuine glass phase, and an additional critical fixed point separating high and low T phases. Since we have not found a solution to the SCSA equations corresponding to such a fixed point, this possibility is unlikely. Our conclusion is thus in agreement with the RG analysis of Ref.[28], which also concluded that temperature is a marginally relevant perturbation at the $T = 0$ fixed point. Since the RG flow away from $T = 0$ is marginal, this also implies an exponentially large (in $1/T$) crossover length scale at low temperature. This crossover can, in principle also be studied using the SCSA, but we do not pursue it here.

3. Thermal fixed point with short-range disorder

Next we consider the case 1, $\eta < \eta'$ and $T > 0$, where at long wavelengths $T\Pi_{\kappa\kappa}(\mathbf{q}) \gg \Pi_{\kappa\Delta}(\mathbf{q})$, i.e., thermal fluctuations-induced screening dominates over the disorder one. From (195) and (213) we see that for such a fixed point we have two cases to consider in the small q limit (in all cases we are assuming $0 < \eta < \frac{4-D}{2}$, that we will verify a posteriori):

- $0 < \eta' < \frac{4-D}{2}$, then $\Pi_{\Delta\Delta}(\mathbf{q})$ diverges at small q , and one can neglect the bare random stress variances Δ_μ and Δ_b in the numerators of (197),(198). In this case we find

$$\left(\tilde{\mu}(\mathbf{q}), \tilde{\Delta}_\mu(\mathbf{q})\right) \simeq \left(\frac{1}{2T\Pi_{\kappa\kappa}(\mathbf{q})}, \frac{\Pi_{\Delta\Delta}(\mathbf{q})}{2T^2\Pi_{\kappa\kappa}(\mathbf{q})^2}\right), \quad (257)$$

$$\simeq (D^2 - 1) \left(\frac{Z_\kappa^2}{2T\Pi(\eta, D)} q^{4-D-2\eta}, \frac{Z_\kappa^4\Pi(\eta', D)}{2T^2 Z_\Delta^2 \Pi(\eta, D)^2} q^{4-D+2\eta'-4\eta}\right), \quad (258)$$

$$\left(\tilde{b}(\mathbf{q}), \tilde{\Delta}_b(\mathbf{q})\right) \simeq \frac{2}{D+1} \left(\tilde{\mu}(\mathbf{q}), \tilde{\Delta}_\mu(\mathbf{q})\right). \quad (259)$$

- $\eta' > \frac{4-D}{2}$, then $\Pi_{\Delta\Delta}(\mathbf{q} = 0)$ is finite and simply adds to the bare values Δ_μ and Δ_b in the numerators of (195). To simplify notation we define dressed dimensionless stress variances,

$$d_\mu = \frac{\Delta_\mu + 2\mu^2\Pi_{\Delta\Delta}(\mathbf{q} = 0)}{2\mu^2} \quad , \quad d_b = \frac{\Delta_b + (D+1)b^2\Pi_{\Delta\Delta}(\mathbf{q} = 0)}{(D+1)b^2}. \quad (260)$$

In terms of these we find

$$\left(\tilde{\mu}(\mathbf{q}), \tilde{\Delta}_\mu(\mathbf{q})\right) \simeq \left(\frac{1}{2T\Pi_{\kappa\kappa}(\mathbf{q})}, \frac{d_\mu}{2T^2\Pi_{\kappa\kappa}(\mathbf{q})^2}\right), \quad (261)$$

$$\simeq (D^2 - 1) \left(\frac{Z_\kappa^2}{2T\Pi(\eta, D)} q^{4-D-2\eta}, \frac{(D^2 - 1)Z_\kappa^4 d_\mu}{2T^2 \Pi(\eta, D)^2} q^{2(4-D-2\eta)}\right), \quad (262)$$

$$\left(\tilde{b}(\mathbf{q}), \tilde{\Delta}_b(\mathbf{q})\right) \simeq \frac{2}{D+1} \left(\tilde{\mu}(\mathbf{q}), \frac{d_b}{d_\mu} \tilde{\Delta}_\mu(\mathbf{q})\right). \quad (263)$$

Inserting these expressions into Eqs.(193), (194) we find the following self-consistency equations,

$$\begin{aligned} Z_\kappa k^{-\eta} &= \kappa + \frac{D(D-1)}{d_c} \frac{Z_\kappa \Sigma(\eta, D)}{\Pi(\eta, D)} k^{-\eta} + O(k^{\eta'-2\eta}) - O(k^{\min(2\eta', 4-D)-3\eta});, \\ \frac{Z_\kappa^2}{Z_\Delta} k^{\eta'-2\eta} &= \Delta_\kappa + O(k^{\min(2\eta', 4-D)+\eta'-4\eta}), \end{aligned} \quad (264)$$

where the estimates are valid in both cases. In the first line of (264) we see that the dominant contribution to the correction to the bending rigidity comes from purely thermal fluctuations. We have indicated two other contributions (one positive, one negative) in the order where they appear in (193): they originate from disorder that is subdominant for this case with $\eta' > \eta$ and $4 - D - 2\eta > 0$. In the second line of (264), the second term on the right-hand side is always subdominant compared to the two other terms if $\eta' < (4 - D)/2$, and also if $\eta' > (4 - D)/2$, since then $4 - D + \eta' - 3\eta > 3(\frac{4-D}{2} - \eta) > 0$ from our assumption that $\eta < (4 - D)/2$. Balancing the dominant terms on each side of the first line, canceling the amplitude Z_κ , we obtain an implicit equation

$$\frac{D(D-1)\Sigma(\eta, D)}{d_c \Pi(\eta, D)} = 1, \quad (265)$$

which determines $\eta(D, d_c)$. We note that it is identical to Eq.(80) for a homogeneous membrane, and thus obtain $\eta(D, d_c) = \eta_{\text{pure}}(D, d_c)$. The second line gives

$$\eta' = 2\eta, \quad (266)$$

as well as $Z_{\Delta_\kappa} = 1$. Thus we find that $\tilde{\Delta}_\kappa(\mathbf{q}) \simeq \Delta_\kappa$, i.e., the bare curvature disorder remains essentially unrenormalized, with only subdominant corrections at long wavelength. These corrections are $\sim k^{2(\eta'-\eta)} \sim k^{2\eta}$ at small k for $\eta' < (4 - D)/2$, i.e., $\eta < (4 - D)/4$ and $\sim k^{4-D+\eta'-4\eta} = k^{4-D-2\eta}$ if $\eta > (4 - D)/4$. We note that above is valid for generic disorder, such that $\Delta_\kappa > 0$, and the symmetric case of $\Delta_\kappa = 0$ requires a special discussion given in the next subsection.

Clearly this solution of the SCSA equations corresponds to the non-trivial thermal fixed point of the homogeneous membrane, studied in Sec.III D, with $\eta = \eta_{\text{pure}}$ and thermal roughness exponent $\zeta = (4 - D - \eta)/2 = \zeta_{\text{pure}}$, weakly perturbed by random curvature and stress disorders. We recall that for a physical membrane, $D = 2, d_c = 1$ we have $\eta \approx 0.821$ and $\zeta \approx 0.590$. The disorder is irrelevant at the thermal fixed point. Irrelevance of disorder at the thermal fixed point can also be obtained from a Harris criterion type of arguments, as discussed in [26].

Note that a full detailed crossover from the nontrivial thermal fixed point can in principle be studied using the SCSA. As can be seen from (264), weak disorder corrections at the thermal fixed point scale like k^ϕ (with the positive ϕ corresponding to irrelevant disorder), with the crossover exponent given by $\phi = \min(\phi_1, \phi_2)$, where

$$\phi_1 = \eta' - \eta = \eta, \quad \phi_1 \approx 0.821, \quad \text{for } D = 2, d_c = 1, \quad (267)$$

$$\phi_2 = 4 - D - 2\eta, \quad \phi_2 \approx 0.358, \quad \text{for } D = 2, d_c = 1. \quad (268)$$

While at this fixed point the asymptotic roughness is controlled by thermal fluctuations and is the same as for a homogeneous membrane, there is also a subdominant disorder contribution to the membrane roughness, as described in (30). It is controlled by another non-trivial exponent

$$\zeta' = \frac{4 - D - \eta'}{2} = \zeta - \eta/2 =_{D=2, d_c=1} \frac{1}{7}(9 - 2\sqrt{15}) \approx 0.179, \quad (269)$$

i.e., a smaller, but positive disorder roughness exponent for physical membranes. Hence, quite remarkably, the effect of disorder can still in principle be observed in the scaling of disorder-driven height fluctuations corresponding to the rough wrinkled background (disorder-controlled, disconnected component of height-height correlator). Although challenging, such observation through averaging of thermal fluctuations is in principle possible.

4. Stress-only disorder ($\Delta_\kappa = 0$) analysis

We finish this section on short-range disorder by analyzing a special case of $\Delta_\kappa = 0$, i.e., stress-only disorder. It is clear that $\Delta_\kappa = 0$ is an invariant subspace protected by reflection symmetry, $\vec{h} \rightarrow -\vec{h}$, that, in the absence of

spontaneous breaking of this symmetry implies $\tilde{\Delta}_\kappa(\mathbf{q}) = 0$. Thus we see from (199) that $\Pi_{\Delta\Delta}(\mathbf{q}) = \Pi_{\kappa\Delta}(\mathbf{q}) = 0$, giving

$$(\tilde{\mu}(\mathbf{q}), \tilde{\Delta}_\mu(\mathbf{q})) \simeq \left(\frac{1}{2T\Pi_{\kappa\kappa}(\mathbf{q})}, \frac{\Delta_\mu}{4\mu^2 T^2 \Pi_{\kappa\kappa}(\mathbf{q})^2} \right), \quad (270)$$

$$\simeq (D^2 - 1) \left(\frac{Z_\kappa^2}{2T\Pi(\eta, D)} q^{4-D-2\eta}, \frac{(D^2 - 1)Z_\kappa^4 \Delta_\mu}{4\mu^2 T^2 \Pi(\eta, D)^2} q^{2(4-D-2\eta)} \right), \quad (271)$$

$$(\tilde{b}(\mathbf{q}), \tilde{\Delta}_b(\mathbf{q})) \simeq \left(\frac{1}{(D+1)T\Pi_{\kappa\kappa}(\mathbf{q})}, \frac{\Delta_b}{(D+1)^2 b^2 T^2 \Pi_{\kappa\kappa}(\mathbf{q})^2} \right), \quad (272)$$

$$= (D^2 - 1) \left(\frac{Z_\kappa^2}{(D+1)T\Pi(\eta, D)} q^{4-D-2\eta}, \frac{(D^2 - 1)Z_\kappa^4 \Delta_b}{(D+1)^2 b^2 T^2 \Pi(\eta, D)^2} q^{2(4-D-2\eta)} \right). \quad (273)$$

Using these expressions inside the equation for the renormalized bending modulus, (193) (Eq.(194) identically vanishes) gives

$$Z_\kappa k^{-\eta} = \kappa + \frac{D(D-1)}{d_c} \frac{Z_\kappa \Sigma(\eta, D)}{\Pi(\eta, D)} k^{-\eta} + O(k^{4-D-3\eta}). \quad (274)$$

The second correction term on the right-hand side vanishes identically and the counting in k of the last term has changed. Hence we again find that the thermal fixed point of the homogeneous membrane is stable to stress-only disorder, consistent with the result first found in Ref.[26]. From (274) we see that the crossover exponent is again given by $\phi = \eta_u$, where $\eta_u = 4 - D - 2\eta$, $\eta_u = 0.358$ for the physical membrane.

VII. ANALYSIS OF THE SCSA EQUATIONS FOR THE HETEROGENEOUS MEMBRANE IN LONG-RANGE DISORDER

A. Realization of long-range disorder

In previous sections, our analysis and discussion of membrane's quenched internal disorder was limited to local random heterogeneity, that is *short-range* correlated in space. However, there are a number of physical realizations that also motivate examination of disorder that is *long-range* power-law correlated.

In soft-matter realization of polymerized phospholipid membranes, long-range disorder has been previously addressed by Nelson and Radzihovsky[27] in a context of experiments by D. Bensimon, et. al[55], that observed a wrinkling transition of vesicles partially polymerized with uv irradiation. They argued that correlated disorder, characterized by a power-law exponent $z_\mu = 2$ can arise from randomly distributed disclinations, with (in contrast to a fluid membrane) partial polymerization preventing screening of the long-range strains by immobile dislocations. Also it was found that randomly spaced and oriented lines of impurities (or vacancies or interstitials) can give rise to long-range correlations in the strain and curvature with $z_\mu = z_\kappa = 1$.

Another possible mechanism for a generation of power-law correlated disorder is through a frozen-in lipid tilt order. The latter is well-known to exist in fluid membranes in the β' -phase[34]. The associated in-plane vector projection is an xy-order parameter, \vec{S} , that in the ordered phase exhibits quasi-long-range correlations, characterized by a temperature-dependent exponent η , with $\langle S_\alpha(\mathbf{x}) S_\beta(0) \rangle \sim x^{-\eta}$. One would expect that upon polymerization, these correlations will be frozen in and will couple to elastic strains as quenched-in stress $c_{\alpha\beta}(\mathbf{x}) \sim S_\alpha(\mathbf{x}) S_\beta(\mathbf{x})$. It will thus lead to quenched stress-disorder, characterized by a power-law correlations, with a continuously tunable exponent.

In solid state context, such as graphene and similar atom-thin elastic sheets, long-range disorder can arise from a random distribution of Coulomb impurities. It was also recently pointed out that adatoms, which bind on one side of the membrane, or more generally in a non-symmetric way with respect to the sheet, produce most naturally random curvature disorder. The adatoms have been shown to interact via power-law correlations[23], mediated by the electrons (akin to RKKY interaction of spins), hence their spatial distribution may be long-range correlated. The question of whether ripples, if they have an intrinsic origin, will also produce long-range disorder is also interesting to explore, especially since they can be controlled [24].

Below we will study the effects of power-law correlated disorder and will show that it has dramatic effects on the flat phase of an elastic membrane, leading to a rich phase diagram.

B. Long-range quenched disorder

In this section we thus study the solutions to the SCSA equations for short-range and long-range curvature and stress disorder. In Fourier space both types of disorder can be characterized by disorder variances that are power-laws in the wavevector

$$\Delta_\kappa(\mathbf{q}) \simeq \Delta_\kappa q^{-z_\kappa} \quad , \quad \Delta_\mu(\mathbf{q}) \simeq \Delta_\mu q^{-z_\mu} \quad , \quad , \quad \Delta_\lambda(\mathbf{q}) \simeq \Delta_\lambda q^{-z_\lambda} \quad , \quad (275)$$

where the case of short-range disorder is described by the case $z_\kappa = z_\mu = z_\lambda = 0$. We will specialize to the case $z_\mu = z_\lambda$, although it is trivial to extend our analysis beyond this constraint. Our goal is to compute the roughness exponents $\zeta(z_\kappa, z_\mu)$, $\zeta'(z_\kappa, z_\mu)$ in terms of these two independent range exponents. In the following, instead of Δ_λ , for convenience we will use

$$\Delta_b(\mathbf{q}) \simeq \Delta_b q^{-z_\mu} \quad , \quad \Delta_b = \frac{b^2}{2\mu^2} [2\Delta_\mu + (D-1)\Delta_\lambda] \quad , \quad b = \frac{\mu(2\mu + D\lambda)}{2\mu + \lambda} \quad . \quad (276)$$

In this section we begin with the simplest situation of stress-only disorder, and build up in complexity, considering next the most general situation of long-range disorder in both curvature and stress. The richness of the problem leads us to consider many regimes and identify several new phases, as shown in Fig. 4. In some regimes the long-range disorder is irrelevant, reducing to the results of short-range (SR) disorder of the previous section. Upon increasing the range exponents z_κ , z_μ we find that the long-range disorder becomes relevant. In the phase diagram of Fig. 4 there are several cases. For z_κ , z_μ not too large, there are temperature-dominated phases $\zeta > \zeta'$ (the roughness of the membrane being then dynamic to leading order). For larger values of z_κ , z_μ there are disorder-dominated phases $\zeta' > \zeta$, which are stable at any temperature (qualitatively distinct phases from the case of SR disorder) and hence true glass phases, where the roughness is frozen to leading order. We will refer to these frozen ground state phases as “flat-glasses”, by analogy with spin-glass phases of magnetic spin systems. In between, there is an intermediate range of stability for *marginal phases*, where temperature and disorder play equal role $\zeta = \zeta'$. Each of these three types of phases again subdivides into phases where either stress disorder is more important, or curvature disorder is more important, or, finally, mixed phases where both play a role. Finally upon increasing z_κ , z_μ further, one enters the regime, where the controlling roughness exponent ζ' exceeds unity, signaling an instability to a crumpled-glass phase[30], presumably via a disorder activated crumpling transition.

C. Stress-only disorder

Let us begin with the simpler case of stress disorder only, $\Delta_\kappa(\mathbf{q}) = 0$, which respects the up-down symmetry of the membrane. For $\Delta_\kappa(\mathbf{q}) = 0$, if we assume the absence of spontaneous breaking of the $h \rightarrow -h$ symmetry (or $O(d_c)$ symmetry for $d_c > 1$), we have, from (193)-(199), $\tilde{\Delta}_\kappa(\mathbf{q}) = G_\Delta(\mathbf{k}) = \Pi_\kappa \Delta(\mathbf{q}) = \Pi_\Delta \Delta(\mathbf{q}) = 0$ and our problem is reduced to finding a single exponents $\eta(z_\mu)$ as a function of the stress range exponent z_μ .

In this subspace (195)-(198) give equations similar to Eq.(270) except that in the disorder components in the numerator $\Delta_\mu(\mathbf{q})$ and $\Delta_b(\mathbf{q})$ dominate the vanishing $\Pi_\Delta \Delta(\mathbf{q})$. Using (213) this leads to

$$\begin{aligned} (\tilde{\mu}(\mathbf{q}) , \tilde{\Delta}_\mu(\mathbf{q})) &= \left(\frac{1}{2T\Pi_{\kappa\kappa}(\mathbf{q})} , \frac{\Delta_\mu(\mathbf{q})}{4\mu^2 T^2 \Pi_{\kappa\kappa}(\mathbf{q})^2} \right) , \\ &= (D^2 - 1) \left(\frac{Z_\kappa^2}{2T\Pi(\eta, D)} q^{4-D-2\eta} , \frac{(D^2 - 1)\Delta_\mu Z_\kappa^4}{4\mu^2 T^2 \Pi(\eta, D)^2} q^{8-2D-4\eta-z_\mu} \right) , \\ (\tilde{b}(\mathbf{q}) , \tilde{\Delta}_b(\mathbf{q})) &= \left(\frac{1}{(D+1)T\Pi_{\kappa\kappa}(\mathbf{q})} , \frac{\Delta_b(\mathbf{q})}{(D+1)^2 b^2 T^2 \Pi_{\kappa\kappa}(\mathbf{q})^2} \right) , \\ &= (D^2 - 1) \left(\frac{Z_\kappa^2}{(D+1)T\Pi(\eta, D)} q^{4-D-2\eta} , \frac{(D^2 - 1)\Delta_b Z_\kappa^4}{(D+1)^2 b^2 T^2 \Pi(\eta, D)^2} q^{8-2D-4\eta-z_\mu} \right) . \end{aligned} \quad (277)$$

Using these expressions inside the equation for the renormalized bending modulus, (193) (Eq.(194) identically vanishes) and dropping bare term that is irrelevant at any fixed point with $\eta > 0$, we obtain

$$Z_\kappa k^{-\eta} = Z_\kappa \frac{D(D-1)}{d_c} \frac{\Sigma(\eta, D)}{\Pi(\eta, D)} k^{-\eta} - Z_\kappa A_\kappa \frac{2}{d_c} \frac{\Sigma(2\eta + z_\mu/2 + D/2 - 2, \eta, D)}{\Pi(\eta, D)^2} k^{4-D-3\eta-z_\mu} , \quad (278)$$

where we defined a universal dimensionless amplitude A_κ ,

$$A_\kappa = \frac{(D-1)Z_\kappa^2 \Delta}{b^2 T^2} \quad (279)$$

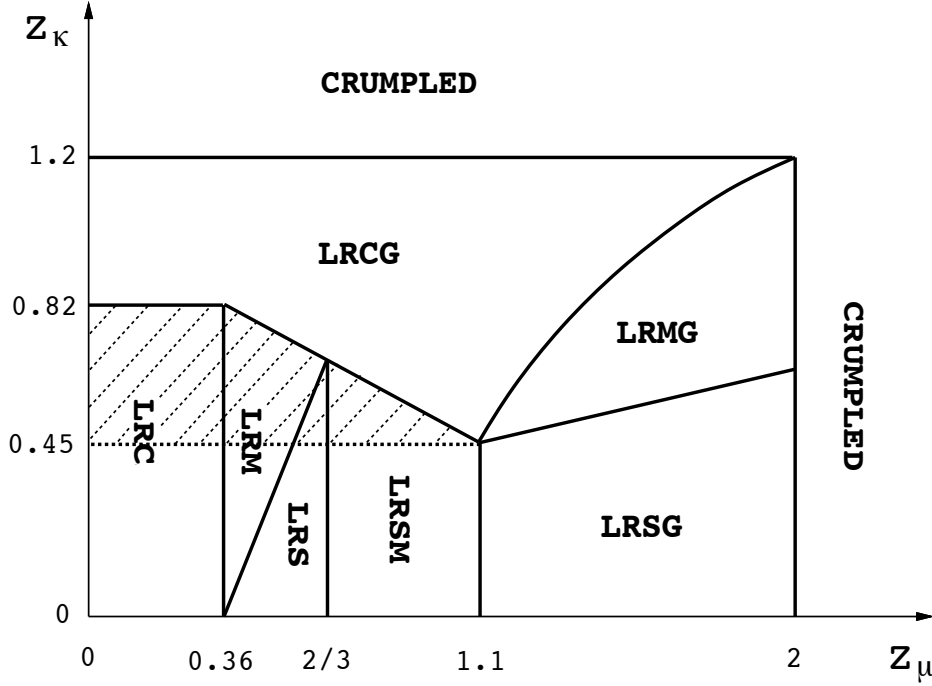


FIG. 4: Domain of stability (phase diagram) of the flat phases as a function of disorder range exponents z_μ, z_κ . (1) Disorder-dominated phases ($\zeta' > \zeta$): long-range stress glass (LRSG), long-range curvature glass (LRCG), long-range mixed glass (LRMG). (2) Temperature-dominated phases ($\zeta' < \zeta$): LR curvature (LRC), LR mixed (LRM) and LR stress (LRS). (3) LRSM: marginal phase with $\zeta = \zeta'$. The shaded area corresponds to a region of thermal phase transitions between several stable phases (LRCG and others). The region where the membrane crumples is also indicated.

in terms of an "effective disorder" bare variance defined as

$$\Delta = \Delta_b + \frac{(D-2)(D+1)^2 b^2}{4\mu^2} \Delta_\mu = (D-1) \frac{b^2}{4\mu^2} ((2+D)(D-1)\Delta_\mu + 2\Delta_\lambda), \quad (280)$$

which is an explicitly positive quantity for $D > 1$.

There are now two cases to consider.

- *Irrelevant disorder: homogeneous thermal fixed point.* If $z_\mu < 4 - D - 2\eta$ the disorder term is irrelevant and can be dropped at long wavelengths. For this solution we find that balancing the remaining two terms lead to the equation for η

$$\frac{D(D-1)}{d_c} \frac{\Sigma(\eta, D)}{\Pi(\eta, D)} = 1, \quad (281)$$

which is identical to Eq. (80) and determines the thermal fixed point of the homogeneous membrane $\eta = \eta_{\text{pure}}(D, d_c)$ studied in detail in Section III D.

- *Relevant disorder: disordered fixed point.* If the stress disorder is longer range than the critical range, with $z_\mu > z_\mu^{\text{cl}} = 4 - D - 2\eta_{\text{pure}} = \eta_u^{\text{pure}}$, then the disorder term (last term) cannot be neglected in Eq.(278). Since it has a negative amplitude (it decreases the bending rigidity), the only choice is to balance all three terms by choosing

$$\eta = 2 - \frac{D}{2} - \frac{z_\mu}{2} < \eta_{\text{pure}} \quad (282)$$

to balance the powers of k . The result is an expression for a z_μ -dependent universal amplitude $A_\kappa(z_\mu)$, which must be positive in the range of stability of this new long-range fixed point,

$$A_\kappa(z_\mu) = \frac{D(D-1)}{2} \Pi(\eta(z_\mu), D) \left(1 - \frac{d_c \Pi(\eta(z_\mu), D)}{D(D-1) \Sigma(\eta(z_\mu), D)} \right), \quad \eta(z_\mu) = 2 - \frac{D}{2} - \frac{z_\mu}{2} < \eta_{\text{pure}}. \quad (283)$$

In the case of the physical membrane, $D = 2, d_c = 1$, we thus find within SCSA that the LR disorder is relevant if $z_\mu > z_\mu^{c1} = \eta_u^{\text{pure}} = \frac{2}{7}(9 - 2\sqrt{15}) \approx 0.3583$. Denoting $z_\mu = z_\mu^{c1} + \delta$ we find that the amplitude increases from zero as

$$A_\kappa(z_\mu) = 0.52874\delta - 2.80214\delta^2 + O(\delta^3) \quad (284)$$

for small δ . We have checked numerically that it is positive for all values in $z_\mu^{c1} < z_\mu < 2$. Hence it is an admissible (i.e., physical) solution of the SCSA equations.

Plugging these results back into (210) one obtains

$$G_\kappa(\mathbf{k}) \simeq \sqrt{\frac{D-1}{A_\kappa(z_\mu)}} \frac{\Delta}{b^2} k^{-\frac{2+D+z_\mu}{2}}, \quad \zeta = \frac{4-D}{4} + \frac{z_\mu}{4} > \zeta_{\text{pure}}. \quad (285)$$

Since the effective bending rigidity is reduced by disorder, we find that in this phase the roughness exponent of the out-of-plane fluctuations is larger than the one of the pure homogeneous membrane. The amplitude is non-universal, depending on the bare disorder (note that the temperature dependence has dropped out since $Z_\kappa \sim T$ at the fixed point). On the other hand one can check that the renormalized elastic and disorder couplings scale as $\tilde{\mu}(\mathbf{q}) \sim \tilde{b}(\mathbf{q}) \sim Tq^{z_\mu}$ and $\tilde{\Delta}_\mu(\mathbf{q}) \sim \tilde{\Delta}_b(\mathbf{q}) \sim T^2q^{z_\mu}$, respectively. Hence there is a thermal renormalization (screening) of these moduli, stronger at small q than for the pure system, that one can summarize by $\eta_u = \eta'_u = z_\mu > \eta_u^{\text{pure}}$. This means that the connected or thermal part $\overline{\langle uu \rangle}_{\text{conn}} \sim T/(\tilde{b}(\mathbf{q})q^2) \sim q^{-2-z_\mu}$ becomes independent of T and similarly the off-diagonal part $\overline{\langle u \rangle \langle u \rangle} \sim \tilde{\Delta}_b(\mathbf{q})/(\tilde{b}(\mathbf{q})^2q^2) \sim q^{-2-z_\mu}$, also is independent of T . So both in-plane displacements and out-of-plane displacements (from (285)) are independent of temperature to leading order, and hence are marginally frozen. The membrane thus exhibits a glassy behavior. Note that the physical interpretation of the condition $z_\mu > z_\mu^{c1} = \eta_u^{\text{pure}}$ for this phase to occur, corresponds to stress disorder producing in-plane displacements that are larger than the thermal phonon fluctuations controlled by the pure fixed point of the homogeneous membrane. Since for physical membranes $\zeta = 1/2 + z_\mu/4$ in this phase, reaching the value 1 at $z_\mu^{c2} = 2$ we expect the membrane to crumple for $z_\mu \geq z_\mu^{c2}$, corresponding to disorder produced by frozen unscreened disclinations [27].

Note that the assumption that we are looking for a solution with $G_\Delta(\mathbf{k}) = 0$, that is $\tilde{\Delta}_\kappa = 0$, is equivalent to assuming that $\langle h_{\mathbf{k}} \rangle = 0$ in each disorder configuration, i.e., no symmetry breaking in each disorder configuration. As we see below this parity symmetric subspace is unstable to introduction of even weak curvature disorder. The local in-plane strains introduced by the stress disorder can be screened by local buckling of the membrane. In the absence of interactions the resulting ground state is highly degenerate with respect to local buckling of any sign. Simple arguments suggest that to minimize the curvature energy, the interactions between "puckers" are expected to be "antiferromagnetic" [26]. In any case the restriction of vanishing curvature disorder (symmetric membrane) does not preclude the possibility of a collective spontaneous buckling transition.

D. Non-zero curvature disorder

We now study the more general problem of non-zero curvature disorder. There are three types of solutions which we describe as disorder-dominated phases, temperature-dominated (dynamic) phases, and marginal phases, characterized by $\zeta' > \zeta$, $\zeta' < \zeta$, $\zeta' = \zeta$, respectively. To study these phases we follow an analysis similar to the previous sections. In each case we first determine the renormalized quartic coupling constants via Eqs. (195) to (198), and then use them inside the Eq.(193). The resulting phases are displayed in Fig. 4.

It is useful to recall that in the case of SR disorder we found only two fixed point solutions: (i) the "thermal" fixed point of the homogeneous membrane, which is stable to weak short-range disorder (although it does exhibit some signature of the presence of disorder, e.g., $\zeta' > 0$) and characterized by two exponents, $\eta = \eta_{\text{pure}}$ (as in the strict absence of disorder) and $\eta' = 2\eta = 2\eta_{\text{pure}}$, which describes the weak (irrelevant) disorder-induced fluctuations, (ii) the SR disorder dominated $T = 0$ fixed point with $\eta = \eta' = \eta_{\text{SRdis}}$. Note that in this Section we will denote systematically the exponents at the SR disorder fixed point with the subscript SRdis. As we will see a much greater variety of phases will arise in the present case of LR disorder.

1. Disorder-dominated phases: $\zeta' > \zeta$

Let us now search for disorder-dominated phases. From the classification in Section VIB it amounts to either studying a membrane at $T = 0$ or a search for solutions of the SCSA equations with $\eta' < \eta$, which implies $\zeta' > \zeta$ from

(32), where temperature is subdominant. In both cases we can neglect $T\Pi_{\kappa\kappa}(\mathbf{q})$ compared to $\Pi_{\kappa\Delta}(\mathbf{q})$, as was done to obtain Eqs.(217), except that here we keep the possibly relevant terms $\Delta_\mu(\mathbf{q}), \Delta_b(\mathbf{q})$ in the numerator of Eqs. (197), (198). We find the renormalized couplings as

$$\left(\tilde{\mu}(\mathbf{q}), \tilde{\Delta}_\mu(\mathbf{q})\right) \simeq \left(\frac{1}{4\Pi_{\kappa\Delta}(\mathbf{q})}, \frac{\frac{\Delta_\mu(\mathbf{q})}{2\mu^2} + \Pi_{\Delta\Delta}(\mathbf{q})}{8\Pi_{\kappa\Delta}(\mathbf{q})^2}\right), \quad (286)$$

$$\simeq (D^2 - 1) \left(\frac{Z_\kappa Z_\Delta}{4\Pi(\eta, \eta', D)} q^{4-D-\eta-\eta'}, \frac{Z_\kappa^2 \Pi(\eta', D)}{8\Pi(\eta, \eta', D)^2} q^{4-D-2\eta} + \frac{(D^2 - 1)\Delta_\mu}{16\mu^2} \frac{(Z_\kappa Z_\Delta)^2}{\Pi(\eta, \eta', D)^2} q^{8-2D-2\eta-2\eta'-z_\mu}\right),$$

$$\left(\tilde{b}(\mathbf{q}), \tilde{\Delta}_b(\mathbf{q})\right) \simeq \frac{2}{D+1} \left(\tilde{\mu}(\mathbf{q}), \frac{\frac{\Delta_b(\mathbf{q})}{b^2(D+1)} + \Pi_{\Delta\Delta}(\mathbf{q})}{8\Pi_{\kappa\Delta}(\mathbf{q})^2}\right), \quad (287)$$

$$\simeq 2(D-1) \left(\frac{Z_\kappa Z_\Delta}{4\Pi(\eta, \eta', D)} q^{4-D-\eta-\eta'}, \frac{Z_\kappa^2 \Pi(\eta', D)}{8\Pi(\eta, \eta', D)^2} q^{4-D-2\eta} + \frac{(D-1)\Delta_b}{8b^2} \frac{(Z_\kappa Z_\Delta)^2}{\Pi(\eta, \eta', D)^2} q^{8-2D-2\eta-2\eta'-z_\mu}\right),$$

where we used (213), and assumed $\eta' < (4-D)/2$ and $\eta + \eta' < 4-D$.

Substituting the resulting coupling constants into Eqs.(193) we find the analog of Eqs.(222), generalized to long-range disorder,

$$Z_\kappa k^{-\eta} = \kappa + \frac{Z_\kappa k^{-\eta} D(D-1)}{4d_c} \left[\frac{2\Sigma(\frac{\eta+\eta'}{2}, \eta', D)}{\Pi(\eta, \eta', D)} - \frac{\Sigma(\eta, D)\Pi(\eta', D)}{\Pi(\eta, \eta', D)^2} \right] \quad (288)$$

$$-D(D-1)Z_\kappa A_\Delta \frac{\Sigma(\eta + \eta' + \frac{z_\mu}{2} + \frac{D}{2} - 2, \eta, D)}{4d_c \Pi(\eta, \eta', D)^2} k^{4-D-\eta-2\eta'-z_\mu},$$

$$\frac{Z_\kappa^2}{Z_\Delta} k^{-2\eta+\eta'} = \Delta_\kappa k^{-z_\kappa} + \frac{D(D-1)Z_\kappa^2}{4d_c Z_\Delta \Pi(\eta, \eta', D)^2} \left[A_\Delta \Sigma(\eta + \eta' + \frac{z_\mu}{2} + \frac{D}{2} - 2, \eta', D) k^{4-D-2\eta-\eta'-z_\mu} \right. \quad (289)$$

$$\left. + \Sigma(\eta, \eta', D)\Pi(\eta', D) k^{-2\eta+\eta'} \right],$$

where we have defined another explicitly positive universal amplitude,

$$A_\Delta = \frac{2Z_\Delta^2 \Delta}{Db^2}, \quad (290)$$

and Δ was defined in (280). If we set the LR disorders $A_\Delta = 0$ and $\Delta_\kappa = 0$, we recover the equations (222) for short-range disorder, which were analyzed in Section VIB. There it was found that in that case there are no disorder dominated solution with $\eta' > \eta$, but there is one disorder-dominated solution at $T = 0$ (although marginal with respect to introduction of temperature, since it is characterized by exponents $\eta = \eta' = \eta_{\text{SRdis}}$).

We now describe the relevance of the two types of LR disorder. By comparing the first term on the right-hand side of Eq. (289) to the left-hand side, one sees that the long-range curvature disorder is irrelevant as long as

$$z_\kappa < 2\eta - \eta' \Leftrightarrow \text{LR curvature disorder irrelevant}. \quad (291)$$

Thus we see that at the $T = 0$ SR disorder fixed point, the LR curvature disorder is irrelevant, as long as

$$z_\kappa < \eta_{\text{SRdis}} \quad (292)$$

By looking at the last two terms of either equations Eqs. (288), (289) we see that the long-range stress disorder is irrelevant for

$$z_\mu < 4 - D - 2\eta' = \eta'_u \Leftrightarrow \text{LR stress disorder irrelevant}. \quad (293)$$

This last condition is consistent with the one we found in analyzing $\Delta_\kappa(\mathbf{q}) = 0$ case, except here it is η' instead of η , that controls the roughness of the phase.

We therefore look for long-range (LR) disordered solutions to the above equations. We find that there are three possible LR phases that we call Long-Range Stress Glass (LRSG), Long-Range Curvature Glass (LRCG), and Long-Range Mixed Glass (LRMG), corresponding to the relevant stress, curvature and both disorders, respectively.

(1-i) **Long-Range Stress Glass (LRSG):**

This solution is defined by relevance of LR stress disorder and irrelevance of the LR curvature disorder term $\Delta_\kappa k^{4-z_\kappa}$ and is therefore only stable for $z_\kappa < 2\eta - \eta'$. The relevance of LR stress requires that all terms in (288) scale similarly, which implies

$$\eta' = \eta'(z_\mu) := 2 - D/2 - z_\mu/2. \quad (294)$$

Combining this result with Eqs.(288), (289) leads to the equation which determines $\eta = \eta(z_\mu)$ (plugging $\eta' = \eta'(z_\mu)$ in the first equation) and the universal amplitude $A_\Delta(z_\mu)$ (plugging both $\eta = \eta(z_\mu)$ and $\eta' = \eta'(z_\mu)$ in the second equation)

$$\begin{aligned} \frac{D(D-1)\Sigma(\frac{\eta+\eta'}{2}, \eta', D)}{2d_c\Pi(\eta, \eta', D)} - \frac{\Sigma(\eta, D)}{\Sigma(\eta, \eta', D)} &= 1, \\ A_\Delta(z_\mu) &= \frac{4d_c\Pi(\eta, \eta', D)^2}{D(D-1)\Sigma(\eta, \eta', D)} - \Pi(\eta', D). \end{aligned} \quad (295)$$

We note that the first equation coincides with the equation obtained from the system (224) (obtained for short-range disorder) when eliminating $\Pi(\eta, \eta', D)^2$ from the second equation there and plugging it into the first. Hence the relation (295) between η and η' also holds for SR disorder, but the value of the exponent η' here is imposed by the LR disorder as in (294). Also, if one sets $A_\Delta(z_\mu) = 0$ in the second equation, one recovers the system (224).

On general grounds, and given the assumptions leading to (294) and (295), we expect that this LRSG phase is stable as long as the following conditions hold

$$\eta'(z_\mu) < \eta(z_\mu), \text{ equivalent to } \zeta'(z_\mu) > \zeta(z_\mu), \text{ and } A_\Delta(z_\mu) > 0, \quad (296)$$

$$\eta'(z_\mu) > 0, \text{ equivalent to } \zeta'(z_\mu) < 1. \quad (297)$$

The first condition is that it is disorder-dominated and corresponds to the assumption made in deriving (295). As we discuss below it corresponds to the condition $z_\mu > z_\mu^{c1} = 2 - 2\eta_{\text{SRpure}}$. The second condition states that the membrane is flat and defines the right boundary of LRSG, with $z_\mu^{c2} = 4 - D$, beyond which the membrane crumples, with $\eta'(z_\mu^{c2}) = 0$. An additional condition used in the derivation, $\eta'(z_\mu) + \eta(z_\mu) < 4 - D$, should also be verified. Finally one also needs

$$z_\kappa < 2\eta(z_\mu) - \eta'(z_\mu), \text{ equivalent to } z_\kappa < 2\eta(z_\mu) + \frac{D}{2} - 2 + z_\mu/2, \quad (298)$$

which is the requirement that the LR curvature disorder is irrelevant. It defines the upper boundary of the LRSG, above which both LR curvature and LR stress disorders are relevant and the membrane is described by the LRMG phase.

To analyze the solutions to (295) we must start with the SR fixed point, which is a solution to (295) with $\eta = \eta' = \eta_{\text{SRdis}}$ and $A_\Delta(z_\mu) = 0$. A true LR solution of (295) with $A_\Delta(z_\mu) > 0$ emerges from this SR fixed point for $z_\mu > z_\mu^{c1}$ where z_μ^{c1} is defined by the condition $\eta'(z_\mu^{c1}) = \eta_{\text{SRdis}}$, which from (294) gives $z_\mu^{c1} = 2 - 2\eta_{\text{SRdis}}$.

Let us now discuss in more details the case of the physical membrane, with $D = 2$ and $d_c = 1$. We find

$$\eta_{\text{SRdis}} = \sqrt{6} - 2 = 0.44949.., \quad z_\mu^{c1} = 6 - 2\sqrt{6} = 1.10102, \quad (299)$$

$$\eta'(z_\mu) = \eta_{\text{SRdis}} - \frac{z_\mu - z_\mu^{c1}}{2}, \quad (300)$$

$$\eta(z_\mu) = \eta_{\text{SRdis}} - \frac{23 - 8\sqrt{6}}{58}(z_\mu - z_\mu^{c1}) - 0.0112487(z_\mu - z_\mu^{c1})^2 + \dots, \quad (301)$$

$$A_\Delta(z_\mu) = 0.0494198(z_\mu - z_\mu^{c1}) - 0.0548815(z_\mu - z_\mu^{c1})^2 + \dots, \quad (302)$$

where $\frac{23-8\sqrt{6}}{58} = 0.0586911...$. One thus verifies that the solution obeys the above conditions (296), as well as $\eta(z_\mu) + \eta'(z_\mu) < 2$. Note that T does not appear and hence for $z_\mu > z_\mu^{c1}$ this phase is stable at any temperature T . At the lower boundary $z_\mu = z_\mu^{c1}$ the marginal phase, characterized by $\eta' = \eta$ becomes the ground state (itself marginally unstable to temperature). Below z_μ^{c1} the LRSG phase becomes unstable to the marginal LRSM phase, which is analyzed below (see Fig. 4). This lower boundary is a straight vertical line because in LRSG phase the

exponents are independent of z_κ . At the upper boundary $z_\mu = z_\mu^{c2} = 2$ the flat membrane is unstable, and we find that $\eta(z_\mu^{c2}) \approx 0.3877$ with $A_\Delta(z_\mu) = 0.0209$.

(1-ii) **Long-Range Curvature Glass (LRCG):**

In this phase the LR stress disorder is irrelevant, i.e., $z_\mu < 4 - D - 2\eta'$ and the LR curvature disorder is relevant. At large scales we can therefore drop terms in Eqs.(288), (289), that involve stress disorder (those involving the amplitude A_Δ). Furthermore, for LR curvature disorder to be relevant we must balance the powers of k of the term $\Delta_\kappa k^{-z_\mu}$ with the remaining terms of (289), which leads to the relation

$$2\eta(z_\kappa) - \eta'(z_\kappa) = z_\kappa, \quad (303)$$

where we denote $\eta(z_\kappa)$ and $\eta'(z_\kappa)$ the (as yet unknown) exponents in the LRCG phase. Dropping the irrelevant stress disorder term, Eq. (288) then gives the condition

$$\frac{D(D-1)}{4d_c} \left[\frac{2\Sigma(\frac{\eta+\eta'}{2}, \eta', D)}{\Pi(\eta, \eta', D)} - \frac{\Sigma(\eta, D)\Pi(\eta', D)}{\Pi(\eta, \eta', D)^2} \right] = 1. \quad (304)$$

These equations together determine the anomalous exponents $\eta(z_\kappa)$ and $\eta'(z_\kappa)$ in this phase. In addition one can define another intrinsically positive amplitude,

$$A_{\kappa\Delta} := \frac{\Delta_\kappa Z_\Delta}{Z_\kappa^2}. \quad (305)$$

Dropping the irrelevant stress-disorder term in Eq.(289) allows to determine the value of this amplitude as

$$A_{\kappa\Delta} = A_{\kappa\Delta}(z_\kappa) := 1 - \frac{D(D-1)\Sigma(\eta, \eta')\Pi(\eta')}{4d_c\Pi(\eta, \eta')^2}, \quad (306)$$

where one must plug in the right-hand side the values of the exponents $\eta = \eta(z_\mu)$ and $\eta' = \eta'(z_\mu)$ of the LRCG phase. It is thus a universal amplitude (i.e., depending only on z_κ) characteristic of the LRCG phase.

From the above derivation we can see that the region of stability of the LRCG ground state is defined by the following boundaries

$$z_\mu < 4 - D - 2\eta(z_\kappa) = \eta_u(z_\kappa), \quad (307)$$

$$\eta'(z_\kappa) < \eta(z_\kappa), \text{ equivalent to } \zeta'(z_\kappa) > \zeta(z_\kappa), \quad (308)$$

$$\eta'(z_\kappa) > 0, \text{ equivalent to } \zeta'(z_\kappa) < 1, \quad (309)$$

where the first condition enforces the irrelevance of the LR stress disorder and determines the lower-right boundary of the LRCG phase towards the LRMG phase, in which both LR curvature and LR stress disorders are simultaneously relevant, as illustrated in Fig. 4. The conditions (308), (309) are identical to Eqs. (296), (297), except that in LRCG the exponents are only functions of z_κ , which is why the lower- and upper-boundaries are straight horizontal lines.

To analyze the system of equations (303) and (304) we must again start from the SR disorder fixed point. That determines the lower boundary $z_\kappa = z_\kappa^{c1}$, such that $\eta'(z_\kappa^{c1}) = \eta(z_\kappa^{c1}) = \eta_{SRdis}$. From (303) it then gives $z_\kappa^{c1} = \eta_{SRdis}$. On this boundary the amplitude $A_{\kappa\Delta}(z_\kappa^{c1}) = 0$. For $z_\kappa > z_\kappa^{c1}$ there is a nontrivial solution for the LRCG with $A_{\kappa\Delta}(z_\kappa^{c1}) > 0$. At the upper boundary, $z_\kappa = z_\kappa^{c2}$, defined by the equation (309), the flat phase is unstable and the membrane crumples. Let us now specialize to the physical membrane $D = 2, d_c = 1$. Then one finds, for z_κ , above, but close to the lower-boundary z_κ^{c1}

$$z_\kappa^{c1} = \eta_{SRdis} = \sqrt{6} - 2 = 0.44949.., \quad (310)$$

$$\eta'(z_\kappa) = \eta_{SRdis} + a'(z_\kappa - z_\kappa^{c1}) + .., \quad a' = 2a - 1 = -0.46305.., \quad (311)$$

$$\eta(z_\kappa) = \eta_{SRdis} + a(z_\kappa - z_\kappa^{c1}) + .., \quad a = \frac{2}{19} (5 - \sqrt{6}) = 0.268475.., \quad (312)$$

$$A_\Delta(z_\kappa) = A(z_\mu - z_\mu^{c1}) + .., \quad A = \frac{1}{95} (108 + 43\sqrt{6}) = 2.24556.., \quad (313)$$

which satisfies all the required stability conditions. More generally, solving Eqs. (303) and (304) in the whole LRCG phase we confirm that $\eta'(z_\kappa)$ decreases and $\eta(z_\kappa)$ increases as z_κ increases. For the upper boundary defined by equation (309) at which the membrane crumples, we find $z_\kappa^{c2} \approx 1.19695$, with $\eta'(z_\kappa^{c2}) = 0$ and $\eta(z_\kappa^{c2}) = z_\kappa^{c2}/2 \approx 0.598473$.

(1-iii) **Long-Range Mixed Glass (LRMG):**

A new glassy ground state and phase results when both types of LR disorder are relevant. The LRMG phase borders the LRSg, LRCG and the Crumpled Glass phases, with the boundaries already defined in the discussion of LRSg and LRCG, above. The relevance of both types of disorders requires us to balance the powers of k in both Eqs.(288),(289) and therefore the exponents are completely determined to be

$$\eta(z_\kappa, z_\mu) = \frac{z_\kappa}{2} - \frac{z_\mu}{4} + 1 - \frac{D}{4}, \quad (314)$$

$$\eta'(z_\mu) = 2 - \frac{D}{2} - \frac{z_\mu}{2}. \quad (315)$$

We expect these expressions to be exact, since they are a result of dimensional analysis. The two universal amplitudes defined in the previous sections are also determined by the Eqs.(288),(289) and are given by

$$A_\Delta = A_\Delta(z_\kappa, z_\mu) = \frac{1}{\Sigma(\eta, D)} \left[2\Pi(\eta, \eta', D)\Sigma\left(\frac{\eta + \eta'}{2}, \eta', D\right) - \Sigma(\eta, D)\Pi(\eta', D) \right] - \frac{4d_c\Pi(\eta, \eta', D)^2}{D(D-1)\Sigma(\eta, D)}, \quad (316)$$

$$A_{\kappa\Delta} = A_{\kappa\Delta}(z_\kappa) = 1 + \frac{\Sigma(\eta, \eta', D)}{\Sigma(\eta, D)} - \frac{D(D-1)\Sigma(\eta, \eta', D)\Pi(\eta', D)}{4d_c\Pi(\eta, \eta', D)^2} \quad (317)$$

$$+ \frac{D(D-1)\Sigma(\eta, \eta', D)}{4d_c\Sigma(\eta, D)} \left[\frac{\Sigma(\eta, D)\Pi(\eta', D)}{\Pi(\eta, \eta', D)^2} - \frac{2\Sigma\left(\frac{\eta + \eta'}{2}, \eta', D\right)}{\Pi(\eta, \eta', D)} \right]. \quad (318)$$

The consistency of these amplitudes with the results of the previous section can easily be checked. We summarize by recalling the equations of the phase boundaries

$$z_\kappa = 2\eta_{LRSg}(z_\mu) + \frac{D}{2} - 2 + \frac{z_\mu}{2}, \quad \text{LRSg-LRMG boundary}, \quad (319)$$

$$z_\mu = 4 - D - 2\eta'_{LRCG}(z_\kappa), \quad \text{LRCG-LRMG boundary}, \quad (320)$$

$$z_\mu = 2 \quad \text{or} \quad z_\kappa = z_\kappa^{(c_2)}, \quad \text{boundary to crumpled phase}. \quad (321)$$

Note that the condition that the LRMG is a disorder-dominated phase is

$$\eta'(z_\mu) < \eta(z_\kappa, z_\mu) \quad \Leftrightarrow \quad 2z_\kappa + z_\mu > 4 - D. \quad (322)$$

As can be seen in Fig. 4 this condition is always satisfied in the LRMG phase: the triple point LRCG-LRMG-LRSg, where the three phases has coordinates given by $z_\mu^{c_1} = 2 - 2\eta_{SRdis}$ and $z_\kappa = \eta_{SRdis}$ is located precisely on the line where (322) holds as an equality.

2. Temperature-dominated phases, $\zeta' < \zeta$

We now examine solutions to the SCSA equations (193), (194), (195)-(198), (199) of the heterogeneous membrane, for which the roughness of the membrane is dominated by (dynamic) thermal fluctuations, i.e., solutions with $\eta' > \eta$. The thermal fixed point of the homogeneous membrane, that we have already examined is an example of this type of a solution, at which disorder is completely irrelevant. This solution falls on the z_μ -axis of Fig. 4 for $0 < z_\mu < 0.358$. We have already seen that there are no short-range disordered solutions and we therefore examine LR disordered fixed points of temperature dominated type. As we will see below, there turns out to be three solutions of this type which we name Long-Range Curvature (LRC), Long-Range Stress (LRS), and Long-Range Mixed (LRM), in analogy with the glass solutions we have studied in the previous section.

For all temperature dominated solutions $\eta' > \eta$ and $T > 0$, at long wavelengths we have, from (210), $G_\Delta(\mathbf{k}) \ll G_\kappa(\mathbf{k})$ and therefore $\Pi_{\kappa\Delta}(\mathbf{q}) \ll T\Pi_{\kappa\kappa}(\mathbf{q})$ from (213), i.e., thermal screening dominates. Hence the term $\Pi_{\kappa\Delta}(\mathbf{q})$ can be neglected in the numerators of the renormalized couplings (195), as was done to derive (261) in the case of SR disorder. Here, however we do not drop $\Delta_\mu(\mathbf{q}), \Delta_b(\mathbf{q})$ in the numerators of Eqs.(197),(198), because they might turn out to be relevant.

Let us assume that $0 < \eta' < \frac{4-D}{2}$, then $\Pi_{\Delta\Delta}(\mathbf{q})$ diverges at small q , and one finds the LR generalization of (257)

or, equivalently the generalization of (277) in presence of curvature disorder,

$$\begin{aligned}
(\tilde{\mu}(\mathbf{q}), \tilde{\Delta}_\mu(\mathbf{q})) &\simeq \left(\frac{1}{2T\Pi_{\kappa\kappa}(\mathbf{q})}, \frac{\frac{\Delta_\mu(\mathbf{q})}{2\mu^2} + \Pi_{\Delta\Delta}(\mathbf{q})}{2T^2\Pi_{\kappa\kappa}(\mathbf{q})^2} \right), \\
&\simeq (D^2 - 1) \left(\frac{Z_\kappa^2}{2T\Pi(\eta, D)} q^{4-D-2\eta}, \frac{Z_\kappa^4\Pi(\eta', D)}{2T^2Z_\Delta^2\Pi(\eta, D)^2} q^{4-D+2\eta'-4\eta} + \frac{(D^2 - 1)\Delta_\mu Z_\kappa^4}{4T^2\mu^2\Pi(\eta, D)^2} q^{8-2D-4\eta-z_\mu} \right), \\
(\tilde{b}(\mathbf{q}), \tilde{\Delta}_b(\mathbf{q})) &\simeq \frac{2}{D+1} \left(\tilde{\mu}(\mathbf{q}), \frac{\frac{\Delta_b(\mathbf{q})}{(D+1)b^2} + \Pi_{\Delta\Delta}(\mathbf{q})}{2T^2\Pi_{\kappa\kappa}(\mathbf{q})^2} \right), \\
&\simeq 2(D-1) \left(\frac{Z_\kappa^2}{2T\Pi(\eta, D)} q^{4-D-2\eta}, \frac{Z_\kappa^4\Pi(\eta', D)}{2T^2Z_\Delta^2\Pi(\eta, D)^2} q^{4-D+2\eta'-4\eta} + \frac{(D-1)\Delta_b Z_\kappa^4}{2T^2b^2\Pi(\eta, D)^2} q^{8-2D-4\eta-z_\mu} \right).
\end{aligned} \tag{323}$$

Plugging these formula into (193) we obtain

$$\begin{aligned}
k^{-\eta} &= \frac{D(D-1)\Sigma(\eta, D)}{d_c\Pi(\eta, D)} k^{-\eta} + O(k^{\eta'-2\eta}) - O(k^{\min(2\eta', 4-D)-3\eta}) \\
&\quad - A_\kappa \frac{2\Sigma(2\eta + z_\mu/2 + D/2 - 2, \eta, D)}{d_c\Pi(\eta, D)^2} k^{4-D-3\eta-z_\mu}, \\
k^{-2\eta+\eta'} &= A_{\kappa\Delta} k^{-z_\kappa} + O(k^{\min(2\eta', 4-D)+\eta'-4\eta}) \\
&\quad + A_\kappa \frac{2\Sigma(2\eta + z_\mu/2 + D/2 - 2, \eta', D)}{d_c\Pi(\eta, D)^2} k^{4-D-4\eta+\eta'-z_\mu},
\end{aligned} \tag{324}$$

where we divided the first line by Z_κ and the second by Z_κ^2/Z_Δ . Note that there are terms which we did not write explicitly as they are subdominant when $\eta' > \eta$ and do not involve LR disorder. Their analysis is exactly as in (264) and they can be dropped. We recall that we defined earlier the two dimensionless amplitudes

$$A_\kappa = \frac{(D-1)Z_\kappa^2\Delta}{b^2T^2}, \quad A_{\kappa\Delta} = \frac{\Delta_\kappa Z_\Delta}{Z_\kappa^2}. \tag{325}$$

The relevance of the stress disorder in these equations is determined by the value of z_μ . We further observe that if we discard irrelevant terms the first equation in the system (324) does not involve curvature disorder, neither η' or z_κ , and therefore is identical to Eq.(278). Hence, in all the temperature-dominated phases studied in this section, all quantities related to the (connected) thermal correlations, i.e., $\eta(z_\mu)$, $A_\kappa(z_\mu)$, the small q behavior of $G_\kappa(\mathbf{q})$ and the thermal roughness exponent ζ , are identical to those found in section VII C, where stress-only disorder was considered (i.e., with $\Delta_\kappa(\mathbf{q}) = 0$). In these thermal phases with LR disorder, the thermal (connected) and disorder (off-diagonal) correlations effectively mutually decouple at large scale. Let us now study these phases in more details.

(2-i) long-range curvature disorder (LRC):

As the name implies, the LRC flat phase is characterized by relevant LR curvature disorder and irrelevant LR stress disorder. Thus it must satisfy the condition of irrelevance of LR stress disorder, which is

$$z_\mu < 4 - D - 2\eta, \tag{326}$$

in which case one can neglect in both equations (324) at small k the terms proportional to A_κ . Consider first the case $z_\kappa = 0$: then the situation is very similar to the case of short-range disorder, studied in Section VIB with both types of disorder. Indeed there, the stress disorder is also irrelevant, and balancing the two first terms in the second equation in (324) we obtain $\eta' = 2\eta_{\text{pure}}$, where $\eta = \eta_{\text{pure}}$ is the exponent of the homogeneous membrane. For physical membranes $D = 2, d_c = 1$ this leads to $\eta' \approx 1.66$. Now when LR curvature disorder is included, i.e., $z_\kappa > 0$, balancing again the two first terms in the second equation in (324) gives $\eta'(z_\kappa)$ and the universal amplitude $A_{\kappa\Delta}$ in the LRC phase

$$\begin{aligned}
\eta &= \eta_{\text{pure}}, \\
\eta'(z_\kappa) &= 2\eta_{\text{pure}} - z_\kappa, \\
A_{\kappa\Delta} &= 1.
\end{aligned} \tag{327}$$

This phase is only stable inside the region $z_\mu < z_\mu^{c3}$, outside of which the LR stress disorder becomes relevant, and a new thermal phase which we call LRM appears. From (326) the boundary separating LRC and LRM phases is attained at

$$z_\mu = z_\mu^{c3} = 4 - D - 2\eta_{\text{pure}} = \eta_u^{\text{pure}}. \quad (328)$$

The upper boundary of LRC, z_κ^{c3} , at which LRCG becomes more stable at all temperatures and all strengths of disorder is determined by the condition $\eta'(z_\kappa^{c3}) = \eta(z_\kappa^{c3}) = \eta_{\text{pure}}$, giving from Eq. (327)

$$z_\kappa^{c3} = \eta^{\text{pure}}. \quad (329)$$

(2-ii) long-range mixed disorder (LRM):

From discussion above and from Eqs. (324) we see that a new marginal, temperature-dominated ground state LRM emerges when $z_\kappa > 0$ and $z_\mu > 4 - D - 2\eta_{\text{pure}} = \eta_u^{\text{pure}}$ (≈ 0.358 for physical membranes) and both LR curvature and LR stress disorders are relevant. A balance between all the terms in equations (324) completely determines both exponents,

$$\eta(z_\mu) = 2 - \frac{D}{2} - \frac{z_\mu}{2}, \quad (330)$$

$$\eta'(z_\kappa, z_\mu) = 2\eta(z_\mu) - z_\kappa = 4 - D - z_\mu - z_\kappa. \quad (331)$$

We expect these expressions to be exact, since they are a result of dimensional analysis. The two universal amplitudes $A_\kappa(z_\mu)$, $A_{\kappa\Delta}(z_\kappa, z_\mu)$ are also determined by (324) and are given by

$$A_\kappa(z_\mu) = \frac{1}{2}D(D-1)\Pi(\eta, D) - \frac{d_c\Pi(\eta, D)^2}{2\Sigma(\eta, D)}, \quad (332)$$

$$A_{\kappa\Delta}(z_\kappa, z_\mu) = 1 + \frac{\Sigma(\eta, \eta', D)}{\Sigma(\eta, D)} - \frac{D(D-1)\Sigma(\eta, \eta', D)}{d_c\Pi(\eta, D)},$$

where one inserts $\eta = \eta(z_\mu)$ and $\eta' = \eta'(z_\kappa, z_\mu)$ using (330). We observe that $A_\kappa(z_\mu)$ is identical to that of Eq.(283), and that it vanishes on the vertical line $z_\mu = \eta_u^{\text{pure}}$ ($= 0.358..$, for $D = 2, d_c = 1$) where the LRM phase borders the LRC phase (see Fig. 4). The LRM phase is also bounded from above by the line

$$z_\kappa = 2 - \frac{D}{2} - \frac{z_\mu}{2}, \quad (333)$$

on which $\eta = \eta'$: there the behavior is no longer temperature dominated, and the disorder-dominated LRCG phase takes over. In other words it is stable only when $2z_\kappa + z_\mu < 4 - D$ which is the exact opposite of the condition (322) of stability of the LRMG phase. Finally in Fig. 4 we see that LRM phase is also bounded from below and on the right by the curve L on which the amplitude $A_{\kappa\Delta}(z_\kappa, z_\mu)$ vanishes, signifying the irrelevance of LR curvature disorder. The boundary L in the (z_μ, z_κ) plane is thus given by

$$\frac{D(D-1)\Sigma(\eta, \eta', D)}{d_c\Pi(\eta, D)} - \frac{\Sigma(\eta, \eta', D)}{\Sigma(\eta, D)} = 1, \quad (334)$$

where one inserts $\eta = \eta(z_\mu)$ and $\eta' = \eta'(z_\kappa, z_\mu)$ using (330).

(2-iii) long-range stress disorder (LRS):

As z_μ is increased and z_κ is lowered past the boundary L, the LR curvature disorder becomes irrelevant, while the LR stress disorder remains important and we enter a new, temperature-dominated LRS phase. Since the LR stress is still relevant in the LRS phase, $\eta(z_\mu)$ is still given by Eq.(330) and the associated amplitude A_κ is the same as in the LRM phase, given by Eq. (332). The irrelevance of the LR curvature disorder in this phase allows us to drop the curvature term in (324), resulting in the equation

$$\frac{D(D-1)\Sigma(\eta(z_\mu), \eta')}{d_c\Pi(\eta(z_\mu))} - \frac{\Sigma(\eta(z_\mu), \eta')}{\Sigma(\eta(z_\mu))} = 1, \quad (335)$$

that, together with the value of $\eta(z_\mu)$ given in Eq.(330) determines the $\eta'(z_\mu)$ exponent. We note that unlike in the LRM phase, in the LRS phase the values of the two exponents $\eta'(z_\mu)$ and $\eta(z_\mu)$ are functions only of z_μ .

We observe that the above equation (335) is identical to the second equation in (332) with the amplitude $A_{\kappa\Delta}$ set to 0 or equivalently to Eq.(334). Hence we find that starting from the LRM phase, where the curvature disorder is relevant and has a finite amplitude given by the second line of Eq.(332), the amplitude first decreases and finally vanishes on the boundary L. Beyond this boundary, inside the LRS phase, the curvature disorder is no longer relevant.

The boundary L separating the LRM and the LRS phases can also be obtained from the second of Eqs. (324) by noting where the LR curvature disorder term becomes irrelevant with respect to the left hand side or with respect to LR stress disorder term (which in the LRC phase have the same scaling with k). Looking at the powers of k we find that L is determined by $z_\kappa = 2\eta(z_\mu) - \eta'(z_\mu)$, which together with the first Eq.(330) becomes

$$z_\kappa = 4 - D - z_\mu - \eta'(z_\mu) . \quad (336)$$

In the above equation it is important to remember to use $\eta'(z_\mu)$ inside the LRS phase, given by Eq.(335). The two determining equations of the L boundary (335),(336) are identical to Eqs.(330),(334) used in the determination of the L boundary from requirement of vanishing of $A_{\kappa\Delta}(z_\kappa, z_\mu)$, but have a very different interpretation. It is satisfying to observe that both analysis gives an identical curve $z_\kappa = z_\kappa^L(z_\mu)$ for the L boundary.

Finally it is easy to see that the LRS phase is also bound by a vertical line separating it from a marginal phase LRSM. On this boundary the temperature roughness no long dominates over disorder and $\eta(z_\mu) = \eta'(z_\mu)$. Using this condition inside Eq.(335) we find that on this boundary, in addition to the first equation in (330), i.e., $\eta(z_\mu) = 2 - \frac{D}{2} - \frac{z_\mu}{2}$, $\eta(z_\mu)$ is also given by

$$\frac{D(D-1)\Sigma(\eta)}{2d_c\Pi(\eta)} = 1 , \quad (337)$$

which together with Eqs.(80), (82) gives

$$\eta = \eta_{\text{pure}}(2d_c) , \quad (338)$$

$$= \frac{2}{3}, \text{ for } D = 2, d_c = 1 . \quad (339)$$

Combining with the above other determination of $\eta(z_\mu)$ from Eq.(330) we obtain the right boundary of the LRS phase,

$$z_\mu = 4 - D - 2\eta_{\text{pure}}(2d_c) = \eta_u^{\text{pure}}(2d_c) , \quad (340)$$

$$= \frac{2}{3}, \text{ for } D = 2, d_c = 1 , \quad (341)$$

as represented in the Fig.4.

3. Marginal phases, $\zeta' = \zeta$

Finally we examine solutions to the SCSA equations (193), (194), (195)-(198), (199) of the heterogeneous membrane in LR disorder that are marginal, i.e., characterized by $\eta = \eta'$. As we will see below there are two such solutions, which we call Long-Range Stress Marginal (LRSM) and Long-Range Curvature Marginal (LRCM). As the names imply, in the LRCM phase the LR curvature disorder is relevant and LR stress disorder is irrelevant, while in the LRSM phase the LR stress disorder is relevant and LR curvature disorder is irrelevant. [87] In the phase diagram of Fig. 4, the LRCM phase is the shaded region that overlaps with the temperature dominated phases LRC, LRM, LRS, as well as the disorder-dominated phase LRCG and the second marginal phase LRSM. It is likely, that, although all these phases are stable in the same region of z_κ and z_μ the degeneracy will be lifted by the other physical parameters of the model, such as temperature T and disorder strengths $\Delta_\kappa, \Delta_\mu, \Delta_\lambda$. Varying these additional parameters will induce real thermodynamic phase transitions between the overlapping phases, that can be detected experimentally or numerically. We have not discuss the nature of these phase transitions and leave it for future investigation. Physically we expect that for membranes with z_κ and z_μ , in the shaded region we expect that at low temperatures and strong disorder LRCG will be the stable phase. In the opposite limit of high temperatures and weak disorder, temperature dominated phases LRC, LRM, LRS will characterize the disorder membrane. The marginal LRSM, LRCM phases will exist at intermediate values of temperature and disorder strength.

For the marginal phases with $\eta = \eta'$ at long wavelengths $\Pi_{\kappa\kappa}(\mathbf{q})$ and $\Pi_{\kappa\Delta}(\mathbf{q})$ will have the same scaling behavior with q . We extend the calculation of Section VIB 2 to include LR disorder.

From Eqs. (195) and (213) we find at small q ,

$$\left(\tilde{\mu}(\mathbf{q}), \tilde{\Delta}_\mu(\mathbf{q})\right) \simeq \left(\frac{1}{2(T\Pi_{\kappa\kappa}(\mathbf{q}) + 2\Pi_{\kappa\Delta}(\mathbf{q}))}, \frac{\frac{\Delta_\mu(\mathbf{q})}{2\mu^2} + \Pi_{\Delta\Delta}(\mathbf{q})}{2(T\Pi_{\kappa\kappa}(\mathbf{q}) + 2\Pi_{\kappa\Delta}(\mathbf{q}))^2}\right), \quad (342)$$

$$\simeq \frac{(D^2 - 1)q^{4-D-2\eta}}{2\Pi(\eta, D)} \left(\frac{1}{TZ_\kappa^{-2} + 2Z_\Delta^{-1}Z_\kappa^{-1}}, \frac{Z_\Delta^{-2} + (D^2 - 1)\frac{\Delta_\mu}{2\mu^2\Pi(\eta, D)}q^{4-D-2\eta-z_\mu}}{(TZ_\kappa^{-2} + 2Z_\Delta^{-1}Z_\kappa^{-1})^2}\right), \quad (343)$$

$$\left(\tilde{b}(\mathbf{q}), \tilde{\Delta}_b(\mathbf{q})\right) \simeq \frac{2}{D+1} \left(\tilde{\mu}(\mathbf{q}), \frac{\frac{\Delta_b(\mathbf{q})}{(D+1)b^2} + \Pi_{\Delta\Delta}(\mathbf{q})}{2(T\Pi_{\kappa\kappa}(\mathbf{q}) + 2\Pi_{\kappa\Delta}(\mathbf{q}))^2}\right), \quad (344)$$

$$\simeq \frac{(D-1)q^{4-D-2\eta}}{\Pi(\eta, D)} \left(\frac{1}{TZ_\kappa^{-2} + 2Z_\Delta^{-1}Z_\kappa^{-1}}, \frac{Z_\Delta^{-2} + (D-1)\frac{\Delta_b}{b^2\Pi(\eta, D)}q^{4-D-2\eta-z_\mu}}{(TZ_\kappa^{-2} + 2Z_\Delta^{-1}Z_\kappa^{-1})^2}\right). \quad (345)$$

We now introduce the dimensionless ratio

$$r = \frac{Z_\kappa}{TZ_\Delta} \quad (346)$$

to characterize the ratio of the disorder amplitude to the thermal amplitude. It can also be written $r = a_\Delta/a_T$ in the notations of Section (VIB 2). Substituting the expressions (342) into Eqs.(193), (194), we obtain the self-consistency equations

$$1 = \frac{D(D-1)}{d_c} \left[\frac{1+r}{1+2r} - \frac{r^2}{(1+2r)^2} \right] \frac{\Sigma(\eta, D)}{\Pi(\eta, D)} - \frac{A_\kappa}{(1+2r)^2} \frac{2\Sigma(2\eta + z_\mu/2 + D/2 - 2, \eta, D)}{d_c\Pi(\eta, D)^2} k^{4-D-2\eta-z_\mu}, \quad (347)$$

$$1 = A_{\kappa\Delta}k^{\eta-z_\kappa} + \frac{D(D-1)}{d_c} \frac{r^2}{(1+2r)^2} \frac{\Sigma(\eta, D)}{\Pi(\eta, D)} + \frac{A_\kappa}{(1+2r)^2} \frac{2\Sigma(2\eta + z_\mu/2 + D/2 - 2, \eta, D)}{d_c\Pi(\eta, D)^2} k^{4-D-2\eta-z_\mu},$$

where in the first line we have divided by $Z_\kappa k^{-\eta}$ and in the second line by $Z_\kappa^2 k^{-\eta}/Z_\Delta$. The definitions of the LR disorder dimensionless amplitudes A_κ and $A_{\kappa\Delta}$ are recalled in (325). We note that as expected from the definition of r these equations reduce to disorder- and temperature-dominated ones for $r = \infty$ and $r = 0$, respectively.

We now use these equation to study the two marginal flat phase of a disordered polymerized membrane.

(3-i) long-range stress marginal disorder (LRSM):

In the LRSM phase the LR curvature disorder is irrelevant and the $A_{\kappa\Delta}k^{\eta-z_\kappa}$ term in the second equation of (347) can be dropped at long wavelengths. The relevance of LR stress disorder then demands that

$$\eta(z_\mu) = \eta'(z_\mu) = 2 - D/2 - z_\mu/2. \quad (348)$$

The sum of the two equations (347) gives the equation

$$\frac{(1+r)D(D-1)\Sigma(\eta, D)}{(1+2r)d_c\Pi(\eta, D)} = 1, \quad (349)$$

which determines r as a function of z_μ by plugging in $\eta = \eta(z_\mu)$ (see below). For $r = 0$ this equation is identical to Eq.(337) for $\eta(z_\mu) = \eta'(z_\mu) = \eta_{\text{pure}}(2d_c)$ ($= 2/3$ for $D = 2, d_c = 1$) on the boundary of LRSM phase with the LRS phase. For $r = \infty$ the above equation correctly reduces to Eq.(227), which determines $\eta(z_\mu) = \eta'(z_\mu) = \eta_{\text{pure}}(4d_c) = \eta_{\text{SRdis}}$ ($= 0.449..$ for $D = 2, d_c = 1$) i.e., the exponents of the $T = 0$ SR disorder fixed point, which is also the exponent on the boundary of LRSM phase with the LRSG phase.

Combining these considerations with Eq.(348) we conclude that the LRSM phase exists in the range $\eta_u^{\text{pure}}(2d_c) < z_\mu < \eta_u^{\text{pure}}(4d_c)$ ($2/3 < z_\mu < 2 - 2\eta_{\text{SRdis}} \approx 1.102$, for $D = 2, d_c = 1$), corresponding (in the language of the renormalization group) to a stable $T > 0$ fixed point moving down, as z_μ is increased, until $T = 0$ is reached for $r = \infty$. Hence as z_μ varies in this range, this marginal phase continuously interpolates between the temperature dominated LRS and the disorder dominated LRSG phases, by having the universal amplitude ratio vary in the range $0 < r(z_\mu) < \infty$.

As can be seen from second of Eqs.(347) the LRSM phase is also bounded from above by the line $z_\kappa = 2 - D/2 - z_\mu/2$, i.e., the line same as the upper boundary of LRM phase (333), where LR curvature disorder becomes relevant.

Equation (349) together with (348) also determine the z_μ dependence of the amplitude ratio $r(z_\mu)$ and, taking the difference between the two equations in (347), also determines the universal amplitude $A_\kappa(z_\mu)$, as

$$r(z_\mu) = \frac{D(D-1)\Sigma(\eta(z_\mu), D) - d_c\Pi(\eta(z_\mu), D)}{2d_c\Pi(\eta(z_\mu), D) - D(D-1)\Sigma(\eta(z_\mu), D)}, \quad (350)$$

$$A_\kappa(z_\mu) = \frac{1}{4}(1 + 3r(z_\mu))D(D-1)\Pi(\eta(z_\mu)). \quad (351)$$

(3-ii) long-range curvature marginal disorder (LRCM):

Finally there is a solution to the SCSA equations (347) for which the LR curvature is relevant and the LR stress disorder is irrelevant. Balancing the first two terms in the second equation of (347) we obtain

$$\eta' = \eta = \eta(z_\kappa) = z_\kappa. \quad (352)$$

Neglecting the LR stress disorder in the first equation of (347) we immediately obtain

$$\frac{(1+2r)^2}{(1+3r+r^2)} = \frac{D(D-1)\Sigma(\eta, D)}{d_c\Pi(\eta, D)}. \quad (353)$$

Solving above equation for $r(z_\kappa)$ we find

$$r(z_\kappa) = \frac{3I(z_\kappa) - 4 + \sqrt{(5I(z_\kappa)^2 - 4I(z_\kappa))}}{2(4 - I(z_\kappa))}, \quad I(z_\kappa) := \frac{D(D-1)\Sigma(z_\kappa, D)}{d_c\Pi(z_\kappa, D)}, \quad (354)$$

which leads, for the physical membrane, $D = 2$, $d_c = 1$, to the explicit expression

$$r(z_\kappa) = \frac{-z_\kappa(5z_\kappa + 4) + \sqrt{2}\sqrt{(z_\kappa - 1)(z_\kappa + 1)(z_\kappa(9z_\kappa + 4) - 10)} + 6}{2(z_\kappa(z_\kappa + 4) - 2)}. \quad (355)$$

Using Eq. (347) to compute $A_{\kappa\Delta}(z_\kappa)$ leads to

$$A_{\kappa\Delta}(z_\kappa) = \frac{1 + 3r(z_\kappa)}{1 + 3r(z_\kappa) + r(z_\kappa)^2}, \quad (356)$$

The physical range of $r(z_\kappa)$ is $0 < r(z_\kappa) < \infty$. From the above equation and by comparing with Eqs.(227) and (265) we find that at $r = 0$ $\eta(z_\kappa) = \eta'(z_\kappa) = \eta_{\text{pure}}(d_c)$ ($= 0.820852..$ for $D = 2$, $d_c = 1$) and at $r = \infty$ $\eta(z_\kappa) = \eta'(z_\kappa) = \eta^{\text{pure}}(4d_c) = \eta^{\text{SRdis}}(d_c)$ ($= 0.449..$ for $D = 2$, $d_c = 1$). Plotting the explicit formula (355) fully confirms these predictions, with $r > 0$ in the range. Since $\eta_{\text{pure}}(d_c) > \eta^{\text{SRdis}}(d_c) = \eta_{\text{pure}}(4d_c)$ we conclude that at the upper horizontal part of the boundary of the LRCM phase, Fig. 4, $r = 0$ and $z_\kappa = \eta = \eta' = \eta_{\text{pure}}(d_c)$, while at the lower boundary $r = \infty$ and $z_\kappa = \eta = \eta' = \eta^{\text{SRdis}}(d_c)$.

The condition that the LR stress disorder is irrelevant implies that other part of the upper boundary separating LRCM and LRCG phases is given by $z_\kappa < 2 - D/2 - z_\mu/2$, same as the boundary of the LRM, LRS and LRSM phases with the LRCG. Thus the LRCM solution exists only in the shaded area illustrated in Fig.4. In this shaded region the LRCM solution “coexists” with the disorder-dominated LRCG phase and one of the temperature-dominated solutions (LRC, LRM, LRS phases), as well as with the other marginal LRSM phase. We expect that a thermodynamic phase transition between these phases can be controlled by varying temperature and the strength (amplitude) of disorder. The present marginal fixed point interpolates continuously between the temperature-dominated ($r = 0$) and the LRCG behavior ($r = \infty$) as z_κ increases within the range $\eta^{\text{SRdis}}(d_c) < z_\kappa < \eta^{\text{pure}}(d_c)$.

VIII. CONCLUSIONS

Motivated by a number of physical realizations, particularly freely suspended graphene, we presented a detailed study of tensionless elastic sheets in the presence of thermal fluctuations and/or local heterogeneities due to quenched random internal disorder. We developed a general continuum elastic theory and used it to study statistical mechanics of the crumpled, flat, and a rich variety of glassy wrinkled phases, that are driven by anomalously strong effects of thermal fluctuations and short- and long-ranged quenched internal disorder. We also presented a detailed analysis of some of the associated phase transitions, with a particular focus on the flat-to-crumpled transition in a “phantom” (i.e., neglecting self-avoiding interaction) membrane.

Throughout, we utilized a powerful field-theoretic method of the Self-Consistent Screening Approximation that complements the renormalization group methods, together with the expansion in intrinsic and embedding dimensionalities. As discussed in detail, the advantage of the SCSA is its ability to reproduce and interpolate between exact results in three complementary limits. It is thus highly constrained and is expected to give both qualitative and quantitative predictions, as has been verified in a number of numerical studies.

Acknowledgments

We thank D. R. Nelson for numerous interactions over the years. For the period 1990-1993, when this work was completed, we also take the opportunity to thank D. Bensimon, D. Bowick, M. Kardar, G. Grest, T. Lubensky, M. Mezard, D. Morse, and J. Toner for stimulating discussions. For the more recent period of finishing the writing of the present manuscript we specially thank F. Guinea for useful comments. We also acknowledge discussion with D. Mouhanna. The research part was done while PLD was on leave from LPTENS at the Harvard Physics Department. We thank LPTENS and University of Colorado at Boulder for hospitality while this manuscript was completed. LR also acknowledges support by the NSF grants DMR-1001240, MRSEC DMR-1420736, PHY-1125915, Simons Investigator Fellowship, and thanks KITP and École Normale Supérieure for hospitality during his sabbatical stay, when part of this work was completed.

Appendix A: Useful integrals and identities

In this appendix we present calculational details for a certain class of integrals that are ubiquitous in calculations with massless field theories. For completeness we derive integrals that are more general than necessary for the SCSA calculations of the main text. The motivation is that these more general integrals are necessary for higher order perturbative loop calculations, e.g., as needed to assess the accuracy of the SCSA (not performed here). For this appendix to function as a useful future reference we attempt to derive most relations from first principles.

1. Area of a D -dimensional Sphere

Let S_{D-1} denote an “area” of a $D - 1$ -dimensional sphere. Then for an arbitrary function $f(x)$ spherical symmetry of the integrand gives

$$\int d^D p f(p^2) = S_{D-1} \int dp p^{2D-1} f(p^2). \quad (\text{A1})$$

Although S_{D-1} can be calculated directly by for example by going to D -dimensional polar coordinates and integrating over the polar angles, we will use a short cut.

Since S_{D-1} is independent of function $f(x)$, let us pick a convenient one and compute the above integral. Let us take $f(x) = e^{-x}$, and calculate the left and right hand sides of Eq.(A1). The left hand side can be easily integrated in rectangular coordinates

$$\int d^D p e^{-p^2} = \prod_i^D \int dp_i e^{-p_i^2}, = \left(\int_{-\infty}^{\infty} dp_1 e^{-p_1^2} \right)^D, = (\pi)^{D/2}. \quad (\text{A2})$$

The right hand side is easily computed by making a change of variables $p^2 \rightarrow x$

$$S_{D-1} \int_0^{\infty} dp p^{D-1} e^{-p^2} = \frac{1}{2} S_{D-1} \int_0^{\infty} dx x^{D/2-1} e^{-x}, \quad (\text{A3})$$

$$= \frac{1}{2} S_{D-1} \Gamma(D/2). \quad (\text{A4})$$

Equating the two results and solving for S_D we find

$$S_{D-1} = \frac{2(\pi)^{D/2}}{\Gamma(D/2)}. \quad (\text{A5})$$

2. A Class of Spherically Symmetric Integrals

$$\int_p \frac{p^{2s}}{(p^2 + r)^t} = r^{s-t-D/2} \frac{\Gamma(s + D/2)\Gamma(t - s + D/2)}{(4\pi)^{D/2}\Gamma(D/2)\Gamma(t)}, \quad (\text{A6})$$

where we use notation $\int_p \equiv \int \frac{d^D p}{(2\pi)^D}$.

Proof:

$$I_1 = \int_p \frac{p^{2s}}{(p^2 + r)^t}, \quad (\text{A7})$$

$$= \frac{1}{\Gamma(t)} \int_0^\infty dy y^{t-1} \int p^{2s} e^{-y(p^2+r)},$$

$$= \frac{S_{D-1}}{(2\pi)^D \Gamma(t)} \int_0^\infty dy y^{t-1} e^{-ry} \int_0^\infty dp p^{2s+D-1} e^{-yp^2}, \quad (\text{A8})$$

$$= \frac{1}{(4\pi)^{D/2} \Gamma(D/2) \Gamma(t)} \int_0^\infty dy y^{t-1} e^{-ry} \int_0^\infty dx x^{s+D/2-1} e^{-yx}, \quad (\text{A9})$$

$$= \frac{\Gamma(s + D/2)}{(4\pi)^{D/2} \Gamma(D/2) \Gamma(t)} \int_0^\infty dy y^{t-s-D/2-1} e^{-ry}, \quad (\text{A10})$$

$$= r^{s-t+D/2} \frac{\Gamma(s + D/2)\Gamma(t - s - D/2)}{(4\pi)^{D/2} \Gamma(D/2)\Gamma(t)}. \quad (\text{A11})$$

3. Spherical Average of $\hat{p}_{\alpha_1} \hat{p}_{\alpha_2} \dots \hat{p}_{\alpha_m}$

We now extend above result to an average of a product of unit vectors over a sphere. This will be needed to derive some of the integral identities in the subsequent sections. We will have to compute integrals of the form

$$\int_p \hat{p}_{\alpha_1} \hat{p}_{\alpha_2} \dots \hat{p}_{\alpha_m} f(p^2), \quad (\text{A12})$$

where $f(x)$ is an arbitrary function. Because of the spherical symmetry of $f(p^2)$, the angular part of the integral can be done and amounts to averaging the fully symmetric tensor $\hat{p}_{\alpha_1} \hat{p}_{\alpha_2} \dots \hat{p}_{\alpha_m}$ over the $D - 1$ -dimensional sphere. We denote this average by angular brackets. Since $\delta_{\alpha\beta}$ is the only spherically symmetric tensor and carries two indices, we immediately conclude that spherical average over a product of odd unit vectors (odd m) vanishes. For m even rotational invariance and unit norm of \hat{p}_{α_1} gives

$$\langle \hat{p}_{\alpha_1} \hat{p}_{\alpha_2} \dots \hat{p}_{\alpha_{2n}} \rangle = \frac{1}{C(D, n)} [\delta_{\alpha_1 \alpha_2} \delta_{\alpha_3 \alpha_4} \dots \delta_{\alpha_{2n-1} \alpha_{2n}} + \text{pairings}], \quad (\text{A13})$$

$$= \frac{1}{C(D, n)} S_{\alpha_1 \alpha_2 \dots \alpha_{2n}}^{(n)}, \quad (\text{A14})$$

where the fully symmetric tensor $S_{\alpha_1 \alpha_2 \dots \alpha_{2n}}^{(n)}$ consists of distinct pairings, i.e., permutations that include all distinct rearrangements of $2n$ indices among the $\delta_{\alpha\beta}$, but do not include permutations such as $\delta_{\alpha_1 \alpha_2} \rightarrow \delta_{\alpha_2 \alpha_1}$, nor permutations of pairs of indices such as $\delta_{\alpha_1 \alpha_2} \delta_{\alpha_3 \alpha_4} \rightarrow \delta_{\alpha_3 \alpha_4} \delta_{\alpha_2 \alpha_1}$. For instance

$$S_{\alpha_1 \alpha_2}^{(1)} = \delta_{\alpha_1 \alpha_2}, \quad S_{\alpha_1 \alpha_2 \alpha_3 \alpha_4}^{(2)} = \delta_{\alpha_1 \alpha_2} \delta_{\alpha_3 \alpha_4} + \delta_{\alpha_1 \alpha_3} \delta_{\alpha_2 \alpha_4} + \delta_{\alpha_1 \alpha_4} \delta_{\alpha_2 \alpha_3}, \quad (\text{A15})$$

and so on, $S^{(n)}$ has $(2n - 1)!!$ terms (see below).

We now prove that the constant $C(D, n)$ for arbitrary space dimensionality D and arbitrary number $2n$ of unit vectors is given by

$$C(D, n) = D(D + 2)(D + 4) \dots (D + 2(n - 1)) = 2^n \left(\frac{D}{2} \right)_n, \quad (\text{A16})$$

where $(x)_n = x(x+1)\dots(x+(n-1)) = \Gamma(x+n)/\Gamma(x)$ is the Pochhammer symbol.

We first note that for $D = 1$ the left hand side of the Eq.(A13) is 1. Since in this case $\delta_{\alpha\beta} = 1$, the expression in the square brackets gives the total number of permutations of $2n$ indices not including the interchanges within the pair nor pair interchanges. We therefore find that

$$C(1, n) = \frac{(2n)!}{(2!)^n n!} = (2n-1)!! , \quad (\text{A17})$$

which agrees with the expression for $C(D, n)$ in Eq.(A16) to be proved.

To derive $C(D, n)$ let us contract all the indices in Eq.(A13) in one particular way, say, by letting $\alpha_1 = \alpha_2, \alpha_3 = \alpha_4, \dots, \alpha_{2n-1} = \alpha_{2n}$, and sum over repeated indices. The left hand side is then identically 1. We now must compute the resulting number in the square brackets on right hand side of Eq.(A13). To make things clear let us first work out an example for $n = 3$. Then fully symmetric tensor $S_{\alpha_1\alpha_2\dots\alpha_6}^{(3)}$ is a sum of $(2 \times 3 - 1)!! = 15$ permutation terms

$$\begin{aligned} & [\delta_{\alpha_1\alpha_2}\delta_{\alpha_3\alpha_4}\delta_{\alpha_5\alpha_6}] \\ & + [\delta_{\alpha_1\alpha_2}(\delta_{\alpha_6\alpha_3}\delta_{\alpha_4\alpha_5} + \delta_{\alpha_6\alpha_4}\delta_{\alpha_3\alpha_5}) + \delta_{\alpha_3\alpha_4}(\delta_{\alpha_6\alpha_1}\delta_{\alpha_2\alpha_5} + \delta_{\alpha_6\alpha_2}\delta_{\alpha_1\alpha_5}) + \delta_{\alpha_5\alpha_6}(\delta_{\alpha_2\alpha_3}\delta_{\alpha_4\alpha_1} + \delta_{\alpha_1\alpha_4}\delta_{\alpha_3\alpha_2})] \\ & + [\delta_{\alpha_6\alpha_1}\delta_{\alpha_2\alpha_3}\delta_{\alpha_4\alpha_5} + 7 \text{ permutations}] \end{aligned} \quad (\text{A18})$$

where the 7 permutations in the last term include only those rearrangements of indices that like the first term of these 8 permutations do not allow the contractible pairs of indices $(\alpha_1, \alpha_2), (\alpha_3, \alpha_4), (\alpha_5, \alpha_6)$ to sit on the same $\delta_{\alpha\beta}$. In above expression we purposely organized the terms into groups inside square brackets with the pattern that will generalize for arbitrary n . The first group (containing one term) has all pairs of indices to be contracted sitting on the same $\delta_{\alpha\beta}$. This group (term) will obviously lead to a D^3 term upon contraction, since each $\delta_{\alpha\alpha} = D$. The second group consists of 3×2 terms that have only one $\delta_{\alpha\beta}$ that has contractible indices on the same $\delta_{\alpha\beta}$, contributing a factor of D . This $\delta_{\alpha\beta}$ is multiplied by the terms in parenthesis that do not have any pairs of indices that are contractible sitting on the same $\delta_{\alpha\beta}$, and therefore these products of two $\delta_{\alpha\beta}$ will collapse into one $\delta_{\alpha\alpha}$ upon contraction, contributing only a single power of D . The total contribution of group two is therefore proportional to D^2 . The third group does not have any $\delta_{\alpha\beta}$ that contains contractible indices and each of the products of three $\delta_{\alpha\beta}$ in this group collapses to a single power of D , much like in group two the products in parenthesis did. Upon a contraction we obtain $C(D, 3)$ which is a 3rd order polynomial in D

$$C(D, 3) = D^3 + 6D^2 + 8D , = D(D+2)(D+4) . \quad (\text{A19})$$

It is obvious that for an arbitrary n this structure will generalize. $C(D, n)$ will be a polynomial of order D^n , with monomial D^{n-k} for $k = 0, \dots, n-1$ coming from a k th group that we described above. As in the example the zeroth group that will contribute D^n will come from the n -product of $\delta_{\alpha\beta}$, with all contractible pairs of indices belonging to the same $\delta_{\alpha\beta}$. It is obvious that there is only one such term and therefore the coefficient of D^n is 1. The D^{n-1} will come from group one. $n-1$ powers of D can be broken up into two contributions. One is a factor of D^{n-2} due to $n-2$ tensors $\delta_{\alpha\beta}$ that have all $2(n-2)$ contractible indices sitting on the same $\delta_{\alpha\beta}$. The additional factor of D comes from the remaining product of two $\delta_{\alpha\beta}$, that has all the contractible indices located on different $\delta_{\alpha\beta}$ and therefore fully collapsible to $\delta_{\alpha\alpha} = D$. A k th term proportional to D^{n-k} will come from the group that contains exactly $n-k-1$ contractible pairs of indices belonging to the same $\delta_{\alpha\beta}$ times an additional factor of D from the fully collapsible $k+1$ -product of $\delta_{\alpha\beta}$.

We must now compute the coefficients of these monomials. For the D^{n-k} term we first count the number of ways of selecting which of the $n-k-1$ pairs of indices will sit on the same $\delta_{\alpha\beta}$. This equals to the number of ways of choosing $n-k-1$ out of n objects giving a multiplicative contribution

$$\frac{n!}{(n-k-1)!(k+1)!} \quad (\text{A20})$$

to the coefficient of D^{n-k} (contributing $n-k-1$ of the powers upon the contraction). For each of these choices of $n-k-1$ pairs of indices, there are $(2k)!!$ permutations of the remaining $k+1$ pairs that will fully collapse to a single $\delta_{\alpha\alpha}$, giving an additional factor of D after contraction. Hence the general $C(D, n)$ polynomial has a following form

$$\begin{aligned} C(D, n) = & D^n + \frac{n!}{(n-2)!2!}(2)!!D^{n-1} + \frac{n!}{(n-3)!3!}(4)!!D^{n-2} + \dots \\ & + \frac{n!}{(n-(k+1))!(k+1)!}(2k)!!D^{n-k} + \dots + (2(n-1))!!D . \end{aligned} \quad (\text{A21})$$

A derivation of above polynomial can be expressed diagrammatically. We denote each of the $\delta_{\alpha_1\alpha_2}$ by a vertex with two legs carrying indices α_1, α_2 . In this representation the fully symmetric tensor $S_{\alpha_1\alpha_2\dots\alpha_{2n}}^{(n)}$ in Eq.(A13) is given by a sum over string of n vertices, with $2n$ indexed legs. A full contraction is then represented by pairwise connection of all the $2n$ legs on each n -vertex. As is the case for standard Feynman diagrammatics, each of the resulting loops contributes a factor of D . The k th term of above polynomial D^{n-k} is generated by a sum over all possible leg connections that end up with $n-k$ loops. Diagrammatic combinatorics then leads to a polynomial identical to Eq.(A21). Although it is not obvious, this polynomial can be factorized into the form of Eq.(A16), proving the result that we will use below.

4. Feynman Parameters Integrals

Often to perform integrals we need to combine denominators of the integrand. This can be done using Feynman identity

$$\frac{1}{\prod_1^n A_i^{a_i}} = \frac{\Gamma(\sum_1^n a_i)}{\prod_1^n \Gamma(a_i)} \prod_1^n \left(\int_0^\infty dx_i x_i^{a_i-1} \right) \frac{\delta(1 - \sum_1^n x_i)}{(\sum_1^n x_i A_i)^{\sum_1^n a_i}}. \quad (\text{A22})$$

Proof:

$$\frac{1}{\prod_1^n A_i^{a_i}} = \frac{1}{\Gamma(a_1) \dots \Gamma(a_n)} \int_0^\infty dx_1 \dots dx_n x_1^{a_1-1} \dots x_n^{a_n-1} e^{-A_1 x_1 - A_2 x_2 - \dots - A_n x_n}, \quad (\text{A23})$$

$$= \frac{1}{\prod_1^n \Gamma(a_i)} \prod_1^n \left(\int_0^\infty dx_i x_i^{a_i-1} \right) e^{-\sum_1^n A_i x_i} \int_0^\infty ds \delta\left(\sum_1^n x_i - s\right), \quad (\text{A24})$$

$$= \frac{1}{\prod_1^n \Gamma(a_i)} \prod_1^n \left(\int_0^\infty dx_i x_i^{a_i-1} \right) \delta\left(\sum_1^n x_i - 1\right) \int_0^\infty ds s^{\sum_1^n a_i - 1} e^{-\left(\sum_1^n A_i x_i\right)s}, \quad (\text{A25})$$

$$= \frac{\Gamma(\sum_1^n a_i)}{\prod_1^n \Gamma(a_i)} \prod_1^n \left(\int_0^\infty dx_i x_i^{a_i-1} \right) \frac{\delta(\sum_1^n x_i - 1)}{(\sum_1^n x_i A_i)^{\sum_1^n a_i}}, \quad (\text{A26})$$

where in above we introduced unity in a form of a δ -function and made a change of variables $x_i \rightarrow x_i s$, followed by integration over s .

5. Two Propagator Integrals of Products $q_{\alpha_1} q_{\alpha_2} \dots q_{\alpha_m}$

We now use results of previous subsections to derive integrals that are necessary for evaluating expressions that arise in the SCSSA of the main text. We will derive somewhat more general integrals required for higher order computations in theory of membranes.

We are interested in the integrals of the form

$$I_{\alpha_1\alpha_2\dots\alpha_m}(a, b, \mathbf{p}) = \int_q \frac{q_{\alpha_1} q_{\alpha_2} \dots q_{\alpha_m}}{(\mathbf{p} + \mathbf{q})^{2a} q^{2b}}. \quad (\text{A27})$$

We will begin with the simplest case of $m = 0$, slowly increasing the level of complexity,

$$I(a, b, \mathbf{p}) = \int_q \frac{1}{(\mathbf{p} + \mathbf{q})^{2a} q^{2b}}. \quad (\text{A28})$$

Using Eq.(A22) with $n = 2$, $A_1 = (\mathbf{p} + \mathbf{q})^2$, $A_2 = q^2$, $a_1 = a$, and $a_2 = b$ to combine the denominators we find

$$I(a, b) = \int_q \frac{1}{(\mathbf{p} + \mathbf{q})^{2a} q^{2b}}, \quad (\text{A29})$$

$$= \frac{\Gamma(a+b)}{\Gamma(a)\Gamma(b)} \int_q \int_0^1 dx \frac{x^{a-1} (1-x)^{b-1}}{[x(\mathbf{p} + \mathbf{q})^2 + (1-x)q^2]^{a+b}}, \quad (\text{A30})$$

$$= \frac{\Gamma(a+b)}{\Gamma(a)\Gamma(b)} \int_0^1 dx x^{a-1} (1-x)^{b-1} \int_q \frac{1}{(q^2 + r)^{a+b}}, \quad (\text{A31})$$

where we first integrated over one of the Feynman's parameters using the δ -function, shifted the q integration variable by $\mathbf{q} \rightarrow \mathbf{q} - x\mathbf{p}$ and defined $r = x(1-x)p^2$. Noting that the remaining rotationally invariant integral over \mathbf{q} is of the form of Eq.(A6) we obtain

$$I(a, b) = p^{D-2a-2b} \frac{\Gamma(a+b-D/2)}{(4\pi)^{D/2}\Gamma(a)\Gamma(b)} \int_0^1 dx x^{a-1} (1-x)^{b-1} [x(1-x)]^{D/2-a-b}, \quad (\text{A32})$$

$$= p^{D-2a-2b} \frac{\Gamma(a+b-D/2)}{(4\pi)^{D/2}\Gamma(a)\Gamma(b)} \int_0^1 dx x^{D/2-b-1} (1-x)^{D/2-a-1}, \quad (\text{A33})$$

$$= p^{D-2a-2b} \frac{\Gamma(D/2-a)\Gamma(D/2-b)\Gamma(a+b-D/2)}{(4\pi)^{D/2}\Gamma(a)\Gamma(b)\Gamma(D-a-b)}. \quad (\text{A34})$$

Performing similar steps for $m = 1$ we obtain

$$I_{\alpha_1}(a, b) = \int_q \frac{q_{\alpha_1}}{(\mathbf{p} + \mathbf{q})^{2a} q^{2b}}, \quad (\text{A35})$$

$$= \frac{\Gamma(a+b)}{\Gamma(a)\Gamma(b)} \int_q \int_0^1 dx \frac{x^{a-1} (1-x)^{b-1} q_{\alpha_1}}{[x(\mathbf{p} + \mathbf{q})^2 + (1-x)q^2]^{a+b}}, \quad (\text{A36})$$

$$= \frac{\Gamma(a+b)}{\Gamma(a)\Gamma(b)} \int_0^1 dx x^{a-1} (1-x)^{b-1} \int_q \frac{q_{\alpha_1} - x p_{\alpha_1}}{[q^2 + r]^{a+b}}, \quad (\text{A37})$$

$$= -p_{\alpha_1} p^{D-2a-2b} \frac{\Gamma(a+b-D/2)}{(4\pi)^{D/2}\Gamma(a)\Gamma(b)} \int_0^1 dx x^a (1-x)^{b-1} [x(1-x)]^{D/2-a-b}, \quad (\text{A38})$$

$$= -p_{\alpha_1} p^{D-2a-2b} \frac{\Gamma(a+b-D/2)}{(4\pi)^{D/2}\Gamma(a)\Gamma(b)} \int_0^1 dx x^{D/2-b} (1-x)^{D/2-a-1}, \quad (\text{A39})$$

$$= -p_{\alpha_1} p^{D-2a-2b} \frac{\Gamma(D/2-a)\Gamma(D/2-b+1)\Gamma(a+b-D/2)}{(4\pi)^{D/2}\Gamma(a)\Gamma(b)\Gamma(D-a-b+1)}, \quad (\text{A40})$$

where in (A37) the integral of the part proportional q_{α_1} obviously vanishes by rotational symmetry. Above result can also be simply obtained by noticing that

$$I_{\alpha_1}(a, b) = \frac{1}{2(b-1)} \frac{\partial}{\partial p_{\alpha_1}} \int_q \frac{1}{(\mathbf{p} + \mathbf{q})^{2(b-1)} q^{2a}}, \quad (\text{A41})$$

$$= \frac{1}{2(b-1)} \frac{\partial}{\partial p_{\alpha_1}} I(b-1, a), \quad (\text{A42})$$

$$= -p_{\alpha_1} p^{D-2a-2b} \frac{\Gamma(D/2-a)\Gamma(D/2-b+1)\Gamma(a+b-D/2)}{(4\pi)^{D/2}\Gamma(a)\Gamma(b)\Gamma(D-a-b+1)}, \quad (\text{A43})$$

where in going from (A42) to (A43) we used Eq.(A34) and the recursion formula for Gamma-functions, $\Gamma(a) = a\Gamma(a-1)$.

For $m = 2$ we have

$$I_{\alpha_1\alpha_2}(a, b) = \int_q \frac{q_{\alpha_1} q_{\alpha_2}}{(\mathbf{p} + \mathbf{q})^{2a} q^{2b}}, \quad (\text{A44})$$

$$= \frac{\Gamma(a+b)}{\Gamma(a)\Gamma(b)} \int_0^1 dx x^{a-1} (1-x)^{b-1} \int_q \frac{q_{\alpha_1} q_{\alpha_2} + x^2 p_{\alpha_1} p_{\alpha_2}}{(q^2 + r)^{a+b}}, \quad (\text{A45})$$

$$= \frac{\Gamma(a+b)}{\Gamma(a)\Gamma(b)} \int_0^1 dx x^{a-1} (1-x)^{b-1} \int_q \left[\frac{\delta_{\alpha_1\alpha_2}}{D} \frac{q^2}{(q^2 + r)^{a+b}} + \frac{x^2 p_{\alpha_1} p_{\alpha_2}}{(q^2 + r)^{a+b}} \right], \quad (\text{A46})$$

$$= \frac{p^{2(D/2-a-b+1)}}{(4\pi)^{D/2}\Gamma(a)\Gamma(b)} \int_0^1 dx x^{a-1} (1-x)^{b-1} \left[\delta_{\alpha_1\alpha_2} \Gamma(a+b-D/2-1) (x(1-x))^{D/2-a-b+1} \right. \\ \left. + \hat{p}_{\alpha_1} \hat{p}_{\alpha_2} \Gamma(a+b-D/2) x^2 (x(1-x))^{D/2-a-b} \right], \quad (\text{A47})$$

$$= p^{2(D/2-a-b+1)} \left[\delta_{\alpha_1\alpha_2} \frac{\Gamma(a+b-D/2-1)\Gamma(D/2-a+1)\Gamma(D/2-b+1)}{2(4\pi)^{D/2}\Gamma(a)\Gamma(b)\Gamma(D-a-b+2)} \right. \\ \left. + \hat{p}_{\alpha_1} \hat{p}_{\alpha_2} \frac{\Gamma(a+b-D/2)\Gamma(D/2-a)\Gamma(D/2-b+2)}{(4\pi)^{D/2}\Gamma(a)\Gamma(b)\Gamma(D-a-b+2)} \right], \quad (\text{A48})$$

where in (A45) again by symmetry the terms with odd number of q_α vanished and to get to (A46) we used Eq.(A13) for $n = 1$. We also introduced a unit vector $\hat{\mathbf{p}} = \mathbf{p}/p$. Another way to obtain above result is to note the recursion relation

$$I_{\alpha_1\alpha_2}(a,b) = \frac{1}{4(b-1)(b-2)} \frac{\partial}{\partial p_{\alpha_1} \partial p_{\alpha_2}} I(b-2,a) + \frac{1}{2(b-1)} \delta_{\alpha_1\alpha_2} I(b-1,a), \quad (\text{A49})$$

and use Eq.(A32).

By repeating the integration steps of Eqs.(A29),(A32),(A35),(A44) for higher values of m we observe a general structure that emerges. For arbitrary m in making the shift in the q integration we will obtain in the numerator m factors $(q_{\alpha_i} + xp_{\alpha_i})$. Upon expanding this product all the terms containing an odd number q_{α_i} vanish by rotational symmetry. For $m = 2n$ even, we organize all the remaining terms into groups by the number of pairs of q_{α_i} contained in the term, because via Eq.(A13) the \mathbf{q} integration for each member of a group is of the same form. Each member of a group of k pairs of q_{α_i} is multiplied by a one of the possible products $2(n-k)$ vectors $x\hat{p}_{\alpha_i}$, carrying the remaining $2(n-k)$ indices. After the \mathbf{q} integration a k th group becomes proportional to a tensor $S_{\alpha_1\alpha_2\ldots\alpha_{2n}}^{(k,2n)}(\hat{\mathbf{p}})$ that is a sum of tensors of the form

$$S_{\alpha_1\alpha_2\ldots\alpha_{2k}}^{(k)} \hat{p}_{\alpha_{2k+1}} \hat{p}_{\alpha_{2k+2}} \cdots \hat{p}_{\alpha_{2n}}, \quad (\text{A50})$$

with the permutations ranging over all possible ways of dividing up the $2n$ indices between the $S_{\alpha_1\alpha_2\ldots\alpha_{2k}}^{(k)}$ and $\hat{p}_{\alpha_{2k+1}} \hat{p}_{\alpha_{2k+2}} \cdots \hat{p}_{\alpha_{2n}}$ tensors.

For odd $m = 2n+1$ the structure is very similar to that of $m = 2n$, but with an additional factor of p_{α_i} multiplying each tensor, symmetrized over all indices. We now summarize the results of integration for several values of m .

$m = 3$:

$$I_{\alpha_1\alpha_2\alpha_3}(a,b) = -p^{D-2a-2b+3} \left[S_{\alpha_1\alpha_2\alpha_3}^{(1,3)} \frac{\Gamma(a+b-D/2-1)\Gamma(D/2-a+1)\Gamma(D/2-b+2)}{2(4\pi)^{D/2}\Gamma(a)\Gamma(b)\Gamma(D-a-b+3)} \right. \\ \left. + S_{\alpha_1\alpha_2\alpha_3}^{(0,3)} \frac{\Gamma(a+b-D/2)\Gamma(D/2-a)\Gamma(D/2-b+3)}{(4\pi)^{D/2}\Gamma(a)\Gamma(b)\Gamma(D-a-b+3)} \right], \quad (\text{A51})$$

where as explained above

$$S_{\alpha_1\alpha_2\alpha_3}^{(1,3)} = \hat{p}_{\alpha_1} S_{\alpha_2\alpha_3}^{(1)} + \hat{p}_{\alpha_2} S_{\alpha_3\alpha_1}^{(1)} + \hat{p}_{\alpha_3} S_{\alpha_1\alpha_2}^{(1)}, \quad (\text{A52})$$

$$S_{\alpha_1\alpha_2\alpha_3}^{(0,3)} = \hat{p}_{\alpha_1} \hat{p}_{\alpha_2} \hat{p}_{\alpha_3}, \quad (\text{A53})$$

$m = 4$:

$$I_{\alpha_1\alpha_2\alpha_3\alpha_4}(a,b) = p^{D-2a-2b+4} \left[S_{\alpha_1\alpha_2\alpha_3\alpha_4}^{(2,4)} \frac{\Gamma(a+b-D/2-2)\Gamma(D/2-a+2)\Gamma(D/2-b+2)}{4(4\pi)^{D/2}\Gamma(a)\Gamma(b)\Gamma(D-a-b+4)} \right. \\ \left. + S_{\alpha_1\alpha_2\alpha_3\alpha_4}^{(1,4)} \frac{\Gamma(a+b-D/2-1)\Gamma(D/2-a+1)\Gamma(D/2-b+3)}{2(4\pi)^{D/2}\Gamma(a)\Gamma(b)\Gamma(D-a-b+4)} \right. \\ \left. + S_{\alpha_1\alpha_2\alpha_3\alpha_4}^{(0,4)} \frac{\Gamma(a+b-D/2)\Gamma(D/2-a)\Gamma(D/2-b+4)}{(4\pi)^{D/2}\Gamma(a)\Gamma(b)\Gamma(D-a-b+4)} \right], \quad (\text{A54})$$

where the tensors are

$$S_{\alpha_1\alpha_2\alpha_3}^{(2,4)} = S_{\alpha_1\alpha_2\alpha_3\alpha_4}^{(2)}, \quad (\text{A55})$$

$$S_{\alpha_1\alpha_2\alpha_3\alpha_4}^{(1,4)} = \hat{p}_{\alpha_1} \hat{p}_{\alpha_2} S_{\alpha_3\alpha_4}^{(1)} + \hat{p}_{\alpha_1} \hat{p}_{\alpha_3} S_{\alpha_2\alpha_4}^{(1)} + \hat{p}_{\alpha_1} \hat{p}_{\alpha_4} S_{\alpha_2\alpha_3}^{(1)} + \\ \hat{p}_{\alpha_2} \hat{p}_{\alpha_3} S_{\alpha_1\alpha_4}^{(1)} + \hat{p}_{\alpha_2} \hat{p}_{\alpha_4} S_{\alpha_1\alpha_3}^{(1)} + \hat{p}_{\alpha_3} \hat{p}_{\alpha_4} S_{\alpha_1\alpha_2}^{(1)}, \quad (\text{A56})$$

$$S_{\alpha_1\alpha_2\alpha_3\alpha_4}^{(0,4)} = \hat{p}_{\alpha_1} \hat{p}_{\alpha_2} \hat{p}_{\alpha_3} \hat{p}_{\alpha_4}. \quad (\text{A57})$$

$m = 5$:

$$I_{\alpha_1\alpha_2\alpha_3\alpha_4\alpha_5}(a,b) = -p^{D-2a-2b+5} \left[S_{\alpha_1\alpha_2\alpha_3\alpha_4\alpha_5}^{(2,5)} \frac{\Gamma(a+b-D/2-2)\Gamma(D/2-a+2)\Gamma(D/2-b+3)}{4(4\pi)^{D/2}\Gamma(a)\Gamma(b)\Gamma(D-a-b+5)} \right. \\ \left. + S_{\alpha_1\alpha_2\alpha_3\alpha_4\alpha_5}^{(1,5)} \frac{\Gamma(a+b-D/2-1)\Gamma(D/2-a+1)\Gamma(D/2-b+4)}{2(4\pi)^{D/2}\Gamma(a)\Gamma(b)\Gamma(D-a-b+5)} \right. \\ \left. + S_{\alpha_1\alpha_2\alpha_3\alpha_4\alpha_5}^{(0,5)} \frac{\Gamma(a+b-D/2)\Gamma(D/2-a)\Gamma(D/2-b+5)}{(4\pi)^{D/2}\Gamma(a)\Gamma(b)\Gamma(D-a-b+5)} \right], \quad (\text{A58})$$

where the tensors are

$$S_{\alpha_1\alpha_2\alpha_3\alpha_4\alpha_5}^{(2,5)} = \hat{p}_{\alpha_1} S_{\alpha_1\alpha_2\alpha_3\alpha_4}^{(2)} + 4 \text{ other permutations} , \quad (\text{A59})$$

$$S_{\alpha_1\alpha_2\alpha_3\alpha_4\alpha_5}^{(1,5)} = \hat{p}_{\alpha_1}\hat{p}_{\alpha_2}\hat{p}_{\alpha_3}S_{\alpha_4\alpha_5}^{(1)} + 9 \text{ other permutations} , \quad (\text{A60})$$

$$S_{\alpha_1\alpha_2\alpha_3\alpha_4\alpha_5}^{(0,5)} = \hat{p}_{\alpha_1}\hat{p}_{\alpha_2}\hat{p}_{\alpha_3}\hat{p}_{\alpha_4}\hat{p}_{\alpha_5} . \quad (\text{A61})$$

In the expression for tensor $S_{\alpha_1\alpha_2\alpha_3\alpha_4\alpha_5}^{(1,5)}$ the permutations are the $5!/2!/3! = 10$ ways of choosing a set of 3 indices that will sit on the $\hat{\mathbf{p}}$ vectors. Similarly, in (A59) the $5!/1!/4! = 5$ permutations correspond to different ways of choosing which one index will sit on $\hat{\mathbf{p}}$. From above expressions, it is quite obvious how to construct the solution to the integrals of this form for an arbitrary m .

6. Summary

Let us define

$$H_{n,m}(a,b) = \frac{\Gamma(a+b-D/2-n)\Gamma(D/2-a+n)\Gamma(D/2-b+m-n)}{2^n(4\pi)^{D/2}\Gamma(a)\Gamma(b)\Gamma(D-a-b+m)} \quad (\text{A62})$$

Then we have shown

$$\begin{aligned} I_{\alpha_1}(a,b) &= -p^{D-2a-2b+1} S_{\alpha_1}^{(0,1)} H_{0,1}(a,b) \\ I_{\alpha_1\alpha_2}(a,b) &= p^{D-2a-2b+2} \left[S_{\alpha_1\alpha_2}^{(1,2)} H_{1,2}(a,b) + S_{\alpha_1\alpha_2}^{(0,2)} H_{0,2}(a,b) \right] \\ I_{\alpha_1\alpha_2\alpha_3}(a,b) &= -p^{D-2a-2b+3} \left[S_{\alpha_1\alpha_2\alpha_3}^{(1,3)} H_{1,3}(a,b) + S_{\alpha_1\alpha_2\alpha_3}^{(0,3)} H_{0,3}(a,b) \right] \\ I_{\alpha_1\alpha_2\alpha_3\alpha_4}(a,b) &= p^{D-2a-2b+4} \left[S_{\alpha_1\alpha_2\alpha_3\alpha_4}^{(2,4)} H_{2,4}(a,b) + S_{\alpha_1\alpha_2\alpha_3\alpha_4}^{(1,4)} H_{1,4}(a,b) + S_{\alpha_1\alpha_2\alpha_3\alpha_4}^{(0,4)} H_{0,4}(a,b) \right] \\ I_{\alpha_1\alpha_2\alpha_3\alpha_4\alpha_5}(a,b) &= -p^{D-2a-2b+5} \left[S_{\alpha_1\alpha_2\alpha_3\alpha_4\alpha_5}^{(2,5)} H_{2,5}(a,b) + S_{\alpha_1\alpha_2\alpha_3\alpha_4\alpha_5}^{(1,5)} H_{1,5}(a,b) + S_{\alpha_1\alpha_2\alpha_3\alpha_4\alpha_5}^{(0,5)} H_{0,5}(a,b) \right] \end{aligned} \quad (\text{A63})$$

Hence each term $H_{n,m}(a,b)$ is paired with the symmetric tensor $S^{(n,m)}$ with m indices and n Kronecker delta, defined above, i.e.,

$$S_{\alpha_1}^{(0,1)} = \hat{p}_{\alpha_1} , \quad S_{\alpha_1\alpha_2}^{(1,2)} = \delta_{\alpha_1\alpha_2} , \quad S_{\alpha_1\alpha_2}^{(0,2)} = \hat{p}_{\alpha_1}\hat{p}_{\alpha_2} , \dots , \quad (\text{A64})$$

i.e., $m-2n$ is the number of \hat{p} 's appearing in the tensor (n,m) . We also note useful recursion relations,

$$H_{n,m+1}(a,b) = \frac{D-2b+2m-2n}{2(D-a-b+m)} H_{n,m}(a,b) , \quad (\text{A65})$$

$$H_{n-1,m}(a,b) = \frac{(2a+2b-D-2n)(-2b+D+2m-2n)}{-2a+D+2n-2} H_{n,m}(a,b) . \quad (\text{A66})$$

Appendix B: Results for the SCSA integrals

Here we give the results for the integrals needed in the text. From (A54) we have

$$\Pi(\eta, \eta', D) = \int_p \frac{(p_\alpha P_{\alpha\beta}^T(\hat{\mathbf{q}}) p_\beta)^2}{|\mathbf{p}|^{4-\eta} |\mathbf{p} + \hat{\mathbf{q}}|^{4-\eta'}} = P_{\alpha_1\alpha_2}^T(\hat{\mathbf{q}}) P_{\alpha_3\alpha_4}^T(\hat{\mathbf{q}}) I_{\alpha_1\alpha_2\alpha_3\alpha_4}(2-\frac{\eta}{2}, 2-\frac{\eta'}{2}, \hat{\mathbf{q}}) , \quad (\text{B1})$$

$$= (D^2 - 1) \frac{\Gamma(2-\frac{\eta+\eta'}{2}-\frac{D}{2})\Gamma(\frac{D}{2}+\frac{\eta}{2})\Gamma(\frac{D}{2}+\frac{\eta'}{2})}{4(4\pi)^{D/2}\Gamma(2-\frac{\eta}{2})\Gamma(2-\frac{\eta'}{2})\Gamma(D+\frac{\eta+\eta'}{2})} \quad (\text{B2})$$

which leads to the integral given in the text in (73). Note that the other terms vanish because of the transverse projectors and we used that

$$P_{\alpha_1\alpha_2}^T(\mathbf{q}) P_{\alpha_3\alpha_4}^T(\mathbf{q}) S_{\alpha_1\alpha_2\alpha_3}^{(2,4)} = D^2 - 1 . \quad (\text{B3})$$

Let us consider now the second integral. We have

$$\begin{aligned}\Sigma(\eta, \eta', D) &= \int_q \frac{(\hat{k}_\alpha P_{\alpha\beta}^T(\hat{\mathbf{q}}) \hat{k}_\beta)^2 |\mathbf{q}|^{4-D-2\eta}}{|\hat{\mathbf{k}} + \mathbf{q}|^{4-\eta'}} , \\ &= I(2 - \frac{\eta'}{2}, \frac{D}{2} + \eta - 2, \hat{\mathbf{k}}) - 2\hat{k}_{\alpha_1} \hat{k}_{\alpha_2} I_{\alpha_1, \alpha_2}(2 - \frac{\eta'}{2}, \frac{D}{2} + \eta - 1, \hat{\mathbf{k}}) + \hat{k}_{\alpha_1} \hat{k}_{\alpha_2} \hat{k}_{\alpha_3} \hat{k}_{\alpha_4} I_{\alpha_1, \alpha_2, \alpha_3, \alpha_4}(2 - \frac{\eta'}{2}, \frac{D}{2} + \eta, \hat{\mathbf{k}}) .\end{aligned}\tag{B4}$$

Using the above expressions (A32), (A44), (A54), (A55) and performing the tensor contractions we obtain

$$\Sigma(\eta, \eta', D) = \frac{(D^2 - 1) \Gamma(2 - \eta) \Gamma\left(\frac{D}{2} + \frac{\eta'}{2}\right) \Gamma\left(\eta - \frac{\eta'}{2}\right)}{4(4\pi)^{D/2} \Gamma\left(2 - \frac{\eta'}{2}\right) \Gamma\left(\frac{D}{2} + \eta\right) \Gamma\left(\frac{D}{2} - \eta + \frac{\eta'}{2} + 2\right)} .\tag{B5}$$

We notice that the results for Π and Σ can be rewritten in a more compact unified way

$$\Pi(\eta, \eta', D) = \frac{D^2 - 1}{4(4\pi)^{D/2}} F_D\left(\frac{D}{2} + \frac{\eta}{2}, \frac{D}{2} + \frac{\eta'}{2}\right) ,\tag{B6}$$

$$\Sigma(\eta, \eta', D) = \frac{D^2 - 1}{4(4\pi)^{D/2}} F_D\left(2 - \eta, \frac{D}{2} + \frac{\eta'}{2}\right) ,\tag{B7}$$

with

$$F_D(a, b) = \frac{\Gamma(a) \Gamma(b) \Gamma(2 + \frac{D}{2} - a - b)}{\Gamma(2 + \frac{D}{2} - a) \Gamma(2 + \frac{D}{2} - b) \Gamma(a + b)} .\tag{B8}$$

Appendix C: Crumpling transition integrals

Here we work out integrals necessary for the analysis of the crumpling transition. To utilize the results of the previous sections, let us rewrite (114) in a generalized form, as

$$\Pi_{\alpha\beta, \gamma\delta}(\mathbf{p}) = \frac{1}{4} \int_q (q_\alpha(p_\beta + q_\beta) + q_\beta(p_\alpha + q_\alpha))(q_\gamma(p_\delta + q_\delta) + q_\delta(p_\gamma + q_\gamma)) \frac{1}{(\mathbf{p} + \mathbf{q})^{2a} q^{2b}} ,\tag{C1}$$

where in the case of interest $2a = 2b = 4 - \eta$. Then in terms of previous derived integrals, it can be rewritten as

$$\Pi_{\alpha\beta, \gamma\delta}(\mathbf{p}) = \text{sym}_{\alpha, \beta} \text{sym}_{\gamma, \delta} [p_\beta p_\delta I_{\alpha\gamma}(a, b, \mathbf{p}) + p_\delta I_{\alpha\beta\gamma}(a, b, \mathbf{p}) + p_\beta I_{\alpha\gamma\delta}(a, b, \mathbf{p})] + I_{\alpha\beta\gamma\delta}(a, b, \mathbf{p}) ,\tag{C2}$$

where $\text{sym}_{\alpha, \beta}$ is a symmetrization over α, β indices.

To calculate the polarization integrals, $\pi_i(\mathbf{p})$, we will use that

$$(D - 1)\pi_3(\mathbf{p}) = P_{\alpha\beta}^T(\mathbf{p}) \Pi_{\alpha\beta, \gamma\delta}(\mathbf{p}) P_{\gamma\delta}^T(\mathbf{p}) ,\tag{C3}$$

$$\pi_5(\mathbf{p}) = P_{\alpha\beta}^L(\mathbf{p}) \Pi_{\alpha\beta, \gamma\delta}(\mathbf{p}) P_{\gamma\delta}^L(\mathbf{p}) ,\tag{C4}$$

$$\sqrt{D - 1}\pi_4(\mathbf{p}) = P_{\alpha\beta}^L(\mathbf{p}) \Pi_{\alpha\beta, \gamma\delta}(\mathbf{p}) P_{\gamma\delta}^T(\mathbf{p}) = P_{\alpha\beta}^T(\mathbf{p}) \Pi_{\alpha\beta, \gamma\delta}(\mathbf{p}) P_{\gamma\delta}^L(\mathbf{p}) .\tag{C5}$$

It is also convenient to define

$$S_{AB}^{(n, 4)} = P_{\alpha\beta}^A(\mathbf{p}) S_{\alpha\beta\gamma\delta}^{(n, 4)} P_{\gamma\delta}^B(\mathbf{p}) .\tag{C6}$$

Thus we have, using that $B_{\alpha\beta} \text{sym}_{\alpha, \beta} A_{\alpha\beta} = B_{\alpha\beta} A_{\alpha\beta}$ for any symmetric tensor B ,

$$(D - 1)\pi_3(\mathbf{p}) = P_{\alpha\beta}^T(\mathbf{p}) I_{\alpha\beta\gamma\delta}(a, b, \mathbf{p}) P_{\gamma\delta}^T(\mathbf{p}) = S_{TT}^{(2, 4)} H_{2, 4}(a, b) = (D^2 - 1) H_{2, 4}(a, b) p^{D-2a-2b+4} ,\tag{C7}$$

where we used $S_{TT}^{(2, 4)} = S_{TT}^{(2)} = D^2 - 1$ and $S_{TT}^{(1, 4)} = S_{TT}^{(0, 4)} = 0$. Thus, we obtain

$$\pi_3(\mathbf{p}) = (D + 1) H_{2, 4}(a, b) p^{D-2a-2b+4} = \big|_{a=b=2-\eta/2} \frac{\Pi(\eta, D)}{D - 1} p^{D-4+2\eta} .\tag{C8}$$

Next we have

$$\sqrt{D-1}\pi_4(\mathbf{p}) = P_{\alpha\beta}^L(\mathbf{p})(I_{\alpha\beta\gamma\delta}(a, b, \mathbf{p}) + p_\beta I_{\alpha\gamma\delta}(a, b, \mathbf{p}))P_{\gamma\delta}^T(\mathbf{p}), \quad (\text{C9})$$

$$\begin{aligned} &= p^{D-2a-2b+4}(S_{LT}^{(2,4)}H_{2,4}(a, b) + S_{LT}^{(1,4)}H_{1,4}(a, b) - P_{\alpha\beta}^L(\mathbf{p})\hat{p}_\beta S_{\alpha\gamma\delta}^{(1,3)}P_{\gamma\delta}^T(\mathbf{p})H_{1,3}(a, b)), \\ &= (D-1)(H_{2,4}(a, b) + H_{1,4}(a, b) - H_{1,3}(a, b)), \\ &= (D-1)(5-2a-2b+D)H_{2,4}(a, b)p^{D-2a-2b+4}, \end{aligned} \quad (\text{C10})$$

using that $S_{LT}^{(0,4)} = 0$ and $P_{\alpha\beta}^L(\mathbf{p})\hat{p}_\beta S_{\alpha\gamma\delta}^{(0,3)}P_{\gamma\delta}^T(\mathbf{p}) = 0$. In the last line we used that $S_{LT}^{(2,4)} = S_{LT}^{(1,4)} = P_{\alpha\beta}^L(\mathbf{p})\hat{p}_\beta S_{\alpha\gamma\delta}^{(1,3)}P_{\gamma\delta}^T(\mathbf{p}) = D-1$. Hence we have

$$\frac{\pi_4(\mathbf{p})}{\pi_3(\mathbf{p})} = \frac{\sqrt{D-1}}{D+1}(5-2a-2b+D) = |_{a=b=2-\eta/2} \frac{\sqrt{D-1}}{D+1}(D+2\eta-3). \quad (\text{C11})$$

Then we have,

$$\pi_5(\mathbf{p}) = \hat{p}_\alpha \hat{p}_\gamma p^2 I_{\alpha\gamma}(a, b, \mathbf{p}) + 2\hat{p}_\alpha \hat{p}_\gamma \hat{p}_\delta p I_{\alpha\gamma\delta}(a, b, \mathbf{p}) + \hat{p}_\alpha \hat{p}_\beta \hat{p}_\gamma \hat{p}_\delta I_{\alpha\beta\gamma\delta}(a, b, \mathbf{p}), \quad (\text{C12})$$

$$= p^{D-2a-2b+4}[H_{1,2}(a, b) + H_{0,2}(a, b) - 6H_{1,3}(a, b) - 2H_{0,3}(a, b) + 3H_{2,4}(a, b) + 6H_{1,4}(a, b) + H_{0,4}(a, b)]. \quad (\text{C13})$$

With this, we obtain

$$\frac{\pi_5(\mathbf{p})}{\pi_3(\mathbf{p})} = \frac{1}{D+1}(4a^2 - 4D(a+b-2) + \frac{4(b-1)(a-b+1)}{-2a+D+2} - \frac{4(a-1)(a-b-1)}{-2b+D+2} + 8ab - 16a + 4b^2 - 16b + D^2 + 15), \quad (\text{C14})$$

$$= |_{a=b=2-\eta/2} \frac{(-22 + 31D - 10D^2 + D^3 + 43\eta - 32D\eta + 5D^2\eta - 24\eta^2 + 8D\eta^2 + 4\eta^3)}{(D+1)(D-2+\eta)}. \quad (\text{C15})$$

For the remaining integrals we use Mathematica. We find

$$\pi_2(\mathbf{p}) = \frac{1}{D-1}(W_2)_{\alpha\beta,\gamma\delta}\Pi_{\alpha\beta,\gamma\delta}(\mathbf{p}), \quad (\text{C16})$$

$$= (2H_{2,4}(a, b) + 2H_{1,4}(a, b) + \frac{1}{2}H_{1,2}(a, b) - 2H_{1,3}(a, b))p^{D-2a-2b+4}, \quad (\text{C17})$$

where $(W_2)_{\alpha\beta,\alpha\beta} = D-1$. This leads to

$$\frac{\pi_5(\mathbf{p})}{\pi_3(\mathbf{p})} = \frac{1}{D+1}\left(\frac{2(b-1)(a-b+1)}{D+2-2a} + \frac{2(a-1)(b-a+1)}{D+2-2b}\right) = |_{a=b=2-\eta/2} \frac{1}{D+1} \frac{2(2-\eta)}{D+\eta-2}. \quad (\text{C18})$$

Finally,

$$\pi_1(\mathbf{p}) = \frac{2}{(D-2)(D+1)}(W_2)_{\alpha\beta,\gamma\delta}\Pi_{\alpha\beta,\gamma\delta}(\mathbf{p}), \quad (\text{C19})$$

$$= 2H_{2,4}(a, b)p^{D-2a-2b+4}, \quad (\text{C20})$$

where $(W_1)_{\alpha\beta,\alpha\beta} = (D-2)(D+1)/2$, which leads to (for any a, b)

$$\frac{\pi_1(\mathbf{p})}{\pi_3(\mathbf{p})} = \frac{2}{D+1}. \quad (\text{C21})$$

We now calculate the height-field self-energy integrals, $b_i(a, b, D)$, defined by (up to a small change in notations and the change $\mathbf{q} \rightarrow -p\mathbf{q}$),

$$b_i(a, b, D) = \int_{\mathbf{q}} q^{-2b} |\hat{\mathbf{p}} + \mathbf{q}|^{-2a} \hat{p}_\alpha (\hat{p}_\beta + q_\beta) (W_i)_{\alpha\beta,\gamma\delta}(\mathbf{q}) \hat{p}_\gamma (\hat{p}_\delta + q_\delta), \quad (\text{C22})$$

which we will need in the text in (123) for $a = 2 - \eta/2$ and $b = D/2 - 2 + \eta$.

Let us start with b_3 . From the definition

$$(D-1)b_3 = \int_q q^{-2b} |\hat{\mathbf{p}} + \mathbf{q}|^{-2a} (\hat{p}_\alpha P_{\alpha\beta}^T(\mathbf{q}) \hat{p}_\beta)^2 = \Sigma(2+b-D/2, 4-2a), \quad (\text{C23})$$

$$= \frac{D^2-1}{4(4\pi)^{D/2}} \frac{\Gamma(D/2-b)\Gamma(\frac{D}{2}+2-a)\Gamma(a+b-\frac{D}{2})}{\Gamma(2+b)\Gamma(a)\Gamma(D+2-a-b)} = (D^2-1)H_{2,4}(a, b+2), \quad (\text{C24})$$

which for $a = 2 - \eta/2$ and $b = D/2 - 2 + \eta$ leads to

$$b_3 = (D+1) \frac{\Sigma(\eta, D)}{D^2-1}. \quad (\text{C25})$$

Using Mathematica we find next,

$$\sqrt{D-1}b_4 = 2(D-1)(1+2b-D)H_{2,4}(a, b+2), \quad (\text{C26})$$

which for $a = 2 - \eta/2$ and $b = D/2 - 2 + \eta$ gives

$$b_4 = 2\sqrt{D-1}(2\eta-3) \frac{\Sigma(\eta, D)}{D^2-1}. \quad (\text{C27})$$

We also find

$$b_5 = \left(-\frac{4(b+1)(-a+b+1)}{-2a+D+2} - \frac{4(a-1)(b+1)}{D-2(a+b-1)} + 4b^2 - 4(b+1)D + 8b + D^2 + 3 \right) H_{2,4}(a, b+2), \quad (\text{C28})$$

which for $a = 2 - \eta/2$ and $b = D/2 - 2 + \eta$ leads to

$$b_5 = -\frac{2D^2 - 4D\eta^2 + 16D\eta - 15D - 4\eta^3 + 24\eta^2 - 43\eta + 22}{D + \eta - 2} \times \frac{\Sigma(\eta, D)}{D^2-1}. \quad (\text{C29})$$

Similarly, we obtain

$$b_2 = \frac{2(D-1)(a^2(8b-4D+4) + 4a(b-D-2)(2b-D+1) + (b-D-3)(b-D)(2b-D) + 4(b+1))}{(2a-D-2)(2(a+b-1)-D)} H_{2,4}(a, b+2). \quad (\text{C30})$$

which for $a = 2 - \eta/2$ and $b = D/2 - 2 + \eta$ reduces to

$$b_2 = -\frac{(D-1)(D^2+2\eta-4)}{D+\eta-2} \times \frac{\Sigma(\eta, D)}{D^2-1}. \quad (\text{C31})$$

Finally, we find

$$b_1 = (D-2)(D+1)H_{2,4}(a, b+2) \quad (\text{C32})$$

which for $a = 2 - \eta/2$ and $b = D/2 - 2 + \eta$ gives

$$b_1 = (D-2)(D+1) \times \frac{\Sigma(\eta, D)}{D^2-1}. \quad (\text{C33})$$

-
- [1] P. LeDoussal and L. Radzihovsky, *Phys. Rev. Lett.* **69**, 1209 (1992).
[2] P. LeDoussal and L. Radzihovsky, *Phys. Rev. B Rapid Comm.* 3548 (1993).
[3] K. S. Novoselov, A. K. Geim, S. V. Morozov, D. Jiang, Y. Zhang, S. V. Dubonos, I. V. Grigorieva, and A. A. Firsov, *Science* 306, 666 (2004).
[4] *The structure of suspended graphene sheets.* J. C. Meyer, A. K. Geim, M. I. Katsnelson, K. S. Novoselov, T. J. Booth, and S. Roth, *Nature* **446**, 60 (2007).

- [5] *Graphene: Exploring carbon flatland*, Andrey K. Geim and Allan H. MacDonald, *Physics Today*, August (2007). Geim-MacDonald
- [6] *The electronic properties of graphene*, A. H. Castro Neto, F. Guinea, N. M. R. Peres, K. S. Novoselov, and A. K. Geim *Rev. Mod. Phys.* **81**, 109 (2009).
- [7] D. R. Nelson and L. Peliti, *J. Phys. (Paris)* **48**, 1085 (1987).
- [8] J. A. Aronovitz and T. C. Lubensky, *Phys. Rev. Lett.* **60**, 2634 (1988); J. A. Aronovitz, L. Golubović, and T. C. Lubensky, *J. Phys. (Paris)* **50**, 609 (1989).
- [9] F. David and E. Guitter, *Europhys. Lett.* **5**, 709 (1988); E. Guitter, F. David, S. Leibler, and L. Peliti, *J. Phys. (Paris)* **50**, 1789 (1989).
- [10] *Scaling behavior and strain dependence of in-plane elastic properties of graphene*, J. H. Los, A. Fasolino, M. I. Katsnelson, *Phys. Rev. Lett.* **116**, 015901 (2016).
- [11] *Increasing the elastic modulus of graphene by controlled defect creation*, G. López-Polín, C. Gómez-Navarro, V. Parente, F. Guinea, M. I. Katsnelson, F. Pérez-Murano, J. Gómez-Herrero, *Nature Physics* **11**, 26-31 (2015).
- [12] *The Effect of Intrinsic Crumpling on the Mechanics of Free-Standing Graphene*, R. J. T. Nicholl, H. J. Conley, N. V. Lavrik, I. Vlassiuk, Y. S. Puzyrev, V. P. Sreenivas, S. T. Pantelides, Kirill I. Bolotin, *Nature Communications* **6**, 8789 (2015).
- [13] *High Precision Fourier Monte Carlo Simulation of Crystalline Membranes* A. Tröster, arXiv:1303.3726, *Phys. Rev. B* **87**, 104112 (2013).
- [14] D. Gazit, *Phys Rev E* **80** (4), 041117 (2009).
- [15] *Collective excitations in a large-d model for graphene* Francisco Guinea, Pierre Le Doussal, Kay Joerg Wiese, arXiv:1312.2854 *Phys. Rev. B* **89**, 125428 (2014).
- [16] *The flat phase of quantum polymerized membranes* O. Coquand, D. Mouhanna, arXiv:1607.03335, *Phys. Rev. E* **94**, 032125 (2016).
- [17] *Electron-induced rippling in graphene* P. San-Jose, J. Gonzalez, F. Guinea, arXiv:1009.1285, *Phys.Rev.Lett.* **106**, 045502 (2011).
- [18] *Gauge fields, ripples and wrinkles in graphene layers* F. Guinea, B. Horovitz, P. Le Doussal, arXiv:0811.4670, *Solid State Commun.* **149**, 1140-1143 (2009), and *Gauge field induced by ripples in graphene* F. Guinea, Baruch Horovitz, P. Le Doussal, arXiv:0803.1958, *Phys. Rev. B* **77**, 205421 (2008).
- [19] *Crumpling transition and flat phase of polymerized phantom membranes* J.-P. Kownacki, D. Mouhanna, *Phys. Rev. E* **79**, 040101 (2009).
- [20] *Thermal crumpling of perforated two-dimensional sheets* D. Yllanes, S. Bhabesh, D.R. Nelson, M.J. Bowick, arXiv:1705.07379.
- [21] *Dislocation-Driven Deformations in Graphene* Jamie H. Warner¹, Elena Roxana Margine¹, Masaki Mukai, Alexander W. Robertson, Feliciano Giustino¹, Angus I. Kirkland, *Science* **337**, Issue 6091, 209-212 (2012).
- [22] *Grains and grain boundaries in single-layer graphene atomic patchwork quilts* P. Y. Huang, Carlos S. Ruiz-Vargas, Arend M. van der Zande, William S. Whitney, Mark P. Levendorf, Joshua W. Kevek, Shivank Garg, Jonathan S. Alden, Caleb J. Hustedt, Ye Zhu, Jiwoong Park, Paul L. McEuen, David A. Muller, *Nature* **469**, 389-392 (2011).
- [23] *Ordered states of adatoms on graphene* Vadim V. Cheianov, Olav Syljuasen, Boris L. Altshuler, Vladimir Falko, *Phys. Rev. B* **80**, 233409 (2009), and *Long-Range Interaction Between Adatoms in Graphene*, Andrei Shytov, Dmitry Abanin, Leonid Levitov, *Phys. Rev. Lett.* **103**, 016806 (2009).
- [24] *Controlled ripple texturing of suspended graphene and ultrathin graphite membranes*, W. Bao, F. Miao, Z. Chen, H. Zhang, W. Jang, C. N. Lau, *Nature Nanotech.* **4**, 562 (2009).
- [25] D. R. Nelson and L. Radzihovsky, *Europhys. Lett.* **16**, 79 (1991).
- [26] L. Radzihovsky and D. R. Nelson, *Phys. Rev. A* **44**, 3525 (1991).
- [27] D. R. Nelson and L. Radzihovsky, *Phys. Rev. A* **46**, 7474 (1992).
- [28] D. C. Morse and T. C. Lubensky, *Phys. Rev. A* **46**, 1751 (1992).
- [29] D. C. Morse, T. C. Lubensky, and G. S. Grest, *Phys. Rev A* **45**, R2151 (1992).
- [30] L. Radzihovsky and P. Le Doussal, *J. Phys. I France* **2**, 599 (1992).
- [31] *Defects in flexible membranes with crystalline order* H. S. Seung and David R. Nelson, *Phys. Rev. A* **38**, 1005 (1988).
- [32] *Anomalous Hooke's law in disordered graphene* I. V. Gornyi, V. Yu. Kachorovskii, A. D. Mirlin, arXiv:1603.00398, *2D Materials* **4**, issue 1, 011003 (2017). *Rippling and crumpling in disordered free-standing graphene*, I. V. Gornyi, V. Yu. Kachorovskii, A. D. Mirlin, *Phys. Rev. B* **92**, 155428 (2015).
- [33] *Thermal Excitations of Warped Membranes*, Andrej Kosmrlj, David R. Nelson, arXiv:1312.4089 *Phys. Rev. E* **89**, 022126 (2013), and *Mechanical Properties of Warped Membranes* arXiv:1306.5941, *Phys. Rev. E* **88**, 012136 (2013).
- [34] For a review, and extensive references, see the articles in *Statistical Mechanics of Membranes and Interfaces*, 2nd edition, edited by D. R. Nelson, T. Piran, and S. Weinberg (World Scientific, Singapore, 1989).
- [35] *Technological Developments of Lipid Based Tubule Microstructures*, A. Rudolph, J. Calvert, P. Schoen, and J. Schnur, *Biotechnological Applications of lipid microstructures*, ed. B. Gaber *et al.* (Plenum, 1988); R. Lipkin, *Science*, **246**, 44 (December 1989).
- [36] A. Elgsaeter, B. Stokke, A. Mikkelsen and D. Branton, *Science* **234**, 1217 (1986).
- [37] *Conformation and elasticity of the isolated red blood cell membrane skeleton*, Karel Svoboda, Christoph F. Schmidt, Daniel Branton, and Steven M. Block, *Biophys J.* **63** 784-793 (1992).
- [38] R. Lipowsky and M. Girardet, *Phys. Rev. Lett.* **65**, 2893 (1990).

- [39] S. Leibler, in Proceedings of the Cargese School on “Biologically Inspired Physics”, (1990).
- [40] T. Hwa, *MIT Ph.D. Thesis*, June 1990, and T. Hwa, E. Kokufuta, and T. Tanaka, *Phys. Rev. A* **44**, 2235 (1991).
- [41] R. R. Chianelli, E. B. Prestridge, T. A. Pecoraro and J. P. DeNeufville *Science* **203**, 1105 (1979).
- [42] Y. Kantor, M. Kardar, and D. R. Nelson, *Phys. Rev. A* **35**, 3056 (1987).
- [43] M. Paczuski, M. Kardar and D.R. Nelson, *Phys. Rev. Lett.* **60**, 2638 (1988).
- [44] P. Hohenberg, *Phys. Rev.* **158**, 383 (1967).
- [45] N. D. Mermin and H. Wagner, *Phys. Rev. Lett.* **17**, 1133 (1966).
- [46] S. Coleman, *Commun. Math. Phys.* **31**, 259 (1973).
- [47] A. M. Polyakov, *Phys. Rev. Lett.*, **59B**, 79, (1975).
- [48] M. Kardar and D. R. Nelson, *Phys. Rev. Lett.* **58**, 1289 (1987).
- [49] J. A. Aronovitz and T. C. Lubensky, *Europhys. Lett.* **4**, 395 (1987).
- [50] B. Duplantier, *Phys. Rev. Lett.* **58**, 2733 (1987).
- [51] Y. Kantor and D. R. Nelson, *Phys. Rev. A* **38**, 4020 (1987).
- [52] F. F. Abraham, W. E. Rudge, and M. Plishke, *Phys. Rev. Lett.* **62**, 1757 (1989).
- [53] M. Plishke and D. Boal, *Phys. Rev. A* **38**, 4943 (1988).
- [54] F. F. Abraham and D. R. Nelson, *Science* **249**, 393 (1990), and *J. de Physique* **51**, 2653 (1990).
- [55] M. Mutz, D. Bensimon, and M. J. Brienne *Phys. Rev. Lett.* **67** 923 (1991).
- [56] *Entropic Interaction between Polymerized Membranes*, S. Leibler and A. C. Maggs, *Phys. Rev. Lett.* **63** 406 (1989).
- [57] *Stretching and buckling of polymerized membranes: a Monte Carlo study*, E. Gitter, S. Leibler, A. C. Maggs, and F. David, *J Phys* **51**, 1055-1060 (1990).
- [58] *Shape fluctuations of polymerized or solid like membranes*, R. Lipowsky, M. Giradet, *Phys Rev Lett* **65** 2893-2896 (1990).
- [59] *Comment on “shape fluctuations of polymerized or solidlike membranes”*, F. F. Abraham, *Phys Rev Lett* **67**, 1669 (1991).
- [60] *Tethered vesicles at constant pressure: Monte Carlo study and scaling analysis*, S. Komura and A. Baumgärtner *J. Phys. France* **51**, 2395 (1990).
- [61] *A polymerized membrane in confined geometry*, G. Gompper and D. M. Kroll, *Europhys Lett.* **15**, 783-788 (1991); *Fluctuations of a polymerized membrane between walls*, G. Gompper and D. M. Kroll, *J. Phys.* **1**, 1411-1432 (1991); *Fluctuations of polymerized, fluid and hexatic membranes: continuum models and simulations*, G. Gompper and D. M. Kroll, *Current Opinion in Colloid & Interface Science* **2**, 373-381 (1997).
- [62] *Molecular dynamics simulations of 52. the structure of closed tethered membranes*, I. B. Petsche, G. S. Grest GS, *J Phys* **1**, 1741-1754 (1993).
- [63] *Scaling behavior of self-avoiding tethered vesicles*, Z. Zhang, H. T. Davis, D. M. Kroll, *Phys Rev E* **48**, R651-R654 (1993).
- [64] *Molecular dynamics simulations of tethered membranes with periodic boundary conditions*, Z. Zhang, H. T. Davis, D. M. Kroll, *Phys Rev E* **53**, 1422-1429 (1996).
- [65] *The Flat Phase of Crystalline Membranes*, M. J. Bowick, Simon M. Catterall, Marco Falcioni, Gudmar Thorleifsson, and Konstantinos N. Anagnostopoulos, *J. Phys. (France) I* **6**, 1321 (1996).
- [66] M. Falcioni, M. J. Bowick, E. Gitter, and G. Thorleifsson, The Poisson ratio of crystalline surfaces, *Europhys. Lett.* **38**, 67 (1997): cond-mat/9610007.
- [67] A. J. Bray, *Phys. Rev. Lett.* **32**, 1413 (1974).
- [68] A generalization to anisotropic in-plane elasticity was considered and extensively explored by Radzihovsky and Toner in *A New Phase of Tethered Membranes: Tubules*, Leo Radzihovsky, John Toner, *Phys. Rev. Lett.* **75**, 4752 (1995); *Elasticity, Shape Fluctuations and Phase Transitions in the New Tubule Phase of Anisotropic Tethered Membranes*, *Phys. Rev. E* **57**, 1832-1863 (1998).
- [69] The other geometrical invariant is the intrinsic Gaussian curvature. However the integral of the Gaussian curvature can be shown to be a topological invariant proportional to the Euler character or the genus of the manifold and therefore will not be considered in this paper.
- [70] In the isotropic description the theory is $O(d) \times O(D)$ invariant and there are a total of Dd independent deformational modes. In the spontaneously broken flat phase the symmetry is reduced to $O(d_c) \times O(D) \times O(D)$. The general principles require that when a group G is broken down to a group H , the number of massless Goldstone modes is equal to the dimension of the coset space G/H , here $O(d)/O(D)/O(d_c)$. We therefore expect Dd_c massless modes and D^2 massive ones corresponding to $\partial_\alpha \vec{h}$ Goldstone modes and $\partial_\alpha u_\beta$ elastic deformations, respectively.
- [71] *Theory of Elasticity*, L.D. Landau and E.M. Lifshitz, Pergamon Press, (1975).
- [72] D. C. Mattis, *Phys. Lett. A* **56**, 421 (1976).
- [73] Y. Imry and S. K. Ma, *Phys. Rev. Lett.*, **35**, 1399 (1975).
- [74] For review of random field and bond disorders see for example article by D. S. Fisher in *Physics Today*, 1989.
- [75] As usual at long wavelengths the higher moments are expected to be irrelevant in renormalization group sense.
- [76] *Aspects of Symmetry: Selected Erice Lectures*, Sidney Coleman, Cambridge University Press (1995).
- [77] *Quantum Field Theory and Critical Phenomena*, Jean Zinn-Justin, Oxford Science Publications (2002).
- [78] *Principles of Condensed Matter Physics*, P. M. Chaikin and T. C. Lubensky, Cambridge University Press, Cambridge (1995).
- [79] L. Radzihovsky, unpublished; B. Jacobsen, Ph.D. Thesis, University of Colorado at Boulder (2003).
- [80] *Liquid Crystal Elastomers*, M. Warner, E.M. Terentjev, Oxford Science Publications (2005).
- [81] *Nonlinear Elasticity, Fluctuations and Heterogeneity of Nematic Elastomers*, Xiangjun Xing and Leo Radzihovsky *Annals of Physics* **323**, 105-203 (2008); *Phases and Transitions in Phantom Nematic Elastomer Membranes*, *Phys. Rev. E* **71**,

- 011802 (2005); *Thermal fluctuations and anomalous elasticity of homogeneous nematic elastomers*, *Europhysics Letters* **61**, 769 (2003); *Universal Elasticity and Fluctuations of Nematic Gels* *Phys. Rev. Lett.* **90**, 168301 (2003).
- [82] O. Stenull and T. C. Lubensky, *Europhys. Lett.* **61**, 776 (2003); *Phys. Rev. E* **69**, 021807(2004).
- [83] E. Guitter, F. David, S. Leibler, and L. Peliti, *Phys. Rev. Lett.* **61** 2949 (1988).
- [84] *Self-Consistent Theory of Normal-to-Superconducting Transition*, L. Radzihovsky, *Europhysics Letters*, **29**, 227 (1995).
- [85] S. F. Edwards and P. W. Anderson, *J. Phys. F* **5** 965 (1975).
- [86] It is not clear whether there is an underlying physical reason for this $d_c \rightarrow 4d_c$ property or that it is just an accident special to the SCSA.
- [87] Actually there is an additional mixed marginal phase in which both LR curvature and LR stress disorders are relevant, analogous to the mixed LRM and LRMG phases and the exponents are completely determined with $\eta = \eta' = z_\kappa$. However, this phase turns out to only exist on a special line $z_\kappa = 2 - D/2 - z_\mu/2$ and is therefore not likely to be experimentally significant. For this reason we do not describe in any further detail.
- [88] D. Espriu and A. Travasset, *Nucl. Phys. B* **468**, 514 (1996).
- [89] Z. Zhang, H. T. Davis, and D. M. Kroll, *Phys. Rev. E* **R48**, 651 (1993).
- [90] C. Lee, X. D. Wei, J. W. Kysar, J. Hone, *Measurement of the elastic properties and intrinsic strength of monolayer graphene*, *Science* **321**, 385 (2008), A. Castellanos-Gomez, M. Poot, G. A. Steele, H. S. J. van der Zant, N. Agrat, G. Rubio-Bollinger, *Elastic properties of freely suspended MoS2 nanosheets*, *Adv. Mater.* **24**, 772 (2012).
- [91] A. Castellanos-Gomez, V. Singh, H. S. J. van der Zant, G. A. Steele, *Mechanics of freely-suspended ultrathin layered materials*, *Annalen der Physik* **527**, 27 (2015).
- [92] A. Baumgartner and W. Renz, *Euro. Phys. Lett.* (1991); A. Baumgartner, *J. de Physique I* **1**, 1549 (1991).